IDENTIFICATION AND CHARACTERIZATION OF AN ALTERNATIVE CANALICULAR BILE ACID TRANSPORTER

by

Ping Lam

B.Sc., The University of Waterloo, 1997

A THESIS SUBMITTED IN PARTIAL FULFILLMENT OF THE REQUIREMENTS FOR THE DEGREE OF

DOCTOR OF PHILOSOPHY

in

THE FACULTY OF GRADUATE STUDIES

(Department of Biochemistry and Molecular Biology)

We accept this thesis as conforming
to the required standard

The University of British Columbia

April 2004

ABSTRACT

In vertebrates, bile flow is essential for movement of water and solutes across the liver canalicular membrane. The formation of bile is contributed by the active transport of bile acids and other organic solutes (Coleman 1987; Nathanson and Boyer 1991; Erlinger 1996). In recent years, the molecular motor of canalicular bile acid secretion has been identified to be a member of the ATP Binding Cassette transporter superfamily, known as Sister of p-glycoprotein (Spgp) or Bile Salt Efflux Pump (Bsep) (Childs et al. 1995; Gerloff et al. 1998). In humans, mutations in *spgp* cause a severe liver disease known as type 2 intrahepatic cholestasis (PFIC2), which is characterized by low bile acid output (Strautnieks et al. 1998; Jansen et al. 1999). *Spgp*$^{-/-}$ mice produce a cholestatic phenotype that is less severe than human PFIC2 (Wang et al. 2001). The work in this thesis investigated the molecular mechanism(s) of bile acid secretion in *spgp*$^{-/-}$ mice. Hepatic responses of bile flow and bile acid secretion were significantly stimulated by cholic acid (CA) feeding in mutant mice. In addition, the capacity of total bile acid secretion was comparable to wildtype mice, compatible with the hypothesis that additional molecular mechanisms exist for bile acid secretion. To investigate whether another ATP-dependent bile acid transport may account for the bile acid clearance in *spgp*$^{-/-}$ mice, mRNA and protein expression data were studied. The expression of Mdr1a associated with resistance to multiple anticancer drugs, was dramatically increased in *spgp*$^{-/-}$ mice. Kinetic studies showed ATP-dependent bile acid transport in canalicular membrane vesicles isolated from control mice but not in those from *spgp*$^{-/-}$ mice. To reconcile this difference between *in vivo* data and *in vitro* canalicular membrane transport measurement, membrane vesicles containing highly overexpressed hamster Pgp (a homolog of mouse *mdr1a*) was used to demonstrate ATP-dependent bile acid transport. The kinetic parameters of Pgp-mediated ATP-dependent taurocholate transport were compatible with a low-affinity transporter. Taken together, these studies have provided evidence that Mdr1a is capable of transporting bile acids, which has not been recognized previously.

TABLE OF CONTENTS

LIST OF TABLES

LIST OF FIGURES

LIST OF ABBREVIATIONS

5'-ND	5'-nucleotidase
ABC	ATP-Binding Cassette
ALP	Alkaline phosphatase
ApoA-I	Apolipoprotein AI
ASBT	A sodium bile acid transporter
AST	Aspartate aminotransferase
BADF	Bile acid dependent bile flow
BAIDF	Bile acid independent bile flow
BFR	Bile flow rate
BMV	Basolateral membrane vesicles
BSEP	Bile acid efflux pump
CA	Cholic acid (3α, 7α, 12α-trihydroxy-5β-cholanic acid)
CDCA	Chenodeoxycholic acid (3α, 7α-dihydroxy-5β-cholanic acid)
CGamF	Cholylglycylamidofluorescein
CMFDA	5-chloromethylfluorescein diacetate
CMOAT	Canalicular multispecific organic anion transporter
CMV	Canalicular membrane vesicles
CsA	Cyclosporin A
CYP7A1	Cytochrome P450 7A1
DBcAMP	Dibutyryl-3'-5'-cyclic monophosphate
DCA	Deoxycholic acid
DCLF	Deoxycholyl-lysyl-fluorescein
E17βG	17-estradiol-17β-glucuronide
EC_{50}	Half maximal effective concentration
EHC	Enterohepatic circulation
FXR	Farnesoid X receptor
GCA	Glycocholate
GGT	γ-glutamyltranspeptidase
GSH	Reduced glutathione
GSSH	Glutathione disulfide

GUDCA	Glycoursodeoxycholate
HDL	High density lipoprotein
HMGCoA-R	3-hydroxyl-3-methylglutaryl-coenzymeA reductase
HPLC	High performance liquid chromatography
HUGO	Human genomic organization
I-BABP	Intestinal bile acid binding protein
LCA	Lithocholic acid (3α-monohydroxy-5β-cholanic acid)
LTC_4	Leukotriene C_4
MDR	Multidrug resistance
MMV	Mixed membrane vesicles
Mrp2	Multidrug resistance related protein
NBD	Nucleotide binding domain
Ntcp	Na^+ dependent taurocholate transporting protein
Oatp	Organic anion transporting polypeptide
PC	Phosphatidylcholine
PCR	Polymerase chain reaction
PFIC1	Progressive familial intrahepatic cholestasis type 1
PFIC2	Progressive familial intrahepatic cholestasis type 2
PFIC3	Progressive familial intrahepatic cholestasis type 3
Pgp	P-glycoprotein
PMV	Plasma membrane vesicles
SHP	Small heterodimer partner
Spgp	Sister of P-glycoprotein
TCA	Taurocholate
TLC-S	Taurolithocholate-3-sulfate
TLDC-S	Taurochenodeoxycholate-3-sulfate
TMCA	Tauro-β-muricholate
TMD	Transmembrane domain
TTBA	Tetrahydroxylated bile acid
TUDCA	Tauroursodeoxycholate

ACKNOWLEDGEMENTS

I would like to thank many people for their help and encouragements:

Victor Ling, for inviting me to his laboratory, for giving me the freedom and resources to explore many areas of research.

Jaclyn Hung, for all her help and support in my graduate training. She sets a high standard for all of us to follow.

Renxue Wang, Carol Soroka and **Dana Forrest** for their collaborations and contributions to this thesis work.

Adam Shapiro, who got me interested in bench work biochemistry and fluorescence spectrofluorometry.

Thanks to all my colleagues and friends: **Lin Liu** and **Camila Alvarez** for their assistance. **Huey-Ling Chen, Maria Ho, Isabella Mak, Masie Lo, Dennis Levinson-Gower** and many others for their support and friendships.

I would like to thank: **Lee Hagey, Alan Hofmann, James Boyer, Dietrich Keppler** for all their help and answers to my questions.

Tania Kastelik for reading my thesis and always happy to give advice and discuss CSI.

Financial support of the Natural Sciences and Engineering Research Council of Canada, Canadian Liver Foundation and University of British Columbia.

To Iris Cheung, I couldn't have done it without you.
To my grandma who is always there for me.
To the rest of my family, for their financial support.

Thesis project overview

Bile acid secretion across the canalicular membranes is the rate-limiting step in the overall transport of bile acids vectorially from blood to bile. This step quantitatively contributes to bile flow, an osmotically driven process whereby water, organic solutes and electrolytes are secreted into bile. This makes up the bile-acid dependent component of bile flow. Bile acid secretion is a key step in maintaining bile acid and cholesterol homeostasis and disruption of this step is expected to lead to liver cholestasis. Lack of bile acid secretion into the small intestine also leads to malabsorption as bile acids are needed for emulsification and digestion of fats and fat-soluble vitamins. Bile acids activate nuclear receptors, thereby affecting diverse physiological functions by transcriptional regulation of many genes. Two factors affect the function of bile acids: the type of bile acid species and the quantity of bile acids. Balance of bile acids in each tissue (liver, bile, blood and small intestine) is thus critical in coordinating normal cellular responses. Understanding the molecular basis for bile acid secretion is therefore important in biliary physiology and in disease (reviewed in (Hofmann 1999))

Many studies have provided strong evidence that a member of the ATP-binding Cassette (ABC) superfamily, Sister of P-glycoprotein (Spgp), is the canalicular membrane bile acid transporter. *In vitro* evidences include results from human, rat and mouse Spgp cDNA transfected insect cell membrane vesicles (Gerloff et al. 1998; Green et al. 2000; Byrne et al. 2002; Noe et al. 2002). Isolated membrane vesicles exhibit a bile acid transport rate and affinity resembling that of isolated canalicular membrane vesicles of rat livers. Furthermore, genetic evidence of *spgp* mutations causing progressive familial intrahepatic cholestasis type 2 (PFIC2), a liver disease characterized by low biliary bile acid output, provided the proof of Spgp's role as a bile acid transporter in humans (Jansen et al. 1999).

In this thesis, the first chapter reviews our present day knowledge of the physiology and biochemistry of bile acid secretion. In the liver, bile acid biosynthesis from cholesterol contributes to most of the bile acid pool in our body. The first part of this chapter reviews the important functions of bile acids in our body. However, buildup of excessive amount of

these bile acids caused liver toxicity and cholestasis. It has become clear that ATP-Binding Cassette (ABC) transporters play important roles in transport processes that occur in the liver. The second part of this chapter is an introduction of the general features of the ABC superfamily with a specific emphasis on the liver ABC transporters, namely ABCB1 (MDR1), ABCB4 (MDR2), ABCC2 (MRP2), ABCC3 (MRP3) and ABCB11 (BSEP/SPGP). The final section of this chapter is an up-to-date analysis of *spgp*$^{-/-}$ mice generated in this laboratory. Although it was expected that disruption of *spgp* gene in mice will phenocopy the human disease counterpart (PFIC2). However, this is not the case. Characterization of these *spgp*$^{-/-}$ mice has led me to investigate alternative bile acid transport mechanism(s) that contribute to biliary function of these mutant mice.

The third chapter entitled "*Bile acid transport capacity in spgp*$^{-/-}$ *mice*" describes the results obtained when *spgp*$^{-/-}$ mice was challenged with a cholic acid (CA) rich diet. Mice deficient in *spgp* displayed hepatomegaly, growth retardation and showed some typical signs of cholestasis such as dramatic reduction in cholic acid secretion. However the phenotype is less severe than those seen in human PFIC2. Liver function measured by biochemical liver indicators e.g. alkaline phosphatase, aspartate aminotransferase, 5'-nucleotidase, and bile flow are normal in *spgp*$^{-/-}$ mice despite the lack of a major bile acid pump in the canaliculi. Furthermore, expression data of a number of liver proteins, e.g. the canalicular multidrug resistance protein (Mdr1), the canalicular multidrug resistance related protein (Mrp2), the basolateral Na^+ dependent bile acid uptake protein (Ntcp) were analyzed for their potential upregulation to assess their roles in compensatory and defense mechanisms against bile acid accumulation in *spgp*$^{-/-}$ mouse liver.

The fourth chapter entitled "*Characterization of Spgp-independent canalicular transport of cholic acid*" is the first *in vitro* study using *spgp*$^{-/-}$ mouse livers to study bile acid transport. *Spgp*$^{-/-}$ mice provide an unique opportunity to investigate transport characteristics of bile acid in native canalicular membrane from both wildtype mice and *spgp*$^{-/-}$ mice. Fluorescent and radiolabel bile acid transport was measured in hepatocyte couplets and in enriched canalicular membrane vesicles to assess the capacity and kinetics of transport.

The fifth chapter entitled "*P-glycoprotein mediated ATP-dependent taurocholate transport: in vitro evidence for an alternative canalicular bile acid transporter*" builds on previous research defining the substrate specificity of Pgp transport. *In vivo* and *in vitro* data obtained in chapter 3 and chapter 4 strongly indicate that a high capacity transporter of bile acids is present in *spgp*$^{-/-}$ mice providing as an alternative bile acid secretory mechanism. Based on the evolutionary closeness of the multidrug resistance (MDR) P-glycoprotein with Spgp and data demonstrating a striking increase in mdr1a mRNA and protein levels in *spgp*$^{-/-}$ mice, it has been postulated that Pgp may serve as an alternative bile acid transporter. Using membrane vesicles that overexpressed hamster pgp1 (homolog of mdr1a in mouse), the ability of Pgp to mediate taurocholate transport was tested. Individual bile acids were tested to determine whether they can inhibit Pgp-mediated transport of substrates. These studies has provided the first evidence of direct interaction with, and bile acid transport activity mediated by, Pgp.

The final chapter entitled "*Conclusions and Perspectives for Future Studies*" discusses how the above results have provided further understanding of substrate diversity and substrate preference of Spgp and Pgp. This chapter also introduces future studies that may arise from work presented in this thesis.

Chapter 1: Introduction

1.1. Enterohepatic circulation of bile acids

The enterohepatic circulation of bile is a process in which bile is reabsorbed from the small intestine, returned to the liver in portal blood and secreted into the biliary tract (Fig. 1) (Carey and W.C. 1994). Bile that exists in the enterohepatic circulation is composed of a complex mixture of different bile acid species, phospholipids, cholesterol, bile pigments in addition to many different organic solutes and electrolytes (Boyer 1986). The enterohepatic circulation of bile acids allows for these biologically important detergents to be reused many times a day. Under most physiological conditions, the bile acid pool remains constant. The adult human synthesizes about 0.2-0.5 g of bile acid every day into the 1.5-4 g total bile acid pool. The entire bile acid pool recirculates 6 to 10 times in one day, in which 95% of bile acids are reabsorbed and only 5% (0.2-0.5g) are lost in feces (Hofmann 1989; Carey and W.C. 1994).

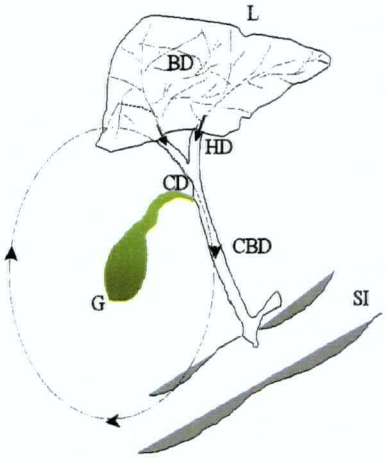

Fig. 1. Enterohepatic circulation of bile acids in vertebrates.

Primary bile acids are synthesized in the liver (L), secreted into bile ducts (BD) and collected into two major ducts called hepatic ducts (HD). Bile acids are transported via the cystic duct (CD) and stored in the gallbladder (G). During food intake, bile acids are pumped into the common bile duct (CBD) and released into the small intestine (SI) where they aid in the digestion of dietary fats and fat-soluble vitamins. Bile acids are then reabsorbed efficiently and taken up into the liver via the portal vein (represented by the circle). Adapted from (Carey and W.C. 1994).

Canalicular bile flow is an active process driven by the secretion of various components across the canalicular membrane. Conventionally, bile flow is made up of a "bile acid-dependent" (BADF) and a "bile acid-independent" (BAIDF) component. Bile acid secretion is the major driving force of the bile acid dependent bile flow (Nathanson and Boyer 1991). Glutathione secretion and many other components are contributors to the bile acid-independent bile flow (Graf 1983; Ballatori and Truong 1992). Hepatic bile originates from transport processes in the bile canaliculus but can be modified by absorption and secretion along the bile ductules and ducts. In addition to the transcellular route for water and solute canalicular bile flow, evidence suggests that fluid and electrolytes pass from the intercellular space across the junctional complex into the canalicular lumen by a paracellular pathway (Boyer et al. 1979). Hormones and secondary messengers appear to regulate several aspects of bile formation. Dibutyrl cAMP increases bile flow and bile acid output in the isolated perfused rat liver (Hayakawa et al. 1990). These observations suggest that endogenous cAMP increases bile acid-dependent bile flow. Protein kinase C and cytosolic Ca^{2+} are important intracellular messengers that have been shown to decrease bile flow in the isolated perfused rat liver (Corasanti et al. 1989; Nathanson et al. 1992). Bile ducts also modify canalicular bile. Under normal condition, the hormone secretin induces a minimal increase in bile flow and biliary bicarbonate secretion (Hardison and Wood 1978; Mathisen and Raeder 1983). Bile ducts can also increase bile flow by reabsorption of some bile acids. The concept of "cholehepatic shunting" has been proposed for bile acid induced hypercholeresis, bile flow that cannot be accounted for only by their secretion into bile (Yoon et al. 1986). According to this hypothesis, unconjugated bile acid such as ursodeoxycholate is secreted into bile and becomes protonated in the canalicular lumen into ursodeoxycholic acid. The proton comes from bicarbonate, and the process generates bicarbonate ion that is secreted by bile ductules and stimulates bile flow. The protonated bile acid is lipid soluble and is absorbed by biliary ductal cells and returns to the hepatocyte. Each cycle of bile acid secretion generates bicarbonate ions and stimulates bile flow.

The magnitude of bile flow and contribution by bile acid dependent and independent components varies greatly between species (Table 1). In some species such as rodent, hamster, guinea pig (Forker et al. 1967; Forker 1968; Guertin et al. 1995), most canalicular

bile flow is bile acid-independent. While in others, such as human, monkey, and dog, most canalicular bile flow is bile acid-dependent (Preisig et al. 1962; Wheeler et al. 1968; Boyer and Bloomer 1974). Comparatively, bile acids secretion generates much lower volume of bile in humans than in rodents (7μl/μmol bile salts vs. 15μl/μmol bile salts respectively). The bile acid-independent component induce more bile flow in rodents, 40μl of bile per min per kg body weight compared to 2μl of bile per min per kg body weight than in humans (Table 1).

Table 1. Comparison of bile flow in different species*

	Man	Rat	Mice	Dog	Rhesus monkey	Rabbit
Total flow (μl/min/kg bw)	5	70	88	10	15	90
Bile acid dependent bile flow (μl/μmol BS)	7	15	28	8	16	70
Bile acid independent bile flow (μl/min/kg bw)	2	40	55	5	7	60

* Adapted from Boyer JL *et al.*, 1986 (Boyer 1986)

1.2. Role and diversity of bile acids

Bile is apparently produced by all vertebrates and bile acids are the most abundant constituents. Most animals make a considerable variety of different bile acids. The actual biliary bile acid composition for each vertebrate is determined by multiple factors: 1) bile acid synthesis in the liver to produce primary bile acids, where the final product is the resultant of hydroxylation by cytochrome P450 enzymes; 2) intestinal conservation by passive and active transport processes; 3) bacterial modification and absorption of bacterially modified bile acids as secondary bile acids; 4) hepatic rate of rehydroxylation of 7-dehydroxylated bile acids and epimerization of 3β- epimers and 3- or 7-oxo bacterial bile acid metabolites.

Bile acid production is essential for cholesterol degradation and represents the most important pathway for cholesterol removal from the body. Since cholesterol has a C3 hydroxyl group, all natural bile acids must have a C3 hydroxyl group. In addition, cholesterol 7α-hydroxylase is the rate-limiting enzyme of bile acid biosynthesis, all bile acids have C7 hydroxyl group. This bile acid is termed chenodeoxycholic acid (3αOH, 7αOH). In most vertebrates, chenodeoxycholic acid can also undergo an additional hydroxylation to form a trihydroxylated bile acid (3αOH, 7αOH and "X" OH).

Two separate pathways in the liver hepatocytes quantitatively contribute to bile acid biosynthesis in mammals: the classic pathway/neutral pathway and the alternative/acidic pathway (Bjorkhem 1985; Fuchs 2003). A condensed overview of the major routes in hepatic bile acid biosynthesis is depicted in Fig. 2. The classic pathway involves the modification of the sterol nucleus before side chain modification. The primary or neutral pathway is initiated by the conversion of cholesterol to 7α-hydroxycholesterol by the first rate limiting enzyme, a microsomal cytochrome P450, cholesterol 7α-hydroxylase (CYP7A1). This pathway starts with hydroxylation of the sterol ring by CYP7A1 followed by side chain cleavage reactions to synthesize cholic acid and chenodeoxycholic acid. The branch point in this pathway is catalyzed by another microsomal P450 sterol 12alpha-hydroxylase (CYP12) that results in the synthesis of cholic acid (Vlahcevic et al. 2000). This

pathway is dominant in human liver when CYP7A1 level is high. When CYP7A1 level is low as in liver disease, an alternative pathway (acidic pathway) predominant to produce chenodeoxycholic acid. The alternative pathway is induced in CYP7A1-/- mice between three to four weeks of life (Schwarz et al. 1996). Most of the enzymes leading to the production of chenodeoxycholic acid remain unknown. It is known that mitochondrial sterol 27-hydroxylase (CYP27) catalyzes the first reaction on cholesterol with side chain modification followed by sterol ring hydroxylation by the microsomal oxysterol 7α-hydroxylase (CYP7B) (Cali and Russell 1991; Wang and Chiang 1994). The production of oxysterols in the liver, brain and extrahepatic tissue also contributes to the alternative pathway of bile acid synthesis (Schwarz et al. 1996; Bjorkhem et al. 2001).

Bile acid composition of >600 vertebrate species, from reptiles, birds to mammals have been determined using modern methods (Hagey 1986). The family of bile acid molecules is composed of a large number of different structures. Most bile acids (5β-cholanic acids) contain a saturated 19-carbon sterol nucleus with an β-oriented hydrogen carbon at C_5 position and a branched, saturated 5-carbon side chain terminating in a carboxyl group, the result is a C_{24} bile acid (see review (Hofmann 1994)). Bile acid differs from each other by the number of hydroxyl groups attached in either α- or β-orientation to the sterol ring and the conjugation status of the side chain. Conjugated bile acids are formed under physiological condition by attaching taurine or glycine to the side chain carboxyl group through an amide bond by bile acid-CoA: amino acid N-acyltransferase (Johnson et al. 1991; Falany et al. 1994; He et al. 2003; O'Byrne et al. 2003).

Table 2 documents the biodiversity of bile acids in some vertebrates. In human bile, cholic acid (3α7α12α) (40%) and chenodeoxycholic acid (3α7α) (40%) comprise the major proportions of bile acids. Bile acids present in lesser amounts are secondary bile acids such as deoxycholic acid (3α12α) (<10%), lithocholic acid (3α) and ursodeoxycholic acid (3α7β) (each less than 1%) (Yanagisawa et al. 1980). In mice and rats, the two major primary bile acids are cholic acid (3α7α12α) (40%) and muricholic acids (50%) (Wang et al. 2001). Muricholic acids (3α, 6β, 7α or 3α, 6β, 7β) are formed in the liver by 6β-hydroxylation and epimerization of the 7α-hydroxyl group (in the case of 3α, 6β, and 7β). In the bear, 7β-

epimerization of 7α-hydroxyl group of CDCA results in the biosynthesis of ursodeoxycholic acid (UDCA) (Hagey et al. 1993).

The relationships between structural properties and biological effects of bile acids have been investigated. Hydrophobic bile acids (chenodeoxycholic acid, deoxycholic acid) but not hydrophilic acids (ursodeoxycholic acid, muricholic acid), significantly suppress hepatic activity of HMG-CoA reductase, the limiting step of cholesterol synthesis, and cholesterol 7alpha-hydroxylation, the limiting step of bile acid synthesis (Bjorkhem et al. 1993; Ellis et al. 2003). The output of biliary cholesterol and phospholipid is also directly related to the hydrophobicity of the bile acid pool (Northfield et al. 1975; Barnwell et al. 1983). Hydrophobic bile acids have been found to induce greater cytotoxic and pro-apoptotic effects in *in vitro* models (Benedetti et al. 1997; van Nieuwerk et al. 1997). In addition, feeding hydrophilic bile acids inhibits intestinal cholesterol absorption (Wang et al. 2003a).

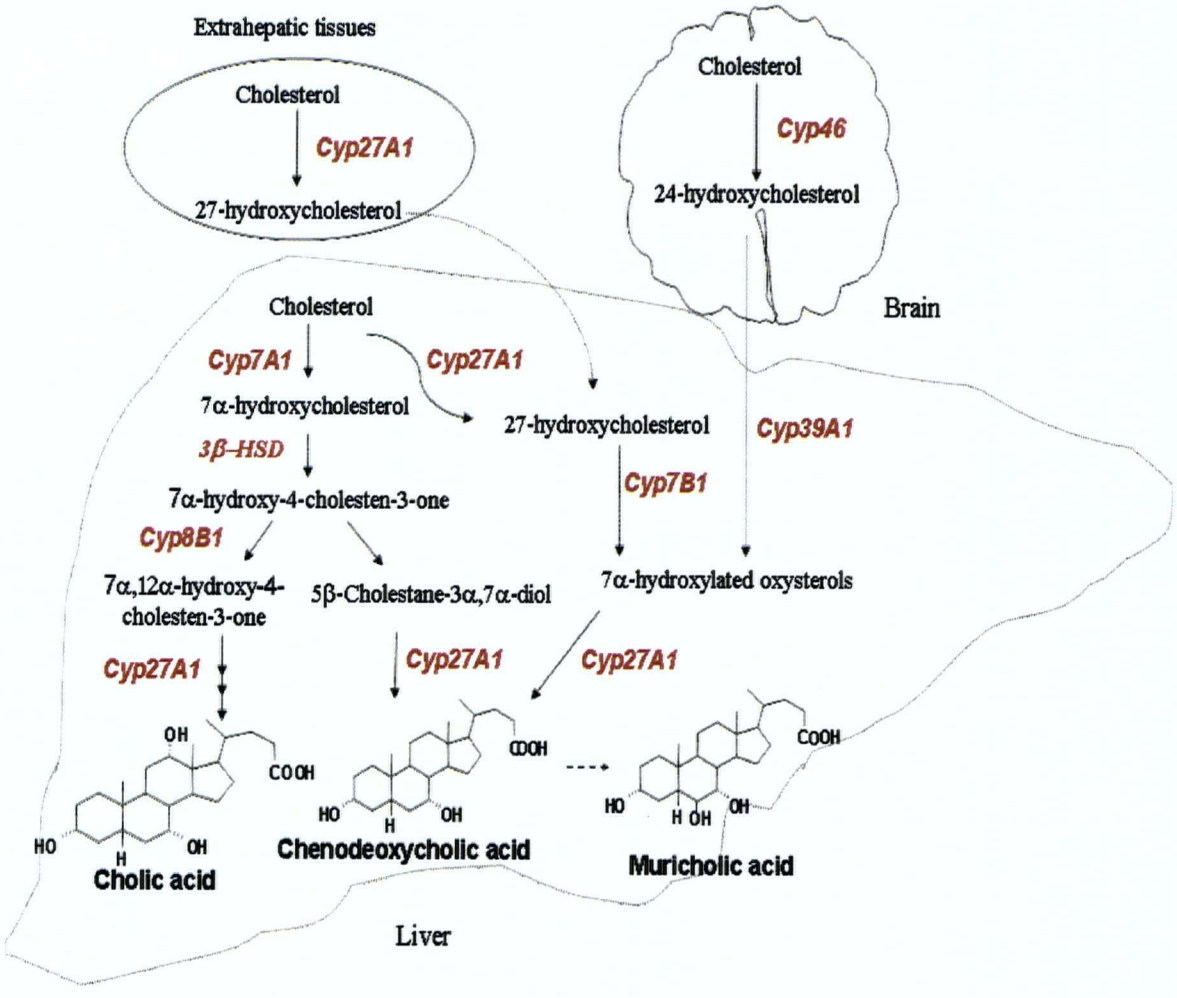

Fig. 2. Bile acid biosynthesis pathways in the liver.

The initial step in the classic pathway is 7α-hydroxylation of cholesterol. The rate-limiting enzyme in this reaction is cytochrome P-450 7α-hydroxylase (Cyp7A1). This activity leads to both cholic and chenodeoxycholic acid biosyntheses. The initial step in the alternative pathway is 27-hydroxylation of cholesterol that involves the cytochrome P-450 enzyme, 27α-hydroxylase (Cyp27) that synthesizes chenodeoxycholic acid. In the intermediate step, cytochrome P-450 enzyme, sterol 12-hydroxylase (Cyp8b1) adds a hydroxyl group to the C-12α-position of bile acid intermediates in the classic bile acid biosynthetic pathway. Its activity is crucial for the determination of the ratio between cholic and chenodeoxycholic acids in human bile. In rodents, hypothetical sequences of steps are likely to be involved in the conversion of chenodeoxycholic acid to muricholic acid drawn as dotted arrows. The molecular components of these steps are not understood (Elliot 1985). Three alternative pathways are also shown. Cholesterol is first converted to oxysterols in the liver, in the extrahepatic tissues (e.g. macrophages) and in the brain. Adapted from (Fuchs 2003).

Table 2. Common bile acids found in the bile of selected vertebrates

Bile acid skeleton

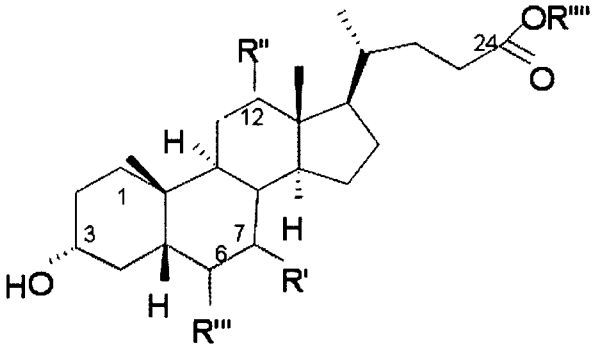

R'''' – taurine or glycine

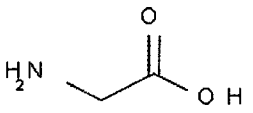

Glycine

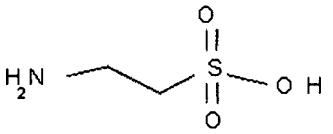

Taurine

Common Name	R'	R"	R""	Commonly found in species
Cholic acid (3α7α12α)	α -OH	α -OH	H	bear, cat, hamster, human, mouse, pig, rabbit, rat
Chenodeoxycholic acid (3α7α)	α -OH	H	H	bear, hamster, human, pig
Deoxycholic acid (3α12α)	H	α -OH	H	cat, human, rabbit
Ursodeoxycholic acid (3α7β)	β -OH	H	H	bear
Lithocholic acid (3α)	H	H	H	human, rat, mouse
β-muricholic acid (3α6β7β)	β -OH	H	β -OH	mouse, rat
α-muricholic acid (3α6α7β)	α -OH	H	β -OH	pig, mouse, rat
Ω-muricholic acid (3α6α7α)	β -OH	H	α -OH	mouse, rat

Adapted from (Hofmann 1994).

In addition to being metabolic end products, bile acids are also functional molecules. Bile acids in the enterohepatic circulation perform several important functions (for a general review on bile acid physiology, refer to (Hofmann 1999). First, bile acids are major end products of cholesterol catabolism and the major pathway for the body to eliminate cholesterol. Bile acids also assist in the secretion of cholesterol into bile. Second, bile acids are responsible for inducing bile flow known as bile-acid dependent bile flow. Bile formation is considered to occur in two stages: (a) hepatocytes secrete bile into canaliculi and drain into hepatic bile ducts. Bile acid secretion promotes bile flow and biliary phospholipids secretion; (b) as bile flows through the bile ducts, it is modified by addition of a bicarbonate-rich solution secreted from ductal epithelial cells. Bile from the liver is then concentrated and stored in the gallbladder or secreted into the duodenum. Third, bile acids are ionic detergents that are required for the digestion, transport and secretion of dietary fats, cholesterol and fat-soluble vitamins in the small intestine. Bile acids that enter the duodenum emulsify dietary fats, thereby increasing and shortening triglyceride digestion by lipases. Bile acids that are secreted into the bile formed mixed micelles with biliary phospholipids/lecithin and cholesterol (Mazer et al. 1984; Cohen et al. 1990; Cohen et al. 1993). These mixed micelles have a hydrophilic exterior and a hydrophobic interior that serve as vehicles for solubilizing and transporting lipids. Fourth, bile acids function as ligands that bind to nuclear receptors and modulate expression of proteins involved in bile acid and cholesterol homeostasis (Fig. 3) (Sinal et al. 2000). Bile acids activated farnesoid X receptor (FXR) inhibits bile acid biosynthesis by suppressing the expression of the rate-limiting enzyme, *CYP7A1*, stimulates secretion of bile acids by upregulating the expression of the bile acid efflux pump (*BSEP*), and stimulates the reabsorption of bile acids by upregulating the expression of the ileum bile acid binding protein (*IBABP*) that interacts with the ileum bile acid transporter (*IBAT*). Bile acids activated pregnane X receptor (PXR) converts the toxic bile acid, lithocholic acid (LCA) into a less toxic bile acid, hyodeoxycholic acid, by upregulating cytochrome P450 enzyme, CYP3A (Staudinger et al. 2001; Xie et al. 2001).

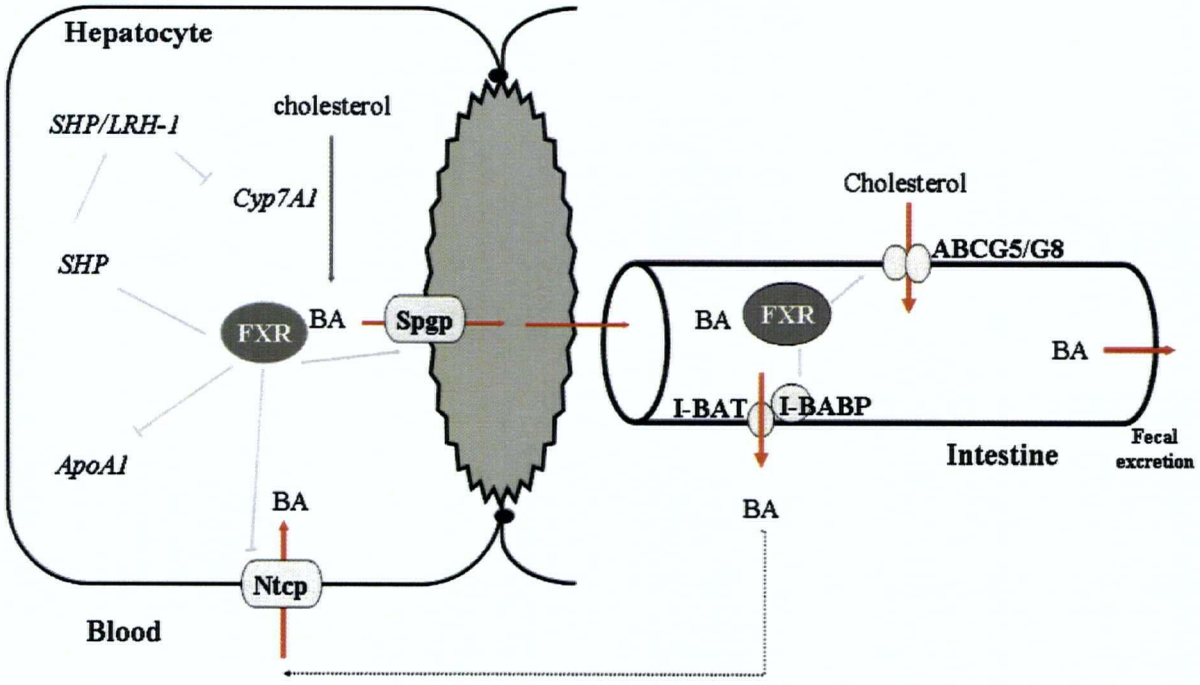

Fig. 3. Coordination of cholesterol and bile acid homeostasis by bile acid activated receptor, FXR.

In the enterocyte, bile acids activate the FXR, which upregulates the ileal bile acid binding protein (*IBABP*), a carrier protein facilitating their reuptake by the gut via the ileal bile acid transporter (*I-BAT*). Bile acids are then delivered into the portal blood and taken up in the hepatocytes by the sodium taurocholate co-transporting polypeptide (*Ntcp*). Inside the hepatocytes, activated FXR decreases further bile acid uptake by reducing the levels of *Ntcp* and stimulating the export of bile acids by increasing the expression of the bile salt efflux pump, *Spgp*. Furthermore, activated FXR indirectly represses the cholesterol 7α-hydroxylase (*cyp7a1*) gene, which controls the rate-limiting step in bile acid biosynthesis from cholesterol. FXR induces the small heterodimer partner (*SHP*) to bind to another orphan nuclear receptor, liver receptor homolog-1 (*LRH-1*), which is a positive regulator of *cyp7a1*. Without the binding of *LRH-1*, the transcription of *cyp7a1* is downregulated. FXR also represses apolipoprotein AI (*ApoAI*) transcription, hence reduces the efflux of cholesterol from extrahepatic tissues and their transfer to the liver. In the small intestine, FXR upregulates the heterodimer ABC transporters, (*ABCG5/G8*) hence lowers the reabsorption of cholesterol. Adapted from (Sinal et al. 2000).

1.3. Experimental tools to study bile acid secretion

Hepatocytes secrete bile into the canalicular lumen, a minute space of 0.75μm in diameter form by apposing membranes of two adjacent hepatocytes (Watanabe et al. 1991). Tight junction complexes are considered to be the blood-biliary barrier that are functionally leaky and permit paracellular exchange of certain solutes between plasma and bile (Lowe et al. 1988). Micelle forming bile acids such as taurocholate do not efflux from the biliary tree when permeability is increased suggesting that there is selectivity in this pathway (Hardison et al. 1991). Therefore, the major pathway for bile acid secretion is postulated to involve a transcellular entry into bile.

A number of *in vivo* and *in vitro* techniques have been devised over the years to study the physiological characteristics of bile secretion. Experimentally, canalicular bile cannot be directly sampled due to an inability to access the canalicular space. Therefore, canalicular bile is collected from the common bile duct or gallbladder in intact animal or isolated perfused liver preparations. The bile collected from these sources have been concentrated and modified from solutes secreted by cholangiocytes (Hofmann 1999). Nevertheless, these techniques are useful for routine quantitation of bile secretion (Dietmaier et al. 1976; Poupon et al. 1988; Deroubaix et al. 1991).

The dissociation of liver tissue into isolated cells suitable for culture has been described over 30 years ago (Berry and Friend 1969). The loss of structural polarity and mixing of membrane domains, however, made them poor models for mechanistic studies. Therefore, improvements in the isolation method to yield functional units of liver cells are required for studies of polarity and bile formation. This is achieved using optimized collagenase perfusion conditions to isolate hepatocytes that are attached as couplets and retained membrane polarity and secretory function (Gautam et al. 1987; Boyer et al. 1990). Hepatocyte couplets are pairs of adjoining hepatocytes that are formed during culture that have functional active bile canaliculi. Hepatocyte couplet model system has certain advantages for studying bile acid secretion than in whole animal or in liver perfusion. The couplet can be viewed as a 'mini-liver' that has the secretory polarity and a canalicular vacuole that represents the functional equivalent of the bile canaliculus of the intact liver

(Boyer 1997). In rat hepatocyte couplet system, fluorescent derivatives of bile acids are secreted into canalicular lumens of active couplets (Weinman et al. 1989; Kitamura et al. 1990a; Boyer and Soroka 1995).

Further advances in understanding of transport processes and their driving forces have been made using functional plasma membrane vesicles that are selectively enriched in either canalicular membranes or basolateral membranes from hepatocytes. An essential requirement for detailed studies of transport processes and their driving forces is the availability of substantial amounts of purified, functionally active membrane vesicles from specific domains of the liver cell. This goal has been achieved using a combination of isopycnic density gradient and rate sedimentation centrifugations procedures (Evans 1980; Inoue et al. 1984, Meier, 1984 #1008). In practice, the most successful and best-documented examples are defined by the specific plasma membrane subfraction preparations from rat liver (Inoue et al. 1982; Inoue et al. 1983a; Inoue et al. 1983b; Meier et al. 1984b). These highly purified membrane vesicles have allowed researchers to investigate the molecular components characteristic of each of the membrane domains and the specific mechanisms of hepatic transport at these cellular fronts.

1.4. Transport processes in the liver

The liver hepatocytes take up conjugated hydrophilic bile acids from the portal vein via the sodium-dependent bile acid transporter (Ntcp) (Boyer et al. 1994; Hagenbuch and Meier 1994). In addition, the organic anion transporting polypeptides (Oatps) take up unconjugated secondary bile acids (Jacquemin et al. 1994; Meier et al. 1997). The uncharged free bile acids can enter the hepatocytes by passive diffusion. Bile acids are trafficked from the basolateral membrane to the canalicular membrane via undefined processes. These processes may involve binding to cytosolic proteins or transported via vesicles (Crawford et al. 1988; Stolz et al. 1989).

The liver metabolizes many endogenous compounds including bile acids, phospholipids, cholesterol, bile pigments and exogenous compounds, such as drugs. Oxidative metabolism and conjugation to amino acid followed by biliary excretion are

common routes of elimination of these metabolites. These compounds are hydrophobic or amphipathic with molecular weights in excess of 400Da. These organic compounds also have a large concentration gradient between the hepatocyte and the bile (up to 1:100 to 1:1000), suggesting that the bile canalicular membrane may contain concentrative and active transport processes for these substrates. Early studies identified a potential sensitive facilitated diffusion pathway in liver cells (Graf et al. 1987; Weinman et al. 1989). In isolated membrane vesicles, bile acids can be transported via a saturable, electrical potential driven process (Meier et al. 1984a; Meier et al. 1987). This suggests that *in vivo* a measurable intracellular negative electrical potential of –25mV to –35mV which is generated by the sodium pump in the basolateral domain of hepatocytes and by an outward potassium conductance, is the primary driving drive for canalicular bile acid secretion (Graf et al. 1987; Weinman et al. 1989). However, based on theoretical calculation, the potential across the canalicular membrane could accumulate bile acids 3 to 4-fold within the bile, more than 25-fold lower than the expected concentration gradient. Thus, the membrane potential cannot be the only driving force for the movement of bile acids across the canalicular membrane. Additional driving forces are thus required for bile acid secretion.

1.5. ABC transporters: an overview

There is increasing evidence that ATP-Binding Cassette (ABC) transporters present on the bile canalicular membrane are responsible for the transport of a number of liver metabolites. The liver hepatocytes are enriched with a number of ABC transporters. Immunostaining studies have localized at least 14 ABC proteins to the apical/canalicular/lateral plasma membrane domain of liver hepatocytes (Table 3 and 4). Fig. 4 illustrates the presence of different ABC transporters in the two different domains of a liver hepatocyte. ABC transporters (Mrp3, Mrp4, Mrp5, Mrp6 and Abca1) are localized to the basolateral membranes (reviewed in (Borst et al. 2000)). These transporters are not as well studied in terms of their transport functions. Some have been demonstrated to transport organic anions. For example, Mrp3 that is localized to the basolateral membrane has been shown to transport bile acids and other organic anions *in vitro* (Hirohashi et al. 2000; Zelcer et al. 2003b). A number of ABC transporters are localized in the canalicular membrane including Mrp2, Spgp, Pgp1 (Mdr1a), Pgp2 (Mdr1b), Pgp3 (Mdr2), Abcg5, Abcg8 and

Abcg2 (Table 3 and 4). These proteins have been postulated to transport organic anions, bile acids, amphipathic drugs, phospholipids and phytosterols. The physiological functions of some of these proteins have been supported by knockout mice studies and mutations in human diseases and will be discussed further below.

ABC proteins represent the largest family of transmembrane proteins in prokaryotes, eukaryotes and archaebacteria (Higgins 1992; Childs and Ling 1994). In the human genome, there are 48 ABC transporters identified and many have been associated with human diseases[1]. ABC proteins are recognized by the presence of highly conserved amino acid sequences of the Walker motifs (Walker A and B) and a "signature" sequence in between the Walker motifs in the ATP-binding sites. An ABC transporter consists of two types of domains, a hydrophobic transmembrane domain (TMD) made up of usually six putative membrane spanning helices and a cytoplasmic nucleotide-binding domain (NBD). The TMD shares little if any homology among all the ABC members and has been suggested to form a transmembrane pore for substrate translocation (Rosenberg et al. 1997). NBD appears to be universally conserved in function. For example, the two NBDs are required for ATP hydrolysis during the catalytic cycle of Pgp transport (Urbatsch et al. 1995).

[1] An inventory of all the known human ABC transporters can be found on the website of M. Muller, University of Wageningen, The Netherlands. (http://www.nutrigene.4t.com/humanabc.htm).

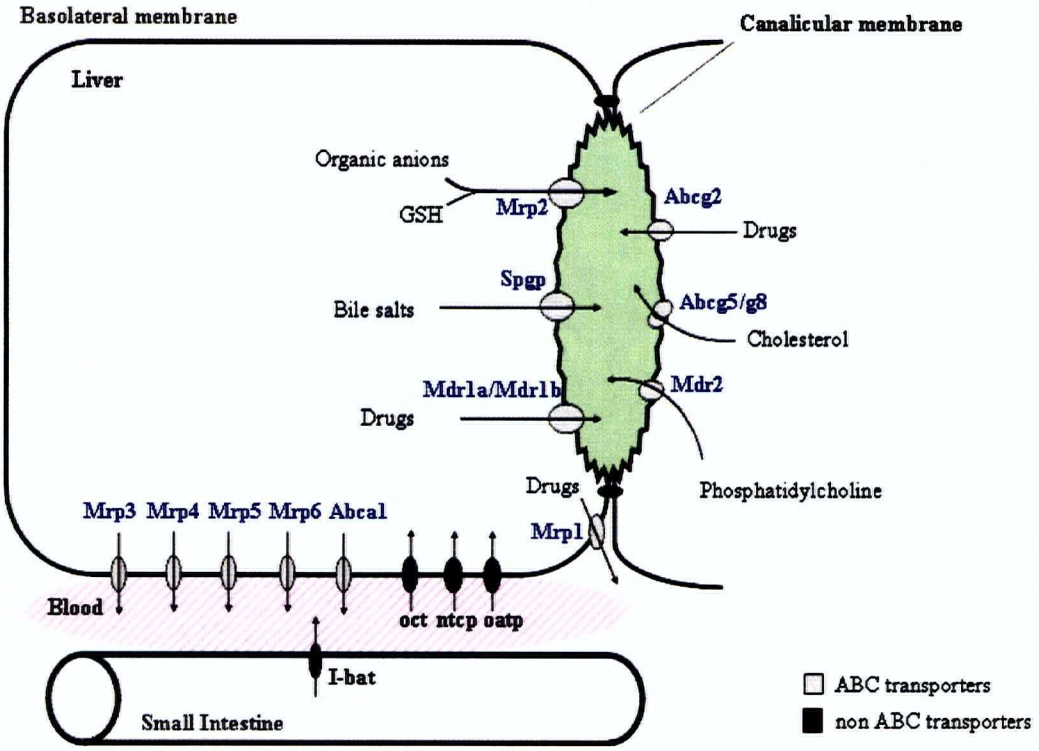

Fig. 4. Canalicular and basolateral transporters involved in hepatobiliary transport.

1.6. ABC transporters in the liver

Some ABC proteins are expressed exclusively in the liver while others are more ubiquitously expressed (Table 3 and 4). With respect to ABC transporters implicated in bile formation, four subfamilies of proteins have been identified to date: ABCA, the Pgps (ABCB subfamily), Mrps (ABCC subfamily), and ABCG subfamily[2]. At least four of these transporters from different subfamilies including Mdr1a (ABCB1), Mdr1b (ABCB1), Mrp2 (ABCC2) and ABCG2 have been demonstrated to exhibit broad substrate specificity (Table 3 and 4). Their substrate transport specificities are consistent with the idea that they have protective roles in the liver and other tissues. Some of these transporters have been shown to transport natural compounds of the liver and will be discussed in sections 1.6.1, 1.6.2 and 1.6.3. Some liver ABC proteins exhibit narrow substrate specificity, and appear to be more specialized in their functions, transporting only one specific type of substrates such as phosphatidylcholine secretion carried out by Mdr2 (Smit et al. 1993).

1.6.1. Drug and lipid transport by multidrug resistance P-glycoprotein

The multidrug resistance (MDR) gene product, P-glycoprotein (Pgp) is the earliest ABC transporter that has been discovered in multidrug-resistant cell lines. Resistance in Pgp overexpressing cell lines is demonstrated by the ability to efflux many classes of chemotherapeutic drugs from the cells thereby lowering the effective concentration inside the cell (Ambudkar et al. 1999). Today, there is solid evidence supporting the model of Pgp as an ATP-dependent drug efflux pump. In isolated membrane vesicles or in biochemically-reconstituted proteoliposomes, Pgp has been demonstrated to transport many structurally different substrates that include anticancer drugs, xenobiotics, peptides, steroids, and fluorescent dyes (Shapiro and Ling 1995; Sharom 1995).

Pgp is present not only in tumor cells but also in normal tissues including the kidney, liver, small and large intestine, brain, testis, adrenal gland, and the pregnant uterus (Georges et al. 1990). The function of Pgp has been investigated in normal rat liver using canalicular

---

[2] All human and mouse ABC genes have standard nomenclature shown in brackets, developed by the Human Genome Organization (HUGO) at a meeting of ABC gene researchers.

and basolateral membrane vesicle preparation. Pgp has been localized exclusively to the rat liver canalicular membrane and not detected in basolateral membrane (Arias 1990). ATP-dependent transport of daunomycin has been demonstrated in the canalicular membrane but not in basolateral membrane (Kamimoto et al. 1989; Sinicrope et al. 1992). Transport is ATP-dependent, temperature-dependent, osmotically sensitive, and saturable. Hydrophobic bile acids and progesterone inhibit daunomycin transport noncompetitively while non-bile acid organic anions such as glutathione conjugates do not inhibit transport demonstrating substrate specificity of the transporter (Kamimoto et al. 1989; Sinicrope et al. 1992). Pgp mediated daunomycin transport has also been observed in rat jejunal and ileal brush border membrane vesicles (Hsing et al. 1992). These studies in normal rat tissues demonstrate that Pgp can transport drugs from epithelial cells into bile, urine or intestine lumen. A possible role of Pgp is in the excretion of naturally occurring toxins and commonly encountered xenobiotics.

The physiological function of the two MDR isoforms remains unanswered. Mice with *mdr1a* or *mdr1b* null mutation are viable and normal in a laboratory environment (Schinkel et al. 1994; Schinkel et al. 1995). When challenged, Pgp appears to serve as a defense mechanism against amphipathic xenotoxins in the gut mucosa, blood-brain barrier, testis and other blood-tissue barriers (Schinkel et al. 1994; Schinkel et al. 1995; van Asperen et al. 1996; Schinkel et al. 1997; Smit et al. 1998a). Whether MDR1 plays a role in bile formation is not understood, as there are no observable changes of bile composition in these mutant mice (Schinkel et al. 1994).

Mdr2 does not confer multidrug resistance in tumour cells and has no demonstrated drug-pumping activity (Buschman and Gros 1994). Its physiological role in the liver is postulated with observations of *mdr2* knockout mice (Smit et al. 1993). *Mdr2*$^{-/-}$ mice developed a liver phenotype associated with defect in phospholipid transport across the canalicular membrane into bile. In *mdr2*$^{-/-}$ mice, the bile lack phospholipid. Biliary secretion of taurocholate is normal, secretion of glutathione is reduced and secretion of chloride is enhanced. The liver pathology is bile ductular proliferation (Smit et al. 1993). .It is postulated that phospholipids in bile form mixed micelles and serve to reduce the detergent

action of bile acids and thereby protect the epithelium of bile ductules and ducts. A surplus of free bile acids may lead to damage of liver canalicular membrane and membranes of bile ducts associated with bile duct proliferation (Leveille-Webster and Arias 1994; Mauad et al. 1994). Phospholipid flippase activity has been demonstrated in bile canalicular membrane (Nies et al. 1996). Mdr2 expressed in yeast secretory vesicles also mediate phosphatidylcholine flippase activity. Transport requires hydrolyzable ATP and is inhibitable by vanadate and verapamil (Ruetz and Gros 1994).

1.6.2. Organic anion secretion by Multidrug resistance associated transporters (Mrp)

The liver secretes a variety of organic anions other than bile acids into bile. These include estradiol-17-β-glucuronide, leukotriene C_4, glucuronide conjugates of bilirubin, and conjugates of hydrophobic bile acids such as lithocholate (Konig et al. 1999a). As with bile acids, the liver/bile concentration gradients of these organic anions are not accounted for by the transmembrane potential difference of -35mV. Studies in canalicular membrane vesicles indicate that these anions are secreted via an ATP-dependent mechanism distinct from that by which bile acids are secreted (Ishikawa et al. 1990; Kobayashi et al. 1990). The identity of the molecular mechanism mediating the ATP-dependent transport of these organic anions was facilitated by the discovery of jaundiced mutant rats in two different strains, Wistar (TR^-) and Sprague-Dawley (EHBR) (Jansen et al. 1985; Hosokawa et al. 1992). Biliary secretion of cholate 3-O-glucuronide, taurochenodeoxycholate-3-sulfate (TLDC-S) and taurolithocholate-3-sulfate (TLC-S), GSH conjugates of sulphobromophthalein (BSP), dinitrophenol (DNP) and leukotriene C_4 are impaired in these deficient rats (Elferink et al. 1989; Kuipers et al. 1989; Sathirakul et al. 1993; Takikawa et al. 1995). Canalicular membrane vesicles from TR^- and EHBR rats lack ATP-dependent transport of many non-bile acid organic anions but not taurocholate or Pgp substrates (Kitamura et al. 1990b; Nishida et al. 1992a; Nishida et al. 1992b). A number of studies have demonstrated Mrp2-mediated transport of organic anions and supports the concept that Mrp2 represents the canalicular multispecific organic anion transporter (cMOAT) of mammalian liver (Leier et al. 1994; Madon et al. 1997).

Another member of the ABC protein, Mrp3 has been demonstrated to transport monovalent bile acids such as taurocholate and glycocholate (Hirohashi et al. 2000). Mrp3 is localized to the basolateral membrane of the liver, cholangiocytes and intestinal epithelium. Under cholestatic conditions, basolateral bile acid efflux can compensate partly for the disrupted canalicular bile acid secretory pathway. This is supported by evidence of upregulation of Mrp3 expression in rat liver during obstructive cholestasis (Ortiz et al. 1999; Soroka et al. 2001), in Mrp2-deficient transport mutant rat strains (Hirohashi et al. 1998), and in liver of patients with Dubin-Johnson syndrome, a human disease caused by Mrp2 deficiency (Paulusma et al. 1996; Konig et al. 1999b).

Table 3. Transport processes in primary bile formation

Superfamily	Gene Product	Species	Tissue Expression	Associated Diseases	Typical substrates/ Physiological substrate	References
ABC sub-family B	MDR1 mdr1a/1b (ABCB1)	Human Rat Mouse	Ubiquitous Blood-brain barrier	Multidrug resistance	Amphiphatic cationic compounds/ Phospholipids? Steroids? Glycosylceramide? Platelet activating factor?	(Schinkel et al. 1994; Schinkel et al. 1995; Smit et al. 1998a; Smit et al. 1998b)
	MDR3 mdr2 (ABCB4)	Human Rat Mouse	Liver	PFIC3 – cholestasis	Phosphatidylcholine	(Jacquemin, 2001; Smit et al. 1993)
	BSEP Bsep (ABCB11)	Human Rat Mouse	Liver	PFIC2 – cholestasis	Monovalent bile acids	(Strautnieks, 1998; (Gerloff et al. 1998)
ABC sub-family C	MRP2 Mrp2 (ABCC2)	Human Rat	Liver, intestine and kidney	Dubin-Johnson Syndrome	Anionic conjugates with GSH, glucuronate, or sulfate. E17βG, LTC_4, GSSH	(Jansen et al. 1985; Kitamura et al. 1990b; Paulusma et al. 1996)
ABC subfamily G	ABCG2	Human	Placenta, breast, liver, endothelium	Multidrug resistance/Drug hypersensitivity	Amphipathic drugs	(Doyle et al. 1998)
	ABCG5/G8	Human	Liver, intestine	Sitosterolemia	Plant sterols, cholesterol	(Berge et al. 2000; Lee et al. 2001)

Table 4. Transport processes in liver basolateral membrane.

Superfamily	Gene Product	Species	Tissue expression	Associated Diseases	Driving Force	Typical substrates/ Physiological substrates	References
ABC sub-family C	MRP1 Mrp1 (*ABCC1*)	Human Rat	Ubiquitous	Multidrug resistance	Primary ATP-dependent	Same as MRP1 and probenecid	(Keppler et al. 1998)
	MRP3 Mrp3 (*ABCC3*)	Human Rat Mouse	Liver, bile ducts, gut, adrenal cortex	-	Primary ATP-dependent	Organic anions including conjugated bile acids	(Hirohashi et al. 2000)
	MRP4 Mrp4 (*ABCC4*)	Human Rat Mouse	Many tissues	-	Primary ATP-dependent	Nucleotide analogs, organic anions	(Reid et al. 2003; Zelcer et al. 2003a)
	MRP5 (*ABCC5*)	Human Rat Mouse	Ubiquitous	-	Primary ATP-dependent	Nucleotide analogs, organic anions	(Reid et al. 2003)
	MRP6 (*ABCC6*)	Human Rat Mouse	Kidney, liver	Pseudo-xanthoma elasticum		BQ-123 (an acidic peptide)	(Belinsky et al. 2002)
Solute carrier family 10	NTCP Ntcp	Human Rat	Liver hepatocyte		Secondary, Na+ gradient	Conjugated bile acids	(Boyer et al. 1994; Hagenbuch and Meier 1994)
Solute carrier family 22	OATP1 Oatp1	Human Rat	Liver hepatocyte		Na+ independent	Unconjugated and conjugated bile acids, uncharged compounds, charged bulk organic cations	(Jacquemin et al. 1994; Meier et al. 1997)
	OATP2	Human Rat	Basolateral membrane		Na+ independent	Bile acids, LTC_4, thyroid hormones, conjugated steroids (E17βG), statins	(Noe et al. 1997; Reichel et al. 1999)

1.6.3. Role of Sister of P-glycoprotein in liver function

Using a low stringency screening strategy, Childs *et al.*, (Childs et al. 1995) has isolated a partial sequence of a novel gene that is most closely related to Pgp, thus named sister of P-glycoprotein (Spgp). Full-length amino acid analysis of human Spgp reveal high similarity to two other members of the ABC superfamily that included class I (MDR1), and class III Pgp (MDR3) (Childs et al. 1995; Childs et al. 1998). Rat Spgp shares 70% similarity and 50% amino acid identity with the Class I Pgp (Table 5). The sequence of the putative TMD is highly variable between the two proteins suggesting that they may have different substrate specificity. On the other hand, substrate preference may be imposed by yet undefined structural motifs that allow Pgp and Spgp to transport the same substrate(s).

Table 5. Sequence comparison of human Sister of P-glycoprotein (BSEP) with other ABC transporters

ABC Protein	Gene Code	Amino Acids	Identity
SPGP/BSEP (human)	*ABCB11*	1321	100 %
SPGP/BSEP (mouse)	*ABCB11*	1321	71.6 %
SPGP/BSEP (rat)	*ABCB11*	1321	82.1 %
ABCB1/MDR1 (human)	*ABCB1*	1280	51.0 %
ABCB5 (human)	*ABCB5*	EST sequence	53.3 %*
ABCB4/MDR3 (human)	*ABCB4*	1279	49.9 %

* only 812 amino acids have been sequenced to date (Frank et al. 2003).

The liver-specific expression of Spgp is reminiscent of the expression pattern of class III Pgp (Mdr2). Both are highly expressed in the bile canalicular membrane of hepatocytes (Buschman et al. 1992; Childs et al. 1998). In the rat liver, the mRNA level of *spgp* and *mdr2* are approximately equivalent. In normal rat liver and freshly isolated rat hepatocytes, *mdr2* and *spgp* have predominant expression. *Mdr1a* is expressed at lower level and *mdr1b* is barely detectable by RT-PCR (Childs 1995). The expression of *spgp* occurs late in liver development. *Spgp* mRNA is transcribed at low but detectable levels in 18 and 21-day rat

embryo, but is upregulated to adult liver levels by one day after birth (Childs et al. 1998; Tomer et al. 2003). The expression of *spgp* in late liver development is also consistent with its function in bile formation, a process that matures during the first few weeks of life (Suchy et al. 1987). *Spgp* gene is distinct from the *pgp* multigene family and has been found as an independent gene in species as distant as chicken, turtle, skate and winter flounder (Gerloff et al. 1998; Ballatori et al. 2000; Cai et al. 2001). This indicates that Spgp may have acquired a more specialized function in the liver that is conserved in evolutionary distant vertebrates. Although the expression of *spgp* in normal adult liver is relatively high, its expression in hepatocyte cultures and hepatoma cell line is downregulated to low level limiting the use of these cells lines for functional studies of Spgp (Childs et al. 1998).

A question is raised, based on the high similarity between Pgp and Spgp would be: Does Spgp exhibit MDR profile, i.e. cross-resistance to unrelated cytotoxic drugs? Childs *et al* (Childs et al. 1998) has studied the drug resistance profile in *spgp* transfected SKOV (human ovarian) cells and has showed that most of the drugs tested except taxol, were still cytotoxic. Furthermore, the Pgp inhibitors, SDZ-PSC 833 and verapamil can reverse the transfected cells' resistance to taxol. Work done by Lecureur *et al.* (Lecureur et al. 2000) revealed that Spgp in transfected cells also transport only a few of the many Pgp substrates such as vinblastine. These studies suggest that Spgp is a more discriminating drug transporter than Pgp.

Rat *spgp* gene express in *Xenopus laevis* oocytes results in a 1.5 fold higher ^{3}H-taurocholate efflux (Gerloff et al. 1998). In addition, membrane vesicles from transfected Sf9 insect cells confer a 5-fold stimulation of ATP-dependent taurocholate transport with a Km of 5.3 μM (Gerloff et al. 1998). The relative rates of bile acid transport and specificity mediated by rat and human Spgp, is in the order of taurochenodeoxycholate > tauroursodeoxycholate = taurocholate > glycocholate = cholate (Gerloff et al. 1998; Noe et al. 2002). These rates are comparable to ATP-dependent transport of taurocholate in rat liver plasma membrane vesicles (Stieger et al. 1992). These observations provide the first *in vitro* evidence of the role of Spgp in bile acid transport. Recent papers also confirm that human and mouse Spgp exhibit comparable bile acid transport kinetics suggesting that Spgp

has similar substrate specificity and transport efficiency in different species (Gerloff et al. 1998; Green et al. 2000; Byrne et al. 2002; Noe et al. 2002).

1.7. Sister of P-glycoprotein in cholestasis

In humans, mutations in *spgp* cause a human liver progressive cholestatic disease, known as progressive familial intrahepatic cholestasis, type 2. Progressive familial intrahepatic cholestasis (PFIC) is a heterogeneous group of pediatric cholestatic liver diseases of which three types have been identified based on molecular abnormalities (Bull et al. 1997; Strautnieks et al. 1997; de Vree et al. 1998; Jansen and Muller 1998; Strautnieks et al. 1998). In 1994, fewer than 100 cases meeting the general description of PFIC have been reported (Whitington et al. 1994). PFIC manifests early onset in infancy, and progresses rapidly to liver failure and patients survive only with liver transplantation (Luketic and Shiffman 1999; van Mil et al. 2001; Lykavieris et al. 2003). The diagnosis of these rare disorders includes accumulation of bile acids and/or their precursors in serum and urine. Common clinical features include pruritus, jaundice, malnutrition, growth retardation, rickets, progressive liver damage leading to cirrhosis and liver failure. Liver histology is consistent with intrahepatic cholestasis with only slight bile duct proliferation, a sign of extrahepatic damage (Luketic and Shiffman 1999; van Mil et al. 2001; Lykavieris et al. 2003). Today, the molecular basis for some of these cholestatic syndromes has been identified (reviewed in (Jacquemin 2000; Jansen and Muller 2000; Thompson and Jansen 2000; Elferink and Groen 2002). All the diseases appear to be direct consequences of transporter defects (Table 6). Identification of these molecular defects has led to functional studies of their role in normal cell. From the clinical standpoint, these molecular defects can now be used as a molecular tool for the diagnosis of subcategories of PFIC.

Table 6. Molecular defect of transporter proteins in progressive familial cholestatic liver disease.

Disorder	Defect	Transporter Function	Genetic Localization
PFIC1 (Byler's)	Fic1	Aminophospholipid transport	18q21-22
PFIC2	Spgp	Bile acid transport	2q24
PFIC3	Mdr3	Phospholipid flippase	7q21

PFIC1 arises from mutations of the *FIC1* or *ATP8B1* gene is located on chromosome 18q21-22 (Carlton et al. 1995; Bull et al. 1997; Bull et al. 1998). The biochemical features resemble those of PFIC2, with elevated serum bile acid levels and severely impaired bile acid secretion (Lykavieris et al. 2003). How mutations in this protein cause cholestasis is unclear. The gene encodes a P-type ATPase with unknown function. P-type ATPases belong to a large gene family mainly encoding ion transport pumps such as Na^+/K^+ ATPase, Ca^{2+} ATPase, and the copper transporting Wilson protein ATP7B (van Mil et al. 2001). FIC1 is highly expressed in cholangiocytes, pancreas, small intestine, urinary bladder, stomach and prostate (Eppens et al. 2001; Ujhazy et al. 2001; Harris and Arias 2003). Transient transfection with FIC1 cDNA mediates ATP-dependent phosphatidylserine (PS) translocation in cells. In canalicular membrane vesicles, translocase activity is demonstrated with an initial velocity of 3.3 nmol/min/mg protein PS translocated and a K(m) (ATP) = 1.2 mmol/L. The translocase activity is inhibited by vanadate, N-ethylmaleimide, sodium azide, and calcium; and is unidirectional (i.e., from the outer to the inner canalicular plasma membrane leaflet). These studies indicate that FIC1 is a canalicular P-type ATPase that participates in maintaining the distribution of aminophospholipids between the inner and outer leaflets of the plasma membrane (Ujhazy et al. 2001).

The PFIC2 locus on chromosome 2q24 has been identified in a genome-wide screening of six consanguineous Middle Eastern families (Strautnieks et al. 1998). The disease has autosomal recessive inheritance and is usually fatal within adolescence life. The primary defect in bile acid secretion leads to malabsorption of fats, fat-soluble vitamins and essential fatty acids resulting in growth defects, hepatic failure, ultimately leading to biliary

fibrosis, cirrhosis and death (Jansen and Muller 1998; Jansen et al. 1999). Somewhat distinct features may be recognized in PFIC2 patients including low serum levels of primary bile acids, low to normal γ-glutamyltransferase (γ-GT), elevated serum liver enzymes, and appearance of amorphous or filamentous bile as seen by transmission electron microscopy (Alonso et al. 1994; Whitington et al. 1994; Jansen et al. 1999; Cabrera-Abreu and Green 2002; Chen et al. 2002). The evidence is compelling that *spgp* mutations caused PFIC2 in children. More than ten different mutations in *spgp* have been reported, ranging from missense mutations, frameshift mutations to premature stop codon (Strautnieks et al. 1998). In patients, *spgp* mutations correlate with lack of Spgp canalicular staining and a dramatic reduction of bile acid concentration in bile (<1% of normal in 9 tested patients) (Jansen et al. 1999). PFIC2 missense mutations has been studied in rat *spgp* transfected insect cells and found to result in improper targeting of the protein or loss of bile acid transport activity *in vitro* (Wang et al. 2002).

Patients with PFIC3 have different clinical and histological characteristics than those observed in other PFICs. A marked elevation in serum γ-GT and extensive bile duct proliferation is the hallmarks of PFIC3. Human PFIC3 is caused by mutations in the *mdr2* gene resulting in defects in biliary phosphatidylcholine (PC) secretion (de Vree et al. 1998; Jacquemin 2001). The pathology of PFIC3 patients is similar to that seen in the *mdr2*$^{-/-}$ mouse model. In *mdr2* null mice (an analog of human MDR3) (Smit et al. 1993), bile acid secretion is normal. The high bile acid concentration in the absence of phospholipids is believed to damage the canalicular membrane of hepatocytes and small bile ducts, resulting in extensive bile duct proliferation (Smit et al. 1993).

1.8. Regulation of Spgp expression

Regulation of *spgp* expression helps to prevent intracellular accumulation of toxic bile acids, and to maintain biliary flow for ongoing hepatic clearance. Spgp is regulated at the transcriptional level by bile-acid activation of farnesoid X receptor (FXR). FXR belongs to a class of nuclear receptors that form heterodimers, which bind to promoter elements and induce gene expression. These proteins contain a central DNA-binding domain consisting of a zinc finger module and a large ligand-binding domain with a lipophilic core that binds

specific small lipid molecules (Laffitte et al. 2000). Human *bsep/spgp* promoter is regulated by concentration-dependent FXR binding after bile acid activation. Reducing endogenous FXR levels using RNA interference fully represses bile acid-activated *spgp* expression (Plass et al. 2002). The promoter region of human and rat *spgp* has been sequenced and studied (Gerloff et al. 2002; Plass et al. 2002). The gene can be transcriptionally regulated by a number of endogenous compounds and xenobiotics. Hydrophobic bile acids such as chenodeoxycholic acid, deoxycholic acid and lithocholic acid, as well as the anti-estrogen, tamoxifen stimulated *spgp* promoter activity, while the estrogen β-estradiol and rifampicin antibiotics suppress the activity (Gerloff et al. 2002).

1.8.1. Spgp expression in various cholestatic models

Spgp mRNA and protein levels are maintained in obstructive, ethinylestradiol (EE) and endotoxin-induced cholestasis (Lee et al. 2000; Wagner et al. 2003). After partial hepatectomy, the mRNA and protein level of Spgp is only slightly affected suggesting that a minimal level of Spgp is required for normal liver function (Gerloff et al. 1999). Bile acid feeding in mice, rats and rabbits leads to upregulation of *spgp* at the mRNA and protein levels, while bile acid depletion by biliary diversion is associated with downregulation (Fickert et al. 2001; Wolters et al. 2002; Xu et al. 2002; Zollner et al. 2003a). These studies indicate that *spgp* expression is sensitive to the flux of bile acids through the hepatocyte.

1.8.2. Posttranslational modifications and effects on Spgp function

As described in section 1.8.1, to meet the constant demand of biliary secretion of bile acids, *spgp* gene expression may be maintained by bile acid feedback transcriptional regulation. In addition to being in the canalicular membrane, immunostaining patterns of Spgp suggest that additional Spgp may also reside in subcanalicular vesicular pools (Gerloff et al. 1998). Spgp has been demonstrated to be sequestered in intracellular pool prior to trafficking directly from Golgi to the canalicular membrane (Kipp and Arias 2000; Kipp et al. 2001). The recruitment and direct stimulation of Spgp mediated activity have been demonstrated to be dependent on cAMP, taurocholate, phosphoinositide 3-kinase (PI-3 kinase) activity and its PI-3 kinase generated lipid products (Misra et al. 1998; Misra et al.

1999; Kipp et al. 2001). Further observations have been made on this dynamic process of Spgp turnover in the canalicular membrane and its intracellular pools. *In vitro*, acute adaptation of Spgp mediated bile acid transport can occur via rapid insertion of Spgp into or retrieval from the canalicular plasma membrane. Rapid insertion of Spgp into the canalicular membrane is stimulated by hypoosmotic swelling (Schmitt et al. 2001) or by infusion of taurocholate (Misra et al. 1998). Spgp is phosphorylated by protein kinase C *in vitro* but the role of phosphorylation on bile acid transport activity has not been examined (Noe et al. 2001).

1.9. Disruption of *spgp* gene in mice and effect on biliary secretion

To gain further insight into the role Spgp plays in bile acid secretion and to understand how Spgp deficiency affects bile acid and cholesterol homeostasis, a line of mice deficient in *spgp* has been created by gene targeting method (Wang et al. 2001). The mouse is a useful experimental model for studies of liver physiology, including bile flow, and canalicular bile acid output. Ablation of the *spgp* gene in the mouse provides an animal system to study how its absence affects liver physiology. It was believed that *spgp* $^{-/-}$ mice phenotype would be lethal or severely compromised, but this proved not to be the case.

1.9.1. Phenotype of *spgp* $^{-/-}$ and ultrastructural analysis

Spgp$^{-/-}$ mice are viable and fertile and do not develop advance cholestasis that characterizes PFIC2. Heterozygotes cross with homozygous mice produce litters with the predicted Mendelian distributions, indicating that prenatal death did not occur in the null pups. Table 7 compares the differences in phenotype between human PFIC2 and *spgp* $^{-/-}$ mice. Null pups are observed to be weaker during the first week of life. Once a deficient animal reaches the age of ~ 2 weeks, survival and weight gain dramatically improve such that adult animals are outwardly indistinguishable from wildtype mice. Mean body weight at weaning (21 days after birth) of *spgp* $^{-/-}$ mice is about 80% of wildtype mice. Serum liver biochemistry is not significantly different between wildtype and *spgp*$^{-/-}$ mice. Contrary, serum liver enzyme activities such as alkaline phosphatase, 5'-nucleotidase, and

transaminases are markedly elevated in PFIC2 patients (Jansen and Muller 1998; Jansen et al. 1999; Chen et al. 2002).

Table 7. Comparison of the phenotype of *spgp*-/- mice with human progressive familial intrahepatic cholestasis type 2

	Human PFIC2	Mouse *spgp* knockout
Phenotype	Disease progression is quick (first decade) to liver failure before adulthood Jaundice, bleeding, pruritus, malnutrition, steatorrhoea, osteodystrophy and growth failure, and fat-soluble vitamin deficiency	Viable, non-progressive Body weight is 20% lower than wildtype Liver size is enlarged to 2-fold of wildtype
Serum Biochemistry	low to normal γ-glutamyltransferase activity	Normal serum liver enzyme activities
Histological Findings	Bile canaliculi widened containing amorphous or filamentous bile Severe fibrosis, cirrhosis, hepatitis	Dilated canaliculi, partial loss of microvilli, steatosis Normal organelles with increased number of peroxisomes
Treatment	Ursodeoxycholic acid therapy not effective Liver transplantation	

This table summarizes major findings of two papers (Strautnieks et al. 1998; Wang et al. 2001).

Ultrastructural findings in liver tissues of *spgp* $^{-/-}$ mice reveal dilation of canalicular lumen, partial loss of microvilli and retained biliary material using transmission electron microscopy (Wang et al. 2001). These pathological findings of *spgp*$^{-/-}$ mice liver are consistent with a mild cholestatic phenotype. In core needle biopsies of liver from infants with PFIC2, pathologists identified "neonatal hepatitis" with ultrastructural changes including absence of microvilli, canalicular lumen dilated and distinctive amorphous bile (Knisely 2000). The liver histological features worsen as the disease progresses. In one

PFIC2 patient, the liver section showed lobular disarray, marked giant cell transformation, and cell necrosis accompanied by pericellular fibrosis (Chen et al. 2002).

At first, the mild phenotype in *spgp*$^{-/-}$ mice is unexpected. In retrospect, the striking difference in the outcome between human and mice without *spgp* may not be as surprising as has been suggested by Hofmann (Hofmann 2001). The physiological process of bile flow relies on two components, a bile acid-dependent component and a bile-acid independent component largely contributed by the secretion of other organic anions. It seems that humans depend more on bile-acid dependent component while rodent are more bile-acid independent (Wang et al. 1997). Hence, the magnitude of the effect will be more significant in humans when *spgp*, which contributes to the bile acid-dependent bile flow, is disrupted. Humans have a relatively hydrophobic bile acid pool when compared to rodents. As a consequence, disruption of *spgp* possibly resulting in accumulated bile acids in vital tissues like liver and intestine will pose a greater toxicity in humans compared to rodents.

1.9.2. Alterations in bile acid secretion and composition in *spgp*$^{-/-}$ mice

Spgp$^{-/-}$ mice are distinguished from wildtype mice by hepatomegaly (about 2 times larger in *spgp*$^{-/-}$ mice), elevated serum and liver bile acid level (4-fold and 5-fold respectively) and reduced biliary bile acid (4-fold). Infused individual conjugated cholic acid (taurocholate or glycocholate) is poorly excreted in *spgp*$^{-/-}$ mice. Table 8 shows the distribution of different bile acid species of human PFIC2 and *spgp*$^{-/-}$ mice bile. In *spgp*$^{-/-}$ mice bile, the amount of biliary cholic acid is reduced by 17-fold. An unusual amount of muricholic acids and atypical bile acid species, tetrahydroxylated bile acid (18% of total biliary bile acids) in bile of *spgp*$^{-/-}$ mice have been detected (Wang et al. 2001). Several investigators have reported the presence of tetrahydroxylated bile acids in human cholestatic diseases (Bremmelgaard and Alme 1980; Whitington et al. 1994; Whitington 1996; Setchell et al. 1997) and also in healthy neonates (Strandvik and Wikstrom 1982; Nemeth and Strandvik 1984). Increased hydroxylation in rodents has also been observed following administration of toxic monohydroxylated bile acids (Yousef et al. 1997) and after bile duct ligation (Greim et al. 1972). Hydroxylation of bile acids in the *spgp*$^{-/-}$ mice is consistent with a cholestatic phenotype. However, presence of tetrahydroxylated or atypical bile acids

in bile of a PFIC2 patient has not been reported (Jansen et al. 1999). It is not known whether other PFIC2 patients also have similar bile acids profile. These findings suggest that in the mouse, altered bile acid metabolism and other canalicular bile acid transport systems are present to modify and eliminate these bile acids. The opportunity now provided by the *spgp*$^{-/-}$ mice is to investigate directly the bile acid transport mechanism(s) that exist in addition to Spgp.

Table 8. Bile acid species in wildtype, *spgp*-/- mice, normal and a progressive familial intrahepatic cholestasis type 2 patient

Bile Acid Species	wildtype mice	*spgp*$^{-/-}$ mice	normal control	patient
Biliary Bile acid, mM (n)	32.33 ± 7.66 (3)	7.60 ± 4.58 (3)	44 ± 19 (1)	0.36 (1)
Lithocholic acid (%)			1	0.2
Deoxycholic (%)	3.6	N.D.	25	N.D.
Chenodeoxycholic (%)	1.5	1.4	29	12.9
Cholic (%)	66.7	16.6	44	85.3
Ursodeoxycholic (%)	1.6	0.8	trace	1.6
Muricholic (alpha) (%)	3.0	1.3	-	-
Muricholic (omega) (%)	7.7	20.7	-	-
Muricholic (beta) (%)	15.9	41.6	-	-
Total Tetrahydroxy (%)	N.D.	18.0	-	-

This table summarizes major findings of two papers (Jansen et al. 1999; Wang et al. 2001).

1.10. Present studies and thesis objectives

This thesis addresses the question whether Spgp is the only canalicular bile acid transporter. Previously, other candidate Spgp-independent systems of bile acid transport have been reported (Ruetz et al. 1988; Weinman et al. 1989; Sippel et al. 1994). However, most of these proposed mechanisms unlikely to play a significant role based on *in vitro* transport characteristics. In my work, the *spgp*$^{-/-}$ mouse has been chosen as a model to investigate the presence of other alternative transporters because ablation of the *spgp* gene provides the opportunity to delineate Spgp-mediated and Spgp-independent bile acid transport activities. The *spgp*$^{-/-}$ mice do not show progressive liver disease, and biochemical studies show that significant amounts of bile acids, different from those found in wildtype mice, are present in

the bile of *spgp*$^{-/-}$ mice. This was the first clue that an alternative bile acid output system exists in mice. Therefore, I was interested in addressing the following question: what is the capacity and response of this newly revealed bile acid secretory process in *spgp*$^{-/-}$ mice?

To assess this capacity, cholic acid, a potential toxic bile acid has been added to the diet design to stress the *spgp*$^{-/-}$ mice biliary bile acid secretory system (Chapter 3). This study provides a physiological model of bile acid secretion by Spgp and a Spgp-independent mechanism. To determine the mechanism of bile acid transport in *spgp*$^{-/-}$ mice, three different methodologies are used. These approaches include bile acid transport studies involving isolated hepatocyte couplets, enriched canalicular membrane vesicles (Chapter 3) and a Pgp- overexpressing cell line (Chapter 4). In addition, the expression of selective liver proteins including ABC canalicular membrane transporters is studied. The hypothesis is that if there is upregulated ABC mRNA and protein levels with concomitant increase in bile acid output, the protein may represent a compensatory mechanism in bile acid transport. Together, results from these studies provide a possible candidate Spgp-independent bile acid transporter and define its role in the canalicular membrane. Hence, the four thesis objectives are:

1) To characterize alterations in biochemical and biliary bile acid secretion in *spgp*$^{-/-}$ mice under a challenged condition of cholic acid feeding;
2) To identify selective molecular changes that are correlated with bile acid output in *spgp*$^{-/-}$ mice;
3) To delineate Spgp-dependent and Spgp-independent bile acid transport pathways in hepatocyte couplets and in isolated canalicular membrane vesicles of wildtype and *spgp*$^{-/-}$ mice;
4) To determine whether a highly similar canalicular membrane transporter, P-glycoprotein (Pgp) can transport a specific bile acid, taurocholic acid, in membrane vesicles.

Chapter 2: Materials And Methods

2.1. Mouse

2.1.1. Generation of *Spgp*$^{-/-}$ mutant mice

Mice with a targeted deletion of the *spgp* gene were produced using the strategy described in the experimental procedures by Renxue Wang (Wang et al. 2001). The heterozygous mutant mice from each generation were crossed into C57BL/6J. Homozygous mutant mice were produced by intercross of the heterozygous mice. The expression level of the *spgp* gene was determined by Northern and Western blot analysis using standard methods (Childs et al. 1995). Antiserum IW is specific for Spgp while monoclonal antibody C219 detects Pgp, Spgp and Mdr2 (Childs et al. 1998).

2.1.2. Survival of C57BL/6 *spgp*$^{-/-}$ mice

Originally, the generation of homozygous *spgp*$^{-/-}$ mice was in the C57BL/6J background. These mice were used for experiments in the original work described in the introduction and published in (Wang et al. 2001). The pups were weaned at 21 days and the genotype determined by PCR. Wildtype and heterozygous pups were obtained by crossing male heterozygous with female wildtype mice. The survival rate was 100%. Litter size was 9 pups average. Heterozygous females used for breeding had smaller litters and less frequent pregnancies than wildtype females. The used of foster mothers increased the survival rate of the pups. Knockout animals were obtained by crossing male knockout with female heterozygous mice. The survival rate was 74% (147 mice were born in 21 different litters, 108 pups survived). Litter size was 7 pups average. Knockout pups were smaller than wildtype pups at weaning (8.2 ± 0.7 g vs. 10.4 ± 0.74 g respectively) and heterozygous pups were similar in size to wildtype.

2.1.3. Survival of FVB/NJ *spgp*$^{-/-}$ mice

The work in this thesis is done on *spgp*$^{-/-}$ mice generated in two different genetic backgrounds, FVB/NJ and a mixed background of C57Bl/6J/NJ. Mice of backcross

generations 7 to 10 on a genetic background of FVB/NJ mice were used. We used FVB/NJ for the reasons that they are better breeders than C57BL/6J. Both strains were similar in response to inactivation of *spgp* gene. In the first week of birth, the bigger pups were sacrificed to enhance survival rate of knockout pups. The survival rate was 100% for the wildtype and 64% for the knockout (84 pups from 10 different litters, from which 56 survived). The pups were weaned at 21 days and the genotype determined by PCR technique. Heterozygous females used for breeding had smaller litters and less frequent pregnancies than wildtype females. Litter size was an average of 11 pups for wild type mothers and 9 pups for heterozygous mothers. There was a higher rate of perinatal mortality; therefore, the use of foster mothers was necessary to assure the survival rate of the pups. The body weight of the mice was recorded every three days for the first month, then every week for the duration of the experiment.

2.1.4. Survival of hybrid strain of *spgp*$^{-/-}$ mice

Analyses were also done on mice with a mixed genetic background (effectively F1 of a C57BL and FVB backcross). We used the hybrids also for reasons that they are better breeders than C57/Bl/6. Hybrid wildtype animals were obtained by crossing male wildtype C57BL/6 with female wild type FVB/NJ mice. The pups were weaned at 21 days. Male wean pups weighted an average of 11.4 g and female wean pups weighted an average of 10.6 g. Litter size had an average of 8 pups. Hybrid knockout animals were obtained by crossing male knockout C57BL/6J with female heterozygous FVB/NJ mice. Genotype was determined by PCR technique; heterozygous pups were discarded and knockout mice separated by sex. Knockout pups were 35% smaller than wildtype pups at weaning, with an average of 7.6 grams for males and 7.2 grams for females on weaning day. The survival rate was 84% (134 pups were born from 19 litters, 113 survived). Litter size had an average of 7 pups. Mice two months old did not have any considerable difference in body weight between wildtype and knockout mice. Older knockout animals tend to become obese and gain more weight than wildtype.

Regardless of strains, mice lacking the bile salt transporter, *spgp* developed normally and adult mice were outwardly identical to wildtype littermates. *Spgp*$^{-/-}$ mice were

distinguished from wildtype mice by larger liver size, elevated plasma bile salt, and liver bile salt and reduced biliary bile salt.

2.1.5. Mice feeding experiments

Animals were housed in plastic cages in a temperature-controlled room with 12-hour-light/12-hour dark cycling. Prior to the administration of a special diet, mice were fed *ad libitum* standard mouse diet (Pico Lab Rodent Diet 20, PMI LabDiet, Richmond, Indiana) containing 41.6% carbohydrate, 21.0% protein, 9.9% fat, 4.4% fiber, and 5.7% ash and 10% moisture (control diet). Experimental diet consists of the control diet supplemented with 0.5% (w/w) cholic acid (CA). CA is a common bile acid found in human and mice. CA supplement is often used in mice to recapitulate CA-induced cholestatic liver disease. Sex-matched groups of 2 to 6 months old mice were used for all experiments. Housing conditions and animal surgery were performed under approved protocols of the Committee on Animal Care, University of British Columbia, according to the guidelines of the Canadian Council on Animal Care.

2.2. Biochemistry and physiology of mice

2.2.1. Liver enzyme tests

Plasma samples were stored at $-80^{O}C$ until analysis of bilirubin, gamma glutamyltransferase (γ-GT), alkaline phosphatase (ALP), 5'-nucleotidase (5'-ND) and aspartate aminotransferase (AST) by routine enzyme tests using kits obtained from Sigma-Aldrich chemical Co (USA) according to the manufacturer's instructions.

2.2.2. Plasma and hepatic lipid analysis

Plasma and hepatic levels of cholesterol and triglyceride were measured enzymatically with cholesterol oxidase using Cholesterol kit (Sigma) and Infinity Triglycerides Reagent (Sigma). HDL cholesterol was measured after selective precipitation of non-HDL lipoproteins by phosphotungstic acid and magnesium chloride. Total choline content of phosphatidylcholine was determined enzymatically with phospholipase D and

choline oxidase using Phospholipids kit (Wako Chemicals, U.S.A). Content of cholesterol, phospholipids and triglycerides in liver tissues were determined after lipid extraction and expressed as nmoles/g liver.

2.2.3. Bile duct canulation and collection of bile

Mice were anesthetized by intraperitoneal injection of Ketamine (112.5 mg/kg) and Xylazine (11.3 mg/kg) after 2 to 4 hours fast. The abdomen was opened, and gallbladder was cannulated using a PE-10 catheter after distal common bile duct ligation (Smit et al. 1993). After 20 minutes of bile flow equilibration, bile was collected into pre-tared tubes at 5-minute intervals for 10 minutes. A bolus of 10μmol/kg taurocholate or 10μmol/kg tauroursodeoxycholate was then infused into the tail vein over a 20-second interval. Bile was then collected at 2-minute intervals for 10 minutes, followed by 10-minute intervals for 20 minutes. We then measured the bile flow rate (BFR) and biliary bile acid output and individual bile acid species in the bile by HPLC.

2.2.4. Bile flow rate (BFR)

The BFR was calculated by weighing the tared tubes containing the collected bile and reported as the volume collected per minute collected per liver weight of the mice (μl/min/g liver).

2.2.5. Bile acid output (BAO)

Bile samples were stored at –80°C until analysis with high performance liquid chromatography (HPLC). The biliary bile acid output (nmol/min/g liver) was determined by the concentration of bile acid (mM) (see bile acid determination section) in the bile multiplied by bile flow rate.

2.3. Quantification of bile acids

2.3.1. High performance liquid chromatography (HPLC)

In this laboratory, the bile samples were quantified by HPLC using the technique

established by Rossi *et al* (Rossi et al. 1987) and modified by Hagey *et al* (Hagey et al. 1998). Chromatography was performed using a Waters HPLC instrument equipped with a wavelength UV detector at 210nm. Bile sample (4µl) was diluted with 100% methanol to 20µl total volume. The sample was directly injected into the HPLC. The chromatographic conditions were as follows: column, 250 x 4.0mm Waters Spherisorb S5 ODS2 (Nova Pack, Waters, Toronto, ON, Canada). Mobile phase gradient: solvent A (methanol) and solvent B (50:45 methanol:0.01M potassium phosphate, 0.02M sodium phosphate, pH 5.35) at a flow rate of 0.7ml/min. Complete run is 50min, the first 25min consists of 100% solvent C (methanol) which separates out the more hydrophilic bile acids; tetrahydroxylated bile acids, taurine conjugated muricholic acids and tauroursodeoxycholic acids. The following 25min was a linear gradient from solvent B to solvent A. This portion of the gradient separates out the taurocholate. Integration of the peaks was carried out using Millennium 2010 software and the concentration determined from calibration curves using commercially available bile acids (Steraloids, Newport, Rhode Island, U.S.A). Standard curves for tauro-β-muricholate, tauroursodeoxycholate, glycoursodeoxycholate, taurocholate, taurochenodeoxycholate, taurodeoxycholate, ursodeoxycholate, cholate, taurolithocholate, chenodeoxycholate and deoxycholate were generated. The detection limits for the two major rodent bile acids tauro-β-muricholate is 0.33mM and taurocholate is 0.28mM, therefore, this method appears to be suitable for biliary bile acid analysis. The identities of the peaks were further identified by gas chromatography/mass spectrometry (GC/MS) (Dr. Yousef, University of Montreal, Canada) and electrospray mass spectrometry (ESI-MS) (Dr. Lee Hagey, University of San Diego, USA).

2.3.2. Statistical methods

Significance of differences between groups was determined using the two-tailed Student t-test and a p value of 0.05.

2.4. Purification of liver membrane vesicles

2.4.1. Materials

Sucrose and all other chemicals used were of commercial grade from Sigma (St. Louis, MO). The densities of all sucrose solutions were determined with a MISCO refractometer. All ultracentrifugation steps were carried out in a GS-6R Beckman centrifuge and L-6 Beckman ultracentrifuge (Mississauga, ON). Percoll solution was obtained from Pierce (Rockford, IL).

2.4.2. Isolation of crude membranes from mice liver

Fig. 5 illustrates a purification scheme for the isolation of enriched plasma membrane subfractions from wildtype and *spgp*$^{-/-}$ mice liver. Plasma membrane enriched in bile canaliculi were prepared by a modification of the discontinuous sucrose gradient methods of Bohme M. *et al.*, 1994 (Bohme et al. 1994). Upon sacrifice of 7 to 10 +/+ mice and 3 to 4 -/- mice, blood samples were removed by heart puncture; livers were rapidly removed, weighed and immersed in buffered citrate saline on ice. The livers were then rinsed free of blood three times in cold buffered citrate saline. Approximately 10g of livers were minced through 1mm metal sieve to remove connective tissue. The minced livers were washed with 100ml of Buffer A (250mM sucrose; 5mM HEPES-HCl pH 7.4; 0.5mM $CaCl_2$ and 2 tablets of EDTA-free protease inhibitors and 0.1mM PMSF). Minced livers (50-ml portions) were then homogenized with 7 up-and-down strokes using a 50-ml loose-fitting Dounce homogenizer (Pestle Clearance 0.0035 to 0.0050", Wheaton). Dounce homogenate (1-ml) was saved for protein and enzyme assays and the remainder centrifuged (1500g, 10 min, 4^{O}C, GS-6R Beckman rotor). The pink, gelatinous nuclear and plasma membrane pellets were collected, combined and diluted to 50 ml with Buffer B (250mM sucrose; 5mM HEPES-HCl pH 7.4; 1mM EGTA), homogenized with 20 passes up-and-down strokes using a 50-ml tight-fitting Dounce homogenizer (Pestle Clearance 0.0010 to 0.0030", Wheaton) then diluted to 100ml and passed through a second 1mm metal sieve. After 30 min on ice, the homogenate was mixed with 12ml (14%) of percoll (density = 1.044, Pharmacia) for wildtype animals and 14ml for knockout animals, and were evenly suspended by gentle mixing with transfer pipette. The volume of percoll used was optimal to produce a clear single band after

ultracentrifugation. The percoll-membrane suspension (26 to 27ml) was transferred to polycarbonate tube (for Beckman SW28 rotor) carefully overlayered with 5ml Buffer B, and centrifuged in a SW28 rotor (37,000xg, 40mins, 4^{O}C). Crude membrane sheets (4ml each) were recovered and diluted to 40ml with Buffer B and homogenized by 10 up-and-down strokes with a 50-ml tight fitting Dounce homogenizer.

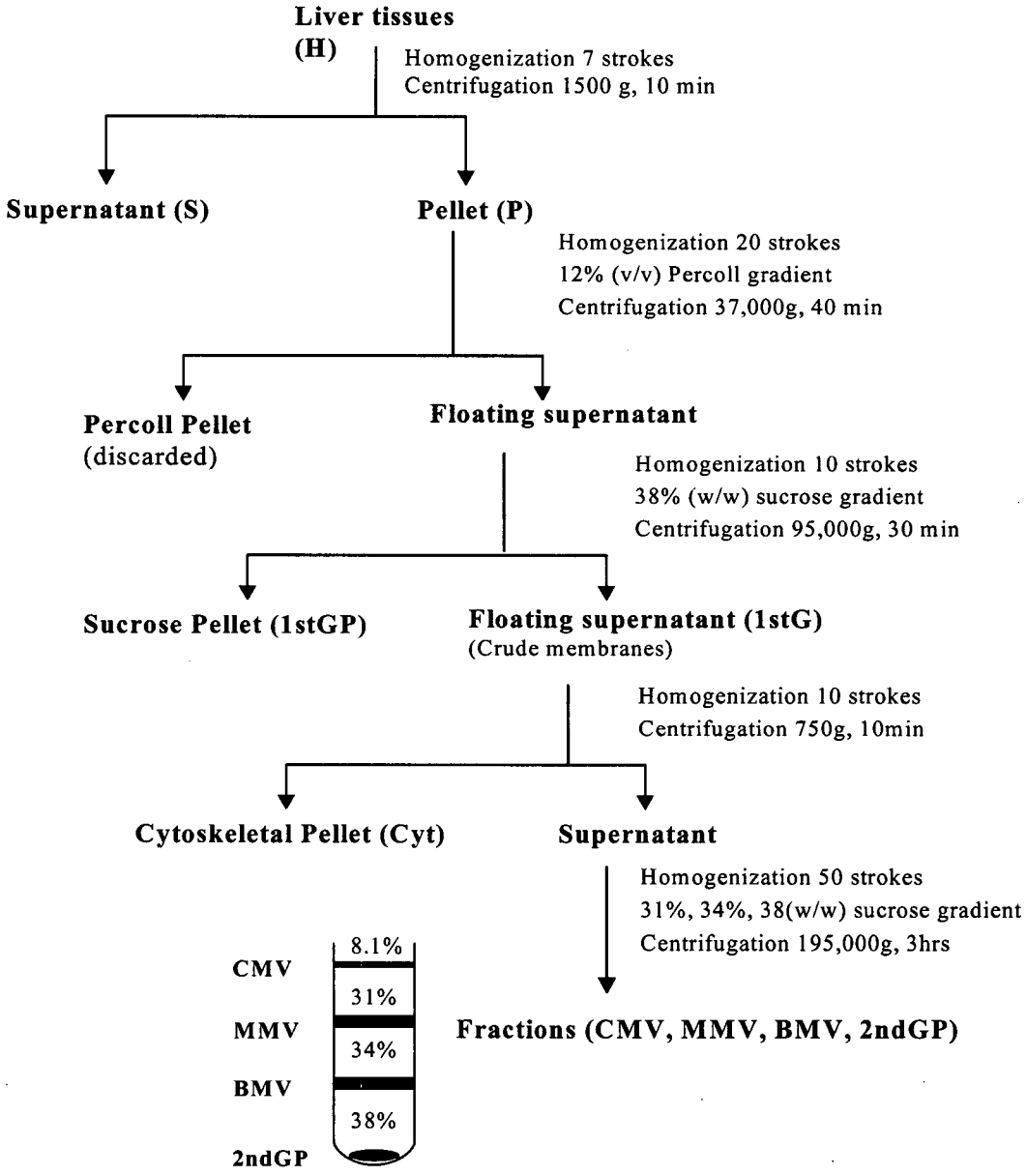

Fig. 5. Purification scheme for different plasma membrane fractions from mice liver.

2.4.3. Isolation of plasma membrane vesicles from mice livers

The homogenate was layered on a 15-ml sucrose solution (38% w/w, density = 1.164 g/ml). The gradients were then centrifuged in a SW28 rotor at 95,000 g for 30 min, 4^{O}C. Plasma membrane sheets were recovered from the 38%(w/w) sucrose interface, diluted to 50-ml with Buffer D (10mM HEPES-Tris pH 7.4; 0.25M sucrose), homogenized with 5 up-and-down strokes using tight-fitting Dounce homogenizer, and spun (750g, 10min, 4^{O}C) to remove cytoskeleton. The supernatant was then centrifuged (100,000g, 30min, 4^{O}C) to collect membrane pellets. The washed pellets were then diluted to 6ml with Buffer D, homogenized by 50 up-and-down strokes with a 15-ml tight fitting Dounce homogenizer, snap frozen in liquid N_2 and stored at –80^{O}C.

2.4.4. Isolation of canalicular membrane vesicles from mice livers

Separation of canalicular and sinusoidal membranes was performed by sucrose density gradient centrifugation. The enrichment of each collected fraction was monitored by enzyme markers described below (Section 2.5). The suspension of membranes was thawed out from –80^{O}C in a 37^{O}C water bath and immediately placed on ice. The membranes were homogenized again with 50 up-and-down strokes using tight-fitting Dounce homogenizer. The vesiculated membrane was layered over a three-step discontinuous sucrose gradient consisting of, 2ml of 31%(w/w) sucrose (density = 1.130 g/ml), 2ml of 34% (w/w) sucrose (density = 1.146 g/ml) and 2.5ml of 38% (w/w) sucrose (density = 1.164 g/ml). The gradient was centrifuged (195,000xg, 3hr, 4^{O}C) to obtain different subfractions of plasma membrane.

The sharply defined band of fine particles which layered just above d = 1.130 interface was collected using a 25-gauge needle. About 3 to 4ml of membranes were collected in one preparation. These membranes were diluted to 4 to 5 times its volume with Buffer D. These membranes constitute the light density vesicular "canalicular" membranes fraction (CMV). The large band which layered between d =1.130 and just above 1.146 was recovered using a 25-gauge needle. About 4ml of membranes were collected in this fraction; diluted to 4-5 times volumes with Buffer D. These membranes constitute the middle fraction representing the "Mixed" membranes (MMV), which consist of intact canaliculi, sinusoidal

sheets, as well as, tight junctions and gap junctions. The very small layer just above d=1.164g/ml was also recovered using 25-gauge needle. This fraction was sometimes not readily visible especially in the -/- mice preparation. Approximately 2ml or less are collected and diluted 5 times in Buffer D. This fraction representing basolateral vesicles (BMV) contains unbroken sheets and some gap junctions. The yellow tan pellet at the bottom of the tube were covered also and diluted in 1ml of Buffer D, resuspended using 50 up and down strokes with a 7-ml tight fitting Dounce homogenizer. This fraction contains mainly unbroken lateral membrane sheets and desmosomes.

All the diluted samples are centrifuged (100,000xg, 30 min, $4^{O}C$) to pellet the fractions. The CMV, MMV and BMV pellets were recovered with 300µl, 1-ml and 400µl Buffer D respectively by resuspending 50 strokes up-and-down with a 1ml-pipetman. The membranes were frozen in liquid N_2 and stored at $-80^{O}C$ for up to 2 months.

2.5. Biochemical analysis of canalicular membrane vesicles

2.5.1. Marker enzyme assays

The following enzyme activities were tested in various membrane fractions: alkaline phosphatase was measured using a commercial kit (Sigma) using p-nitrophenyl-5'-monophosphate as substrate; Mg^{2+}-ATPase and the oubain-sensitive $Na^{+}K^{+}$-ATPase activities were measured according to the method of Scharschmidt *et al.*, (Scharschmidt et al. 1979). Alkaline phosphatase activity is a marker for the enrichment of canalicular membrane; $Na^{+}K^{+}$ ATPase activity is a marker for the enrichment of basolateral membrane. Contaminations by other intracellular organelles have been determined by Western immunoblotting (See section 2.6). The $Na^{+}K^{+}$ ATPase activity was assayed in a medium containing 20µg of protein in 469µl of buffer containing 125mM Tris pH 7.4, 1.5mM EGTA, 125mM NaCl, 12.5mM KCl, 3mM phosphoenolpyruvate (PEP), 6mM NaN_3 incubated in the presence or absence of 60µl of 10mM oubain. The reaction was initiated by adding 6µl of 50mM NADH, 30µl of 100mM MgATP, 20µl of pyruvate kinase and L-lactate dehydrogenase (450U/ml each in ammonium sulfate) enzymes mixture. The $Na^{+}K^{+}$-ATPase

activity was linear over a 5-minute period. Basal Mg^{2+}ATPase activity was the activity not inhibited by oubain.

2.5.2. Orientation of membrane vesicles

The amount of inside-out vesicles was determined by ectoenzyme nucleotide pyrophosphatase activity. The catalytic activity of the enzyme is concentrated on the luminal size of the canalicular plasma membrane domain of hepatocytes. The enzyme substrate p-nitrophenyl 5'-monophosphate is hydrolyzed but not taken up by intact cells. The activity measured with intact vesicles, therefore, corresponds to the fraction of right-side-out vesicles. On the other hand, the activity measured in Triton X-100-solubilized membrane vesicles corresponds to the total enzyme activity from inside-out and right-side-out membrane vesicles. The difference between these two activities provides a means to estimate the amount of inside-out-oriented vesicles. CMV (10μg of total protein) were incubated with 2mM of p-nitrophenylthymidine 5'-monophosphate in 0.25M sucrose, 10mM Tris-HCl pH 7.8 in the presence or absence of 0.3% Triton X-100 for 5 min at 37°C in a final volume of 500μl. The reaction was stopped by addition of 200μl of cold 3M $HClO_4$. After microcentrifugation (14,000 rpm, 10min, 4°C), 500μl of supernatant was added to 340μl 3.3M KOH to reach pH 8-9. The $KClO_4$ precipitate was centrifuged at (14,000rpm, 10min, 4°C) and the supernatant was measured at 405 nm using the molar extinction coefficient of 18.5 $M^{-1}cm^{-1}$.

2.6. Protein Analysis

2.6.1. Materials

All protein gels and transfer for Western immunoblotting were performed using an Invitrogen gel apparatus. The C219 monoclonal antibody recognizes all Pgps including mouse Mdr1a, Mdr1b, Mdr2 and Spgp, was generated in this laboratory (Georges et al. 1990). The polyclonal IW antibody recognizes specifically Spgp protein was generated in this laboratory (Childs et al. 1998). The Ntcp and ectoATPase antibody that recognizes the basolateral sodium taurocholate transporting polypeptide, (Ntcp) and canalicular ectoATPase

were gifts from Dr. F. Suchy (Mount Sinai Medical Center, New York, U.S.A). The Mrp2 antibody recognizes canalicular multidrug resistance related protein (Mrp2) was a gift from Dr. D. Keppler (Division of Tumor Biochemistry, Heidelberg, Germany). The two antibodies that recognizes class I multidrug resistance protein (Mdr1a) and class III multidrug resistance protein (Mdr2) were gifts from Dr. P. Gros (McGill University, Montreal, Canada). The antibody that recognizes basolateral multidrug resistance related protein (Mrp3) was a gift from Dr. Kruh (Fox Chase Cancer Center, Philadephilia, U.S.A). Other primary antibodies that recognize mitochondrial alcohol dehydrogenase and endoplasmic reticulum calnexin were purchase from Stressgen Biotechnologies, Victoria, Canada). Golgi antibody α Golgi 58K was purchased from Sigma. Horseradish conjugated anti-mouse or anti-rabbit secondary antibodies were purchased from Jackson ImmunoResearch Laboratories, Inc (WestGrove, PA). Fluorescent Cy3 or Alexa 488 anti-mouse or anti-rabbit was purchased from Molecular Probes (Eugene, OR).

2.6.2. Protein concentration of different fractions of isolated liver

Protein concentration was determined by BCA assay (Pierce, Rockford, IL) using bovine serum albumin as standard according to manufacturer's instructions.

2.6.3. SDS-PAGE and Western immunoblotting

Protein (20μg) was loaded on an 8% SDS polyacrylamide reducing gel using an Invitrogen minigel apparatus. Gels were either stained with 0.02% Coomassie brilliant blue. Gibco BRL molecular weight standards were used as protein marker. For Western immunoblotting, the gel was directly transferred to Immobilon-P using Invitrogen transfer apparatus with MOPS SDS running buffer (Burlington, ON). The blots were stained with Ponceau S-solution (0.3% Ponceau S (w/v)) to confirm equal transfer of proteins. The blots were blocked with either 10% skim milk or 3% BSA in tris-buffered saline (TBS) that contained 0.05% Tween-20 (TTBS). The blots were incubated with monoclonal antibody C219 (dilution 1:2000), polyclonal antibody Spgp-IW (dilution 1:5000), polyclonal antibody Ntcp (1:2500), polyclonal antibody Mrp2 (1:5000), polyclonal antibody Mdr1a (1:500), polyclonal antibody Mdr2 (1:100), or monoclonal antibody Mrp3 (1:5000) in 1% skim milk

in TTBS containing 1% Tween-20. The blots were incubated with horseradish peroxidase-conjugated secondary antibody (dilution 1:10,000) in TTBS. Protein bands were detected using the ECL system (Amersham). Quantitative comparison of the Western blots was accomplished by determination of the band using Molecular Dynamics densitometer and Image Quant scan software (Amersham Biosciences, Canada).

2.6.4. Immunofluorescence

Liver sections were cut and fixed with 100% methanol for a few minutes at $4^{O}C$. All procedures were then carried out at room temperature in a moisturized chamber. The liver section was then permeabilized 0.05% Triton X-100 in phosphate-buffered saline (PBS), 15min) and blocked (5% bovine serum albumin, 0.05% Triton X-100 in PBS, 15min). The liver section was then stained first with 1:100 primary antibody (C219, Mrp2, Spgp-IW, 1hr) and followed by 1:500 secondary antibody conjugated Cy3 or Alexa 488 conjugated anti-rabbit IgG.

2.7. mRNA analysis

2.7.1. Real time PCR

The methods have been described in (Wang et al. 2003c). Samples from two to four mice for each group were isolated. For real-time PCR analysis, total RNA was extracted from frozen liver using Absolutely RNA RT-PCR Miniprep Kit from Stratagene (La Jolla, CA, USA). Reverse transcriptions were performed with Superscript First-strand Synthesis System for RT-PCR from Invitrogen (San Diego, California, USA). PCR reactions were done with the SYBR Green PCR Master Mix (Foster City, California, USA) in a PRISM 7900HT Sequence Detection System from Applied Biosystems (Foster City, California, USA), using the "Standard Curve Method"(ABI PRISM User Bulletin #2). Aliquots (5-10 ng) of total RNA were used for each RT-PCR reaction and the results were normalized against the expression level of ribosomal protein S15 (Rps15).

2.8. Hepatocyte couplet isolation

2.8.1. Materials

Materials for hepatocyte couplet isolation and secretion studies were made available by Dr. James Boyer at Yale Liver Center (New Haven, CT). Collagenase (type I) was purchased from Boehringer Manheim Biochemicals (Indianapolis, IN). Leibovitz L-15 medium was obtained from Gibco (Grand Island, NY). Two fluorescent bile acid derivative cholylglycylamidofluorescein (CGamF) and deoxycholyl-lysyl-fluorescein (DCLF) were used. All the fluorescent compounds were prepared in DMSO as 1000x stock and stored at $-20^{o}C$. The fluorescent compounds were gifts from Dr. Alan F. Hofmann (University of California, San Diego, USA). CGamF is a cholylglycine derivative with the isothiocyanate group of fluorescein linked to the carboxylate group of the bile acid by formation of an amide bond. Another fluorescent compound, 5-chloromethylfluorescein diacetate (CMFDA), a substrate of Mrp2 was used as control was purchased from Molecular Probes (Eugene, OR). Dibutyryl-3',5'-cyclic monophosphate (DBcAMP) nocodazole, and all other chemicals were from Sigma (St Louis, MO).

2.8.2. Perfusion and isolation procedure

All hepatocyte couplets studies were done at Yale Liver Center (New Haven, CT) in collaboration with Dr. James Boyer and Dr. Carol Soroka. The isolation of hepatocyte couplets from mice liver was performed as previously described for rat hepatocyte couplets (Boyer et al. 1990). Fig. 6 illustrates the procedures for preparing and using hepatocyte couplets for bile acid secretion studies. After anesthesia with phenobarbital (100mg/kgbody weight, intraperitoneal), the portal vein was cannulated with a 16-gauge cannula and perfused *in situ* for 10 minutes with Hanks' buffer A (120.0mM NaCl, 5.0mM KCl, 5.5mM D-glucose, 0.4mM KH_2PO_4, 0.2mM Na_2HPO_4, 25mM $NaHCO_3$, 0.5mM EGTA); pH 7.4) at $37^{o}C$ and then for 10 minutes with Hanks' B medium (120.0mM NaCl, 5.0mM KCl, 5.5mM D-glucose, 0.4mM KH_2PO_4, 25mM $NaHCO_3$, 0.4mM $MgSO_4$, 0.5mM $MgCl_2$, 3mM $CaCl_2$); pH 7.4) at $37^{o}C$ containing 0.05% (w/v) collagenase and 0.8 units trypsin inhibitor per unit tryptic activity in the collagenase. The liver was removed, placed in Leibovitz L-15 medium, minced, passed through serial nylon mesh filters, and washed with Leibovitz L-15 medium at

$4^{O}C$. The cells were spun down (500xg, 5min, $4^{O}C$) to remove medium. The cells were resuspended gently in 90% (v/v) percoll in phosphate-buffered saline and spun (500xg, 5min, $4^{O}C$) to remove floating dead cells. The loose pellet was washed with L-15 medium and spun (500xg, 5min, $4^{O}C$). The procedure was repeated twice. The pellet was then resuspended gently with 3ml of L-15 medium containing 50 IU/ml penicillin, 50μg/ml streptomycin and 10% fetal calf serum, for counting and plating.

2.8.3. Culturing of hepatocyte couplet

Mean cell viability by trypan blue exclusion varied from 50%-90%. Hepatocytes were resuspended from 1 to 5 x 10^6 cells/ml in L-15 medium containing 50 IU/ml penicillin, 50μg/ml streptomycin and 10% fetal calf serum, plated on coverslips in polystyrene Petri dishes (0.1 x 10^6 cells/cm^2) and cultured for 3 hours at $37^{O}C$ in an air atmosphere. Treatments of the cells were carried out as previously described for rat hepatocyte couplets (Boyer and Soroka 1995). Control condition was to maintain cells in L-15 medium alone for 4 hours. Inhibition of microtubule-mediated vesicular movement was accomplished by addition of nocodozole (20μmol/L) at the time of plating and treated for 4 hours at $37^{O}C$. DBcAMP (100μmol/L) was added to dishes after 2 hours of culture and cells were incubated in their presence for an additional 2 hours.

2.8.4. Vectorial transport in hepatocyte couplet

The coverslips containing plated cells were then washed twice in a HEPES-buffered saline solution (HBS, 135mM NaCl, 4.7mM KCl, 1.2mM KH_2PO_4, 1.25mM $CaCl_2$, 1mM $MgSO_4$, 10mM HEPES, pH 7.4). The reaction was started by removing the coverslips and placing into HBS solution containing, 1μM CGamF or 1μM CLF or 5μM CMFDA. After 15 minute, the reaction was stopped by immersing the slide into ice-cold HBS solution.

To visualize fluorescent bile acid accumulation, coverslips were transferred from the dishes to a chamber on the stage of a Zeiss Axiovert microscope (Oberkochen, Germany) and were observed using a BioRad MRC-600 confocal imaging system (Cambridge, MA) and COMOS software (Biorad). Images were collected with the same confocal settings (gain,

aperture, black level and neutral density filter) for all culture conditions. Couplets were selected for study if they had expanded canaliculi using light microscopy and were subsequently scanned with the laser and the data were stored on disk for later analysis. Couplets were excluded from analysis if the lumens were not expanded because a portion of isolated couplets either fail or seal their canalicular spaces and thus do not retain secretory polarity or the canalicular spaces have collapsed before the time of measurement because of continued secretion into the closed luminal space. Ten images of these couplets were collected and were processed using NIH image program (http://rsb.info.nih.gov/nih-image). The fluorescence was quantified by determining the pixel intensity within the area defined by tracing the vacuolar space or the entire area of the hepatocyte couplet. The percentage of secretion was determined by dividing the fluorescence intensity of the vacuolar space and the fluorescence intensity of the area of the hepatocyte couplet. Measurements of the canalicular circumferences were also obtained in the same couplets that were used for quantitation of canalicular fluorescence by tracing the fluorescent canalicular lumens.

2.8.5. Immunocytochemistry

For studies of distribution of Pgps, Spgp and Mrp2, cells were cultured at 37^{O}C on coverslips for 3 hours and fixed in 100% methanol at –20^{O}C for 10 minutes and then rehydrated in PBS (20 minutes). The monoclonal antibody C219 that recognizes all Pgp isoforms including Mdr1a, Mdr1b, Spgp and Mdr2 or polyclonal antibody IW or EAG15 that recognizes the carboxyl terminus of Spgp and Mrp2 respectively were used. The antibody was diluted 1:100 in 1% BSA in PBS containing 0.25% Triton X-100 and incubated with the cells for 2 hours at room temperature. After washing in PBS, the cells were incubated with Cy3-conjugated or Alex488-conjugated anti-rabbit and anti-mouse IgG respectively, for 30 minutes in 1% BSA/PBS at room temperature. Immunolabeling was detected using confocal microscopy.

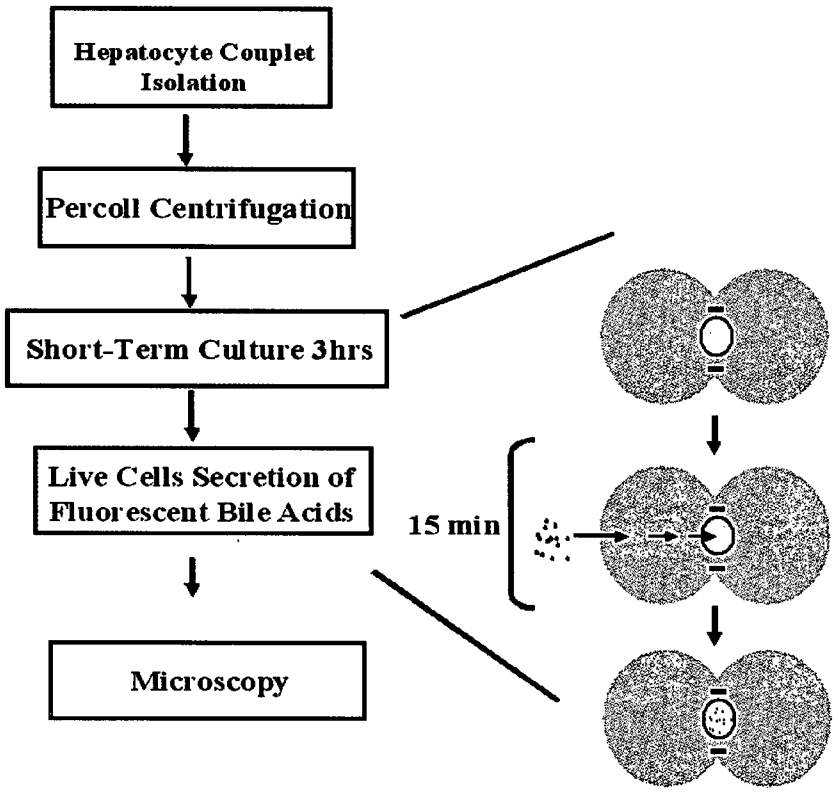

Fig. 6. Isolation and canalicular vacuolar accumulation of fluorescent bile acids

Hepatocyte couplets are isolated from freshly prepared wildtype and *spgp*$^{-/-}$ mice liver perfusion. Preparation usually results in 10 to 20% couplets. Short-term culture of 3 to 4 hour at 37^{O}C re-establishes both morphological and functional polarity of the couplets. The cellular polarity of these cells is determined by the distribution of canalicular membrane transporters by immunofluorescent staining of these couplet cells. The cells are then incubated with a low concentration 1μM CGamF or 1μM DCLF or 5μM CMFDA for 15min and monitored for secretion into canalicular vacuole. The effects of choleretic or cholestatic agents that increases or decreases any of the processes (uptake, transcellular transit, canalicular secretion, vacuolar retention) are then studied.

2.9. *In vitro* bile acid uptake assays

2.9.1. Materials

The enzyme substrates ATP, AMP, NADH, phosphoenolpyruvate (disodium salt), alkaline phosphatase kit, sucrose were obtained from Sigma Chemical Co. (Mississauga, ON). Disodium adenosine triphosphate, taurocholic acid, taxol, and E17-β-glucuronide were obtained from Sigma. ^{3}H-Taurocholic acid (3-5Ci/mmol) was obtained from New England Nuclear (Boston, MA). Other cold bile acids including, β-tauromuricholic acid, α-muricholic acid, tauroursodeoxycholic acid and glycoursodeoxycholic acid were obtained from Steraloids Inc (Newport, Rhode Island). Nitrocellulose filters (HAWP045; pore size, 0.45μm) was from Millipore Corporation (Bedford, MA).

2.9.2. Radiolabel taurocholate uptake

Transport experiments were performed using a rapid filtration assay. Frozen membrane samples were thawed quickly at 37^{O}C, incubated on ice for 30 min until use. Reaction buffer (110μl, 10mM Hepes-Tris pH 7.4, 250mM sucrose, 5mM ATP disodium salt or AMP monosodium salt, 10mM $MgCl_2$, 10mM creatine phosphate tris-salt and 100μg/ml creatine kinase) containing 3μM ^{3}H-taurocholic acid was incubated at 37^{O}C for 5 min and then rapidly mixed with 50μl of 0.8μg/μl membrane vesicle suspension (40μg protein). Control experiments were carried out at 4^{O}C. At the times indicated, 20μl aliquots were removed and added to 1ml of ice-cold washing buffer A (10mM Hepes-Tris pH 7.4, 250mM sucrose and 1mM cold taurocholic acid) and filtered through 0.45μm pore size prewetted nitrocellulose (HAWP045 Millipore) filters. In order to reduce non-specific binding to the filters, the filters were first prewashed with water and then with Buffer A. The filters were then washed with 5-ml buffer A and rinsed twice with 5-ml buffer B (10mM Hepes-Tris HCl pH 7.4, 250mM sucrose). Radioactivity was measured by liquid scintillation counting in 5-ml liquid scintillation fluid.

2.9.3. Osmotic sensitivity assay

The experimental setup is the same as described in the radiolabel taurocholate uptake section. Membrane vesicles were preincubated in the reaction buffer containing different concentration of sucrose (0.2, 0.25, 0.33, 0.5, 1M) for uptake of ^{3}H-taurocholate.

2.9.4. Inhibition of taurocholate uptake studies

CMV was preincubated with the inhibitors for 5 min at 37^{O}C prior to the start of the ^{3}H-taurocholate uptake assay (see time-dependent sodium taurocholate uptake of the materials and method section). α-muricholic acid, β-tauromuricholic acid and cyclosporin A were dissolved in ethanol. Ursodeoxycholic acid was dissolved in aqueous buffer.

2.10. *In vitro* fluorescent substrate uptake assay

2.10.1. Chemicals

Hoechst 33342, rhodamine 123 and were obtained from Molecular Probes. The sodium acids of taurocholate, tauro-β-muricholate, taurochenodeoxycholate, tauroursodeoxycholate and taurodeoxycholate and most fine chemicals were obtained from Sigma Chemical Co. Prenylamine, Cis-(*Z*)-flupentixol, haloperidol and *R*(+)-propanolol were from Research Biochemicals International (Natick, MA, U.S.A). CHAPS was obtained from Calbiochem (San Diego, CA, USA).

2.10.2. Pgp containing plasma membrane vesicles

Plasma membrane vesicles were prepared from Chinese hamster ovary CH^{R}B30 cells as previously described (Shapiro and Ling 1994), which expresses Class I P-glycoprotein about 15% of the plasma membrane protein and negligible amounts of Class II and III P-glycoprotein (Shapiro and Ling 1994). The plasma membrane fraction was collected from the sucrose gradient 16%/31% interface. Protein concentration was determined using BCA assay as described earlier. The protein concentration is determined individually for each experiment (usually 0.4mg/ml to 0.6mg/ml depending on number of cells used for preparation). The vesicles are about 50% inside-out based on enzyme activity.

2.10.3. Fluorescence measurements of substrate uptake

All experiments were performed in Buffer A (100mM Tricine-NaOH (pH 7.4), 75mM NaCl, 1mM EDTA, 1mM EGTA, 1mM NaN_3 and 0.1mM oubain). EGTA, NaN_3 and oubain were present to inhibit the activities of ATPases other than P-glycoprotein.

For assays, a 1-ml portion of plasma membrane vesicles was thawed, diluted with 9 ml of cold Buffer A, and pelleted by centrifugation at 100,000 x g for 45 min at $4^{O}C$. The pellet was resuspended in 1ml cold Buffer A. Approximately 40μg of total protein/ml was used in each assay (Shapiro and Ling 1995).

Rhodamine 123 and Hoechst 33342 transport initial rates were measured as described (Shapiro and Ling 1997b). Fluorescence measurements were made with an SLM-8100 spectrofluorometer (SLM-Aminco) equipped with a double excitation monochromator. The cuvette holder was maintained at $37^{O}C$. Samples of 950μl were incubated in the excitation light beam for 5 min to equilibrate and to stabilize the fluorescent intensity prior to injection of 50μl of a solution containing 100mM Tricine/NaOH pH 7.4, 30mM Na_4ATP, 60mM $MgCl_2$ and 40mM dithiothreitol. The fluorescence was subsequently monitored for 400 s. Fluorescence traces were normalized to a value of 1 immediately after the injection of MgATP so that the slope of the initial linear part of the fluorescence decrease equals the fraction of fluorescence lost per second. Initial rates of fluorescence decrease were measured during the linear part of the trace, typically 4 s and 10s for the rhodamine 123 and Hoechst 33342 transport measurements, respectively.

For rhodamine 123 transport measurements, data were collected at 0.2-s intervals. The excitation and emission wavelengths were 497 nm and 526 nm, respectively. The excitation and emission bandwidths were 1 nm and 4 nm, respectively with 1μM rhodamine 123.

For Hoechst 33342 transport measurements, data were collected at 0.5-s intervals. The excitation and emission wavelengths were 355 nm and 457 nm, respectively. The excitation and emission bandwidths were 2 nm and 16 nm, respectively. Initial rates of

fluorescence decrease were measured during the linear part of the trace, typically the first 4s and 10s for the rhodamine 123 and Hoechst 33342 transport measurements, respectively.

2.10.4. Permeability of membrane vesicles

The effect of bile acids on the permeability of CH^RB30 plasma membrane vesicles to ionic solutes was determined by the pyranine/p-xylene bispyridinium bromide fluorescence quenching assay, as previously described (Shapiro and Ling 1997b). Briefly, the vesicles were loaded with the fluorescent dye pyranine by sonicating in a bath-type sonicator (Laboratory Supplies) for 2 min in the presence of 10mM pyranine. Free external pyranine was removed by passing the vesicles through a column of Sephadex G-50 (fine) (Sigma) equilibrated with Buffer A. The pyranine fluorescence of the vesicles was measured at excitation and emission wavelengths of 454 nm and 511 nm, respectively, with excitation and emission bandwidths of 1nm and 4nm, respectively, in the SLM-Aminco spectrofluorometer. *P*-xylene bispyridinium bromide dissolved in Buffer A was added to 10mM to quench the fluorescence of external pyranine. The addition of agents that increase the permeability of the vesicle membranes to p-xylene bispyridinium bromide or pyranine results in a time-dependent fluorescence decrease. The permeability of CH^RB30 plasma membrane vesicles was tested in the presence of different bile acids at concentrations up to 100μM.

2.10.5. ATPase activities.

ATP hydrolysis was linear with time and was measured by a single-time point assay of phosphate (Chifflet et al. 1988) in buffer A. Blank samples of ATPase assays contained plasma membrane vesicles from AuxB1 cells, the parental cell line from which CH^RB30 cell line was derived and which expresses negligible amounts of P-glycoprotein. Corrections were made for differences between the protein concentrations of samples containing membranes from AuxB1 and CH^RB30 cells.

Chapter 3: Bile acid transport capacity in *spgp*$^{-/-}$ mice

3.1. Introduction

Spgp$^{-/-}$ mice display normal bile flow, elevated level of abnormal hydrophilic bile acid metabolites, and mild intrahepatic cholestasis (Wang et al. 2001). The liver pathology in these animals has been characterized by slight dilation of the canalicular lumen and partial loss of microvilli without advanced or progressive worsening in liver pathology (Wang et al. 2001). Such features do not recapitulate the characteristics of human PFIC2. Initial experiments have revealed that this may involve a canalicular transport process that is selective for hydrophilic bile acids, muricholic acids and tetrahydroxylated bile acid species (Wang et al. 2001). On the basis of these findings, it has been hypothesized that redundant bile acid secretory mechanism(s) and active hydroxylation of toxic bile acids are responsible for the mild phenotype. To test this hypothesis, *spgp*$^{-/-}$ mice were fed with diet supplemented with 0.5% cholic acid (CA), which rendered the bile acid pool more hydrophobic. Such mice developed severe cholestasis characterized by jaundice, weight loss, elevated plasma bile acid, elevated transaminases, liver necrosis, and high mortality. Indeed, these characteristics resembled a PFIC2 phenotype. The capacity and hepatic responses in bile acid output and bile flow under acute taurocholate infusion and feeding experiments in *spgp*$^{-/-}$ mice were also addressed. A surprising observation was that the bile acid output and bile flow in CA-fed mutant mice were significantly higher than anticipated. Results presented in this chapter provide a potential physiological model of a large capacity bile acid transporter in *spgp*$^{-/-}$ mice. A portion of this chapter has been published (Wang et al. 2003b).

3.2. Results

3.2.1. Characteristics of *spgp*$^{-/-}$ mice

Liver weight to body weight ratio was similar in wildtype mice regardless of diet and sex of mice (Fig.7). Heterozygous mice had similar liver weight to body weight ratio as wildtype mice in normal diet and CA diet (data not shown). However, there was a 2-fold increase in liver weight to body weight ratio (with body weight constant but liver weight is approximately 2 times the size) in both male and female knockout mouse liver compared to

wildtype mice fed with the control diet. An even higher ratio was observed in mutant mice fed with CA diet (greater than 15%) compared to wildtype, indicating further biochemical changes in the mice. Based on these results, we focused the majority of our studies on mice fed with the CA diet for 2 days since by this time toxicity were readily apparent in the *spgp*$^{-/-}$ male but mortality was minimal. *Spgp*$^{-/-}$ mice contain approximately two times more liver cells than controls (10 x 10^6 cells versus 23 x 10^6 cells respectively) as estimated by total cell count and the number of viable cells using the trypan blue exclusion method.

3.2.2. Physiological and biochemical responses to CA feeding

Under standard housing and dietary conditions, *spgp*$^{-/-}$ mice were viable, fertile and displayed growth retardation. We attempted to induce the PFIC2-like phenotype in *spgp*$^{-/-}$ mice by feeding the mice with a diet containing 0.5% cholic acid (CA). This was the same concentration used previously for inducing atherogenesis and cholesterol gallstone formation (Paigen et al. 1985; Wang et al. 1999a) and for studying the molecular changes of murine hepatocellular transporters under feeding condition (Fickert et al. 2001). The *spgp*$^{-/-}$ male mice fed with this diet exhibited severe weight loss and hypoactivity and death of all *spgp*$^{-/-}$ male mice occurred within 5-9 days of CA feeding (Fig. 7A). In stark contrast, wildtype mice appeared to tolerate the CA diet well and displayed no overt signs of toxicity or mortality. Interestingly, female *spgp*$^{-/-}$ mice under CA feeding conditions lived up to 102 days without showing terminal illness (Fig. 7A).

With the normal diet, biochemical parameters of liver function in the *spgp*$^{-/-}$ mice have been shown to be very similar to those in wildtype (Wang et al. 2001). However, with CA feeding, alkaline phosphatase (ALP), 5'-nucleotidase, aspartate aminotransferase (AST) and bilirubin levels were significantly elevated in *spgp*$^{-/-}$ mice compared to wild-type mice (Table 9). This biochemical profile, along with relatively normal γ-glutamyltranspeptidase (γ-GT) (Table 9) and a high serum bile acid level (see below for mice bile acid analysis), resembled that seen in PFIC2 patients (Jansen et al. 1999). This profile was consistent with severe hepatocellular damage but relatively mild bile ductular damage and suggested a common hepatological basis for the induced cholestasis and PFIC2.

Fig. 7. Change in relative body weight and liver weight in *spgp*-/- mice.

(A) Relative body weight gain of adult (2-4 months) male and female mice fed with a diet containing 0.5% CA. Relative body weight was calculated as a function of starting body weight at the beginning of CA feeding. A trend line is drawn with all the data points.

(B) Liver weight/Body weight ratio was reported for male and female wildtype and *spgp*$^{-/-}$ mice. Heterozygotes had similar ratio as wildtype animals (data not shown). -/-, *spgp*$^{-/-}$; wt, wild-type. Each point represents the mean of 3 to 5 animals. Error bars represent standard deviation. Asterisks indicate statistical significance between *spgp*$^{-/-}$ mice and wildtype of the same sex on the same diet ($P<0.001$).

Figure 7.

(A)

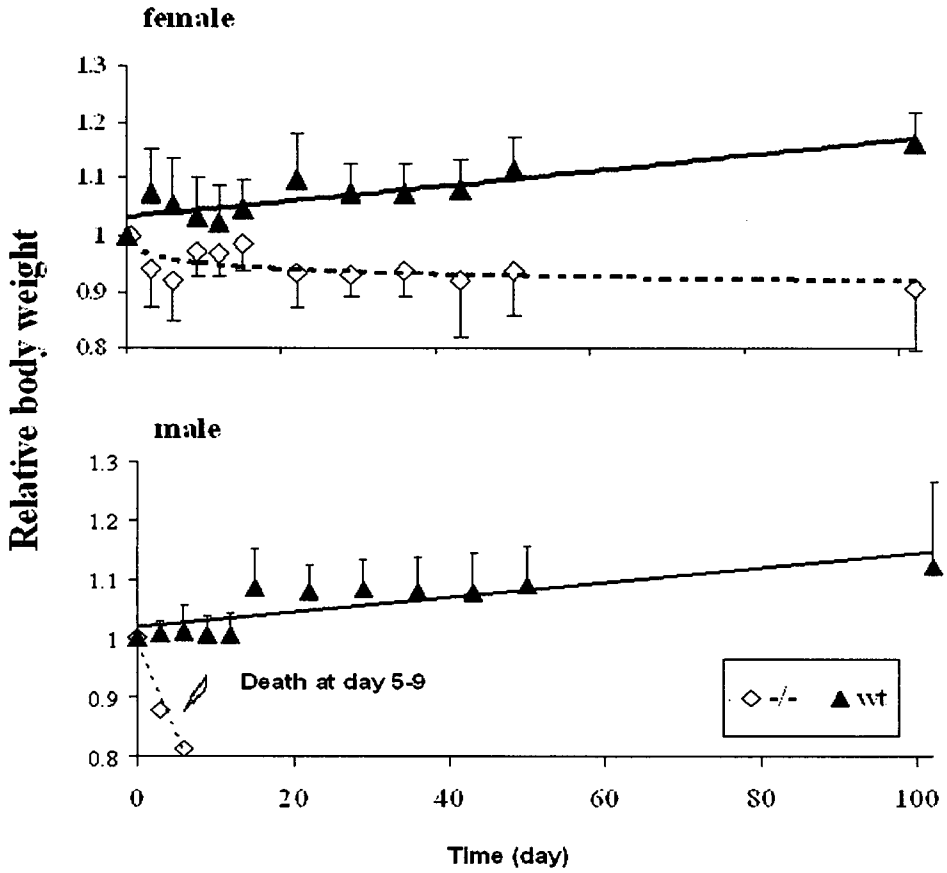
female
male
Relative body weight
1.3
1.2
1.1
1
0.9
0.8
Death at day 5-9
-/-
wt
0
20
40
60
80
100
Time (day)

Figure 7.

(B)

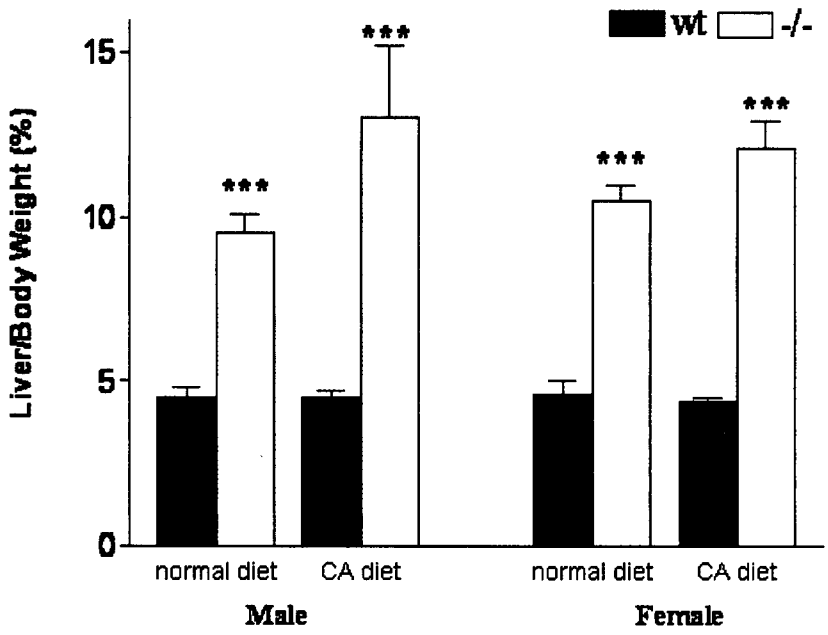
wt
-/-
Liver/Body Weight (%)
15
10
5
0
***
***
***
***
normal diet
CA diet
normal diet
CA diet
Male
Female

Table 9. Serum levels of proteins and enzymes in *spgp*$^{-/-}$ mice and controls fed with cholic acid diet.

Genotype	Bilirubin (μM)		Gamma-glutamyltransferase (U/L)		Alkaline phosphatase (U/L)		5'nucleotidase (U/L)		Aspartate aminotransferase (U/L)	
	M	F	M	F	M	F	M	F	M	F
+/+	4.7 ± 2.2	2.4 ± 0.6	19.8 ± 8.8	31.1 ± 10.9	123.6 ± 16.8	74.9 ± 3.4	197 ± 110	200 ± 48	100.4 ± 35.3	189± 92
+/-	4.6 ± 3.3	3.1 ± 1.6	12.2 ± 0	18.2 ± 6.6	88.2 ± 29.7	72.7 ± 12.0	301 ± 61	206 ± 25	45.0 ± 39.0	121 ± 37
-/-	66.8 ± 32.6	18.6 ± 8.3	12.5 ± 2.1	14.9 ± 7.3	209.0 ± 22.5	287.3 ± 83.1	299 ± 60	249 ± 30	513.3 ± 57.6‡	382 ± 112
Ratio (-/-):(+/+)	14.2	7.8	0.6	0.5	1.7	3.8	1.5	1.2	5	2
P value	0.009	0.008	0.159	0.048	0.001	0.002	0.211	0.354	0.002	0.038

Four wildtype and *spgp*$^{-/-}$ and three to seven heterozygote animals were used for analysis. Plasma was collected from mice fed with CA diet for 12 days, but plasma from male *spgp*$^{-/-}$ mice was collected between day 6-9 when they were terminally ill. M = male; F = female

‡Plasma from this group was analyzed from mice on CA diet for only four days. No analysis could be performed on plasma collected later due to the presence of interfering turbidity.

3.2.3. Bile acid concentration and distribution in *spgp*$^{-/-}$ mice after CA feeding

Bile acid secretion across the canalicular membrane is generally considered to be the rate-limiting step of the enterohepatic circulation. The relative concentration of bile acids in bile, plasma and liver are indicative of the efficiency of their canalicular secretion. We measured the bile acid concentration in plasma, liver and bile of *spgp*$^{-/-}$ mice to determine the efficiency and capacity of the alternative bile acid transport system to transport CA. Examination of the plasma bile acid concentration in *spgp*$^{-/-}$ mice after 2 days of CA feeding indicated that feeding of CA resulted in a great elevation of bile acids, especially in the plasma and liver of *spgp*$^{-/-}$ male mice (Fig. 8). In male *spgp*$^{-/-}$ mice on CA diet, plasma bile acid was 1.9 mM, 30-fold greater than wildtype (0.05 mM). In females, it was 7-fold greater than wildtype (0.5 mM versus 0.08 mM). Bile acid concentration in the liver of *spgp*$^{-/-}$ mice of both sexes was 2-fold that of wild-type (male 2.7 μmol/g versus 1.3 μmol and female 1.8 μmol/g versus 0.80 μmol). The concentrations of plasma and liver bile acids in male *spgp*$^{-/-}$ mice were correlated with the severity of pathological damage. Bile acid concentration in the bile of *spgp*$^{-/-}$ mice of both sexes was similar to that of wildtype when fed with the 0.5% CA diet (190mM and 160 mM for male *spgp*$^{-/-}$ and male wild-type mice respectively; 120mM and 200 mM for female *spgp*$^{-/-}$ and male wild-type mice respectively).

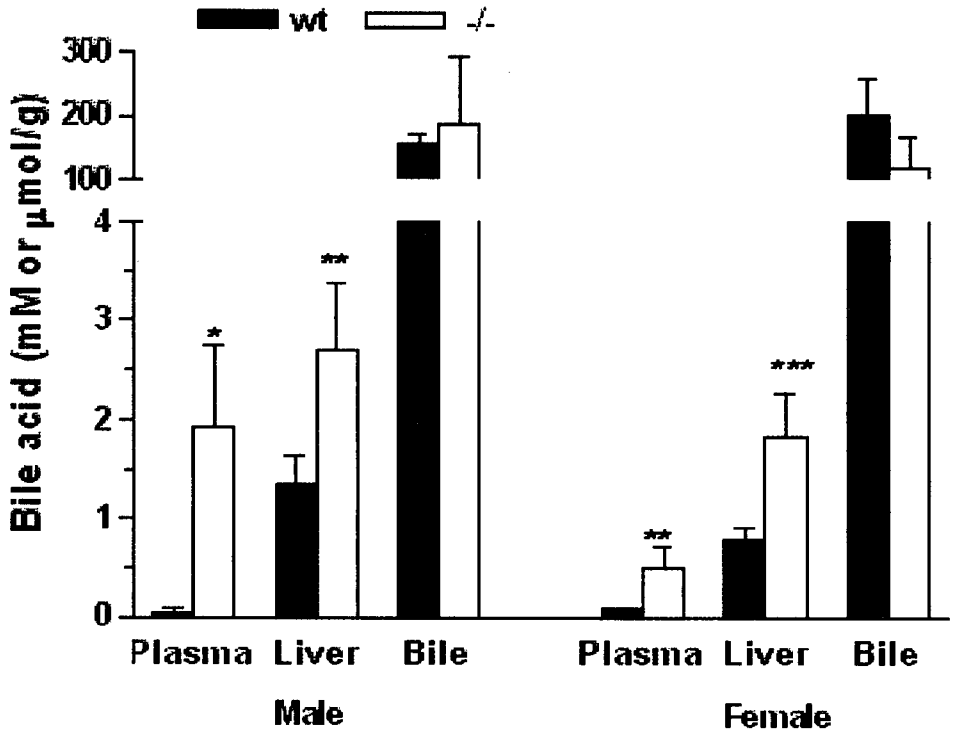

Fig. 8. Distribution of bile acids in plasma, liver and bile of *spgp*-/- mice.

Bile acid levels in plasma (mM), liver (µmol/g) and bile (mM) of mice on a diet containing 0.5% CA were measured. wt, wild-type; -/-, knockout. Asterisks indicate statistical significance between *spgp*$^{-/-}$ mice and wild-type of the same sex. *, 0.05>P>0.01; **, 0.01>P>0.001; ***, P<0.001; no asterisks, no statistical significance (n=3-5).

3.2.4. Cholesterol, phospholipids and triglyceride Levels

By visual inspection, the plasma of *spgp*$^{-/-}$ mice fed with CA diet was lactescent (milky) and showed a cream layer overlaying a turbid plasma layer (Fig. 9). The cause was not known; however, it was speculated that there would be disturbances in plasma lipid balance. Cholestasis has been associated with alterations in the concentrations and compositions of lipids and lipoproteins within the liver and plasma (Claudel et al. 2002). To investigate whether there were abnormalities in plasma lipoprotein metabolism in *spgp*$^{-/-}$ mice, hepatic lipids and plasma lipids concentration were measured. Dietary CA has been shown to have profound effects on plasma lipoproteins. In particular, CA has been shown to lower plasma levels of high-density lipoprotein (HDL) primarily by suppressing apolipoprotein A-I (apoA-I) mRNA level (Srivastava et al. 2000). ApoA-I is a major contributor to the synthesis of HDL particles. Therefore, downregulation of apoA-I leads to lower plasma HDL levels (Srivastava et al. 2000). On the basis of these studies, CA accumulation in *spgp*$^{-/-}$ mice liver has been postulated to regulate apoA-I level and decrease plasma HDL concentration.

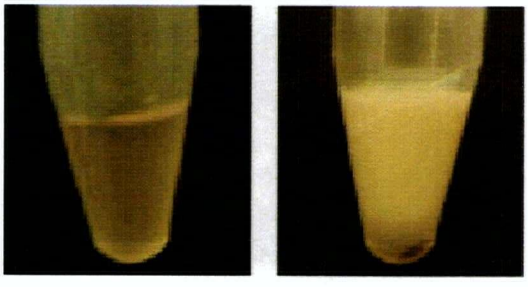

Fig. 9. Appearance of plasma of control and *spgp*-/- mice fed CA diet.

Blood from wildtype and *spgp*$^{-/-}$ mice was collected into tubes containing heparin and centrifuged in a microcentrifuge for 5min at 4^{O}C. Plasma was separated and stored at 4^{O}C for less than 1 week for lipid analysis. A representative example of the appearance of the plasma from wildtype (left panel) and from *spgp*$^{-/-}$ mice was shown.

3.2.4.1. Hepatic lipids

Table 10 summarizes the concentration of cholesterol, phospholipids, and triglycerides in liver and plasma of *spgp*$^{-/-}$ mice and control on normal diet or CA diet. Dietary CA suppressed mRNA expression level of CYP7A1, the rate-limiting enzyme in the classical pathway in bile acid biosynthesis (Chiang et al. 2000). This was expected to lead to slight increase in cholesterol level because cholesterol is the precursor to bile acid biosynthesis. Indeed, hepatic cholesterol concentration was greater (1.6-fold) in both wildtype and *spgp*$^{-/-}$ mice fed with cholic acid diet compared to normal diet. Hepatic cholesterol was slightly elevated in *spgp*$^{-/-}$ mice fed with CA diet compared with wildtype fed with the same diet. No significant difference in hepatic phospholipids or triglycerides in male mice was observed regardless of the diet and the genotype. In females, hepatic cholesterol, phospholipids and triglycerides were ~1.3 to 2.0-fold higher in *spgp*$^{-/-}$ mice fed with CA diet compared to wildtype mice fed with the same diet.

3.2.4.2. Plasma lipids

When maintained on a CA diet, plasma cholesterol, phospholipids concentrations were lower (3.5-fold (female) and 2.0-fold (male)) in *spgp*$^{-/-}$ mice than in wildtype mice (Table 10). Plasma triglycerides were elevated 2-fold in *spgp*$^{-/-}$ female mice compared to wildtype mice fed with CA diet. Notably, administration of CA diet caused a 6 to 8-fold decrease of HDL cholesterol in *spgp*$^{-/-}$ male and *spgp*$^{-/-}$ female mice and did not affect wildtype mice. Plasma triglyceride levels in *spgp*$^{-/-}$ female mice were elevated 2-fold compared to wildtype mice after CA feeding. This observation was consistent with a hyperlipoproteinemia/hypertriglyceridemia serum profile. Further work is necessary to elucidate the mechanism for CA-induced elevation in plasma triglycerides.

Selective gene expression levels that might affect serum HDL cholesterol level were measured (Table 11). Apo-AI mRNA level was decreased in *spgp*$^{-/-}$ mice consistent with the idea that a higher CA level in the knockout suppressed apoAI synthesis pathway. Complete analysis of CA-induced regulation of all potential genes involved lipids and lipoprotein metabolism has not been investigated. The expression of other genes such as low density

lipoprotein receptor (LDLR) and acyl-CoA cholesterol acyltransferase (ACAT) were not significantly changed.

Table 10. Plasma and liver lipid profiles of wildtype and *spgp*-/- mice.

	Male				Female			
	Regular diet		0.5% CA 2 days		Regular diet		0.5% CA 2 days	
Lipid	Wildtype	-/-	Wildtype	-/-	Wildtype	-/-	Wildtype	-/-
Plasma Cholesterol (mg/dl)	124.1± 17.4	99.1 ± 2.4	162.5 ± 9.4	46.1 ± 15.5 ***	98.9 ± 7.2	74.2 ± 10.7 *	156.3 ± 33.0	27.0 ± 8.4 ***
Plasma HDL-cholesterol (mg/dl)	50.7 ± 7.9	34.4 ± 1.7 *	51.2 ± 8.9	6.7 ± 1.4 ***	40.9 ± 2.3	26.1 ± 3.9 *	43.4 ± 4.1	7.0 ± 0.6 ***
Plasma Phospholipids (mg/dl)	187.9 ± 19.7	173.8 ± 27.4	183.8 ± 47.9	82.8 ± 27.0 **	164.6 ± 13.9	134.8 ± 14.6	153.1 ± 30.7	53.6 ± 11.8 **
Plasma triglycerides (mg/dl)	93.4 ± 12.5	184.2 ± 72.8	84.7 ± 24.5	156.2 ± 90.0	102.5 ± 22.8	170.3 ± 20.5 *	56.6 ± 2.7	119.4 ± 12.2 **
Liver Cholesterol (mg/g)	2.53 ± 0.12	2.98 ± 0.49	4.00 ± 0.42	4.89 ± 0.39 **	2.98 ± 0.58	2.88 ± 0.33	4.29 ± 0.81	5.71 ± 0.33 **
Liver Phospholipids (mg/g)	42.90 ± 3.76	40.75 ± 3.57	46.34 ± 4.14	49.87 ± 0.81	44.01 ± 5.74	42.33 ± 3.88	40.36 ± 2.96	60.28 ± 4.96 **
Liver triglycerides (mg/g)	1.17 ± 0.65	1.27 ± 0.51	2.53 ± 1.82	2.02 ± 1.00	1.98 ± 0.26	2.60 ± 0.87	2.10 ± 0.36	6.32 ± 0.51 **

Asterisks indicate statistical significance between the *spgp*$^{-/-}$ mice and the same sex wild-type mice, *, $0.01 < P < 0.05$; **, $0.001 < P < 0.01$; ***, $P < 0.001$.

Table 11. Relative mRNA expression of liver genes and *spgp* gene in wildtype and *spgp*-/- mice fed with normal or CA diet for two days.

Liver genes related to lipid homeostasis	Gene Symbols	Normal diet				CA diet for two days			
		female wt	male wt	female -/-	male -/-	female wt	male wt	female -/-	male -/-
	ApoA1	1.00 ± 0.35	1.13 ± 0.19	0.47 ± 0.17	0.64 ± 0.08 **	0.68 ± 0.26	0.64 ± 0.10	0.27 ± 0.10 *	0.47 ± 0.12
	HMGCoA-R	1.00 ± 0.57	1.19 ± 0.42	3.36 ± 0.60	5.50 ± 1.14 **	0.88 ± 0.17	0.67 ± 0.13	3.73 ± 1.96	4.18 ± 3.33
	LDLR	1.00 ± 0.24	1.21 ± 0.09	1.91 ± 0.08	1.31 ± 0.06	1.18 ± 0.02	0.67 ± 0.02	1.66 ± 0.06 *	1.93 ± 0.17
	ACAT (Soat1)	1.00 ± 0.27	0.72 ± 0.25	1.17 ± 0.11	0.84 ± 0.20	0.97 ± 0.22	0.34 ± 0.25	0.86 ± 0.16	1.35 ± 0.87

Amount of mRNA was determined by Real Time PCR and normalized against ribosomal protein S15 as described in the Materials and Methods. The level of female wild-type mRNA was set at 1. All numbers are expressed as a ratio of female wild-type mRNA, mean ± standard deviation, n = 2-4. Asterisks indicate statistical significance between the *spgp*$^{-/-}$ mice and the same sex wild-type mice, *, $0.01 < P < 0.05$; **, $0.001 < P < 0.01$; ***, $P < 0.001$.

3.2.5. Effect of CA feeding on bile acid output

In agreement with previous reports (Perwaiz et al. 2003), HPLC analysis of various bile samples revealed only two major bile acid species, taurocholic acid and tauromuricholic acid with traces of tauroursodeoxycholic acid (Fig. 10). The individual peaks were compared with a bile acid standard and quantitated by a standard curve generated over a concentration range. Each peak was collected and identity was verified by electrospray mass spectrometry.

Previously, we reported that bile acid output on normal diet was about 20nmol/min/g liver and 4nmol/min/g liver in wildtype and *spgp*$^{-/-}$ mice, respectively (Wang et al. 2001). Under normal diet, bile flow rate was 0.6μl/min/g liver in *spgp*$^{-/-}$ mice, and it was not significantly different from wildtype mice (Wang et al. 2001). Table 12 showed bile flow rate and bile acid output in *spgp*$^{-/-}$ mice compared to controls under CA diet. CA feeding significantly stimulated bile flow of wildtype and *spgp*$^{-/-}$ male mice. There was no significant difference between the genotype (~1.8-2.0μl/min/gliver). Furthermore, total bile acid output rate in male *spgp*$^{-/-}$ mice fed with CA for 2 days was not significantly different than bile acid output rate measured in wild-type controls (86 nmol/min/g liver versus 77 nmol/min/g liver respectively) (Table 12). Although there was no significant difference in total concentration and total bile acid output between wildtype and *spgp*$^{-/-}$ mice, there was significant difference in the output of individual bile acid species (Table 12). CA secretion rate in wildtype and *spgp*$^{-/-}$ mice was 75% and 52% of total bile acid output respectively. Total muricholic acids represented 21% and 39% of wildtype and *spgp*$^{-/-}$ mice respectively. Significant difference was also observed with tetrahydroxylated bile acids output, which represented 7% of total bile acid output in *spgp*$^{-/-}$ mice, while it was barely detectable in the bile of wildtype mice. The high bile acid output in *spgp*$^{-/-}$ mice suggested that the mutant mice had the ability to secrete bile acids under supraphysiological concentration.

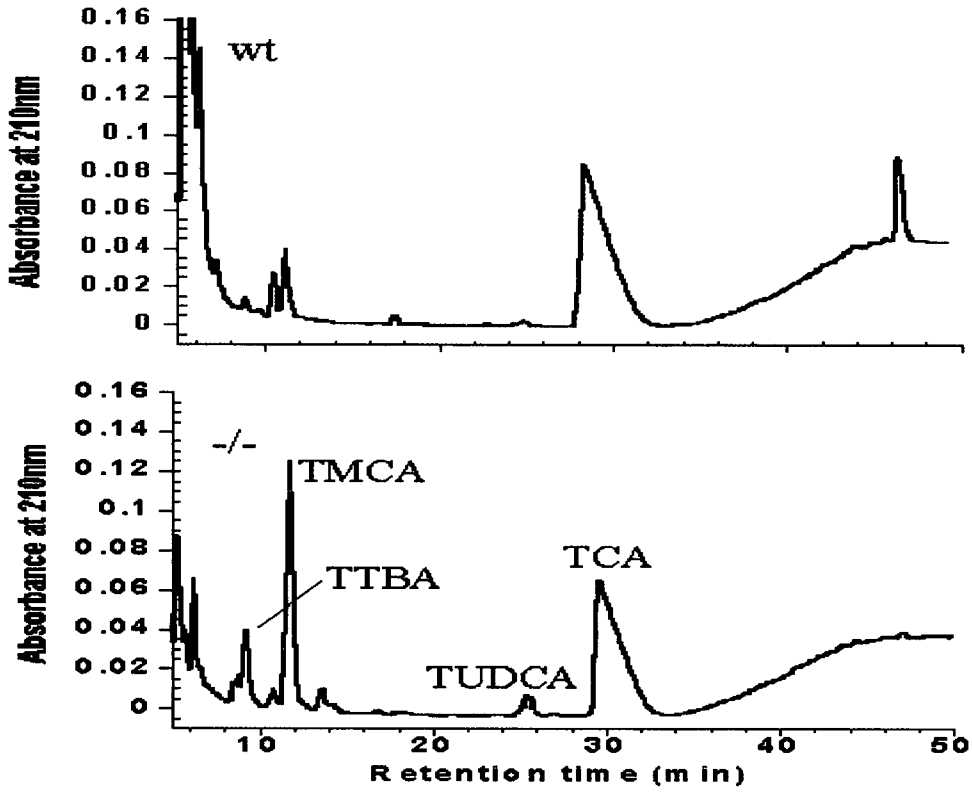

Fig. 10. Representative HPLC profiles of bile samples from wildtype and *spgp*-/- mice fed with CA diet.

Bile samples were collected from both wildtype and spgp-/- mice and separated and quantitated using HPLC measured by absorbance at 210nm as described in materials and methods. The concentration of each bile acid species was determined against a standard. The peaks marked as taurocholate (TCA), tauro-β-muricholate (TMCA) and tetrahydroxylated bile acids (TTBA) were collected and each identity was verified by liquid-chromatography tandem mass spectrometry (LC/MS/MS) and electrospray mass spectrometry (ESI/MS). wt, wildtype; -/-, knockout.

Table 12. Comparison of biliary output of bile acid species in wildtype and *spgp*-/- male mice on CA diet

Bile acid species	Biliary clearance		Significance (p value)
	wildtype (n=4)	*spgp*$^{-/-}$ (n=5)	
Bile flow rate (µl/min/g liver)	2.02 ± 0.29	1.82 ± 0.24	0.35
Total bile acids (nmol/min/gliver)	86.36 ± 14.10 (100%)	77.05 ± 15.98 (100%)	0.38
Taurocholic acid	73.97 ± 15.07 (75%)	42.61 ± 19.64 (52%)	< 0.02
Tauromuricholic acids	20.41 ± 2.27 (21%)	31.76 ± 3.19 (39%)	< 0.01
Tauroursodeoxycholic acid	1.04 ± 0.28 (1%)	1.71 ± 1.02 (2%)	0.20
Tetrahydroxylated bile acids	0.73 ± 0.70 (0.01%)	6.14 ± 1.22 (7%)	0.001

Bile was collected for 40 minutes and its bile acid composition analyzed by HPLC as described in Materials and Method. Bile acid secretion rate (nmol/min/gliver) was calculated from the determined concentration (mM) x bile flow rate measured as the volume of bile collected per unit time per g liver. The percentage of total bile acid secretion is reported in parentheses. Statistical significance was determined using 2-tailed t-test and p-value of 0.05.

3.2.6. Effects of acute taurocholate infusion on short-term taurocholate clearance in *spgp*$^{-/-}$ mice

Hepatocellular secretion of bile acids is a rapid process occurring within a few minutes after intravenous injection or perfusion of a bile acid into an animal. In wildtype mice, the bile to plasma ratio was over 1000-fold, while in knockout mice, this ratio was significantly decreased to 200-fold (Fig. 8). The *spgp*$^{-/-}$ mice on CA diet developed hepatotoxicity despite the large capacity for bile acid secretion. This indicated that Spgp was the more efficient canalicular bile acid transporter. We hypothesized that the efficiency of bile acid transport was affected in knockout mice. To investigate the ability of *spgp*$^{-/-}$ mice to secrete bile acids, taurocholic acid and tauroursodeoxycholic acid were individually infused into the mice and the bile flow rate and biliary taurocholate output were determined. Because bile acids are a major driving force for bile flow, we also determined if there was an expected effect of TCA stimulation of bile flow in *spgp*$^{-/-}$ mice.

As expected, taurocholate infusion at 10-minute time point stimulated bile flow rate in wildtype mice of both sexes regardless of diet (Fig. 11A, C). However, taurocholate infusion did not affect bile flow rate in *spgp*$^{-/-}$ mice in both sexes fed either control or CA diets (Fig. 11A, C). The bile flow rate of female *spgp*$^{-/-}$ mice was significantly less than wildtype control and male *spgp*$^{-/-}$ mice (Fig. 11A, C – lower time trace). These results suggested that there was a strong sex dimorphism in bile flow rate that might not be dependent on Spgp expression because there was no difference observed in wildtype male and female mice. In addition, *spgp* mRNA level was not significantly different in male and female wildtype mice (Table 13). Protein analysis by Western immunoblotting with male and female wildtype mouse livers was also consistent with mRNA expression data (data not shown).

In wildtype mice, acute taurocholate injection at 10-minute time point resulted in the immediate clearance as measured by a peak occurring at 3min after taurocholate injection. Taurocholate output was increased about 20-fold, from the basal level of 12.3 ± 5.2 nmolmin^{-1}g^{-1} liver to the stimulated level of 233.3 ± 124.0 nmolmin^{-1}g^{-1} liver (Fig. 11B). Male and female wildtype mice displayed similar taurocholate output and profile suggesting the same

Spgp-dependent mechanism of transport. The overall profiles of taurocholate output in male and female knockout mice were very different from that of the taurocholate output curve in wildtype mice (Fig. 11B – dotted traces). Taurocholate output rate was at least 25-fold lower in knockout mice compared to controls on normal diet. Taurocholate infusion produced a slight and prolonged increase in output that appeared to saturate at approximately 10 minute after stimulation. A sex-dependent difference was again observed in the knockout mice. In the female knockout mice, taurocholate administration produced an apparent smaller continuous increase in output with no decline within the time analysed (Fig. 11B). Bile salt output was correlated with bile flow rate.

Closer examination of Fig. 11 revealed that a small peak in *spgp*$^{-/-}$ mice immediately after the injection of taurocholate, suggesting that there was an over compensation in bile acid output and bile flow before returning to a lower steady level. Furthermore, basal bile acids output in knockout mice was similar to that as wildtype mice on CA diet. Peak rate of bile acid output was 5-fold lower in *spgp*$^{-/-}$ mice compared to wildtype mice (Fig. 11D). This difference in response between wildtype and *spgp*$^{-/-}$ mice was observed for both taurocholate and tauroursodeoxycholic acids (data not shown). These results suggest a few characteristics of the alternative system. A short-term response was apparent but could only sustain a much lower rate of bile flow and bile acid output. A delayed response was initiated from CA feeding resulting in the same basal rate of bile acid secretion and bile flow in *spgp*$^{-/-}$ mice as in wildtype mice.

Fig. 11. Taurocholate clearance as a function of liver weight in wildtype and *spgp* -/- male and female mice after CA-supplemented diet for 2 days.

Mice were anesthetized by intraperitoneal injection of Ketamine (112.5 mg/kg) and Xylazine (11.3 mg/kg) after 2 to 4 hours fast. The abdomen was opened, and gallbladder was cannulated using a PE-10 catheter after distal common bile duct ligation. After 20 minutes of bile flow equilibration, bile was collected into pre-tared tubes at 5-minute intervals for 10 minutes. Mice were then infused with the sodium salt of taurocholic acid (100μmol/kg) for 10 seconds (arrow). Bile samples were collected at different time points, 0, 5, 10, 12, 14, 16, 18, 20 and 30 minute from the start of bile collection.

Eight different groups of mice were tested: male wildtype, male spgp-/-, female wildtype and female spgp-/- fed normal diet and 0.5% cholic acid diet. Panels *A*, *B* show results of (A) bile flow rate and (B) bile acid output observed with mice fed normal diet. Panels *C*, *D* show results of (C) bile flow rate and bile acid output (D) observed with mice fed 0.5% cholic acid for 2 days.
(■) male wildtype (n = 5); (□) male spgp-/- (n = 4); (●) female wildtype (n = 4); (○) female spgp-/- (n = 4). Data are represented as means ± SEM.

Figure 11A, B

A. Bile flow rate (µl/mingliver)

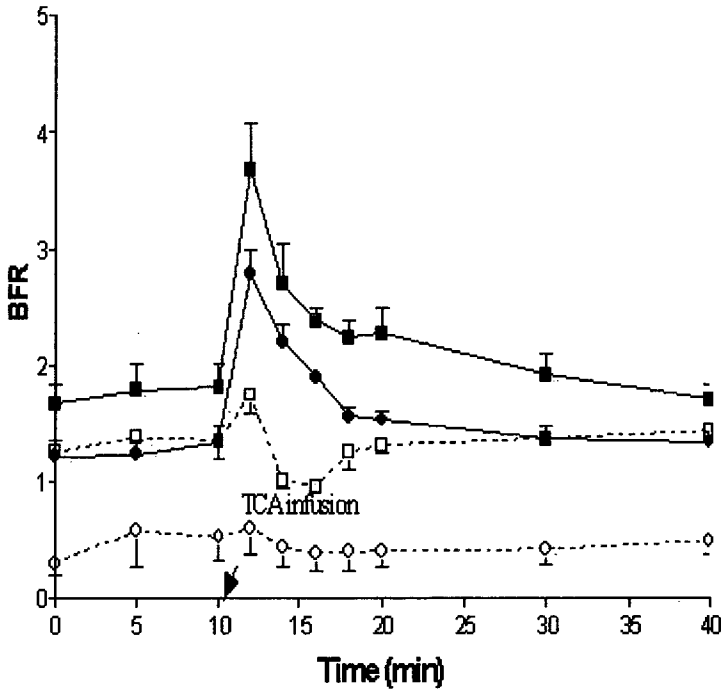

B. Taurocholate output (nmol/mingliver)

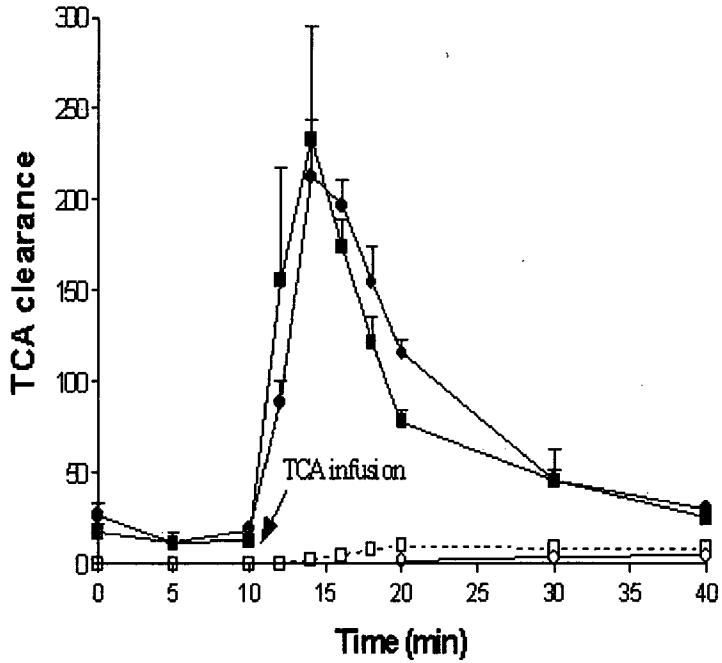

Figure 11 C, D

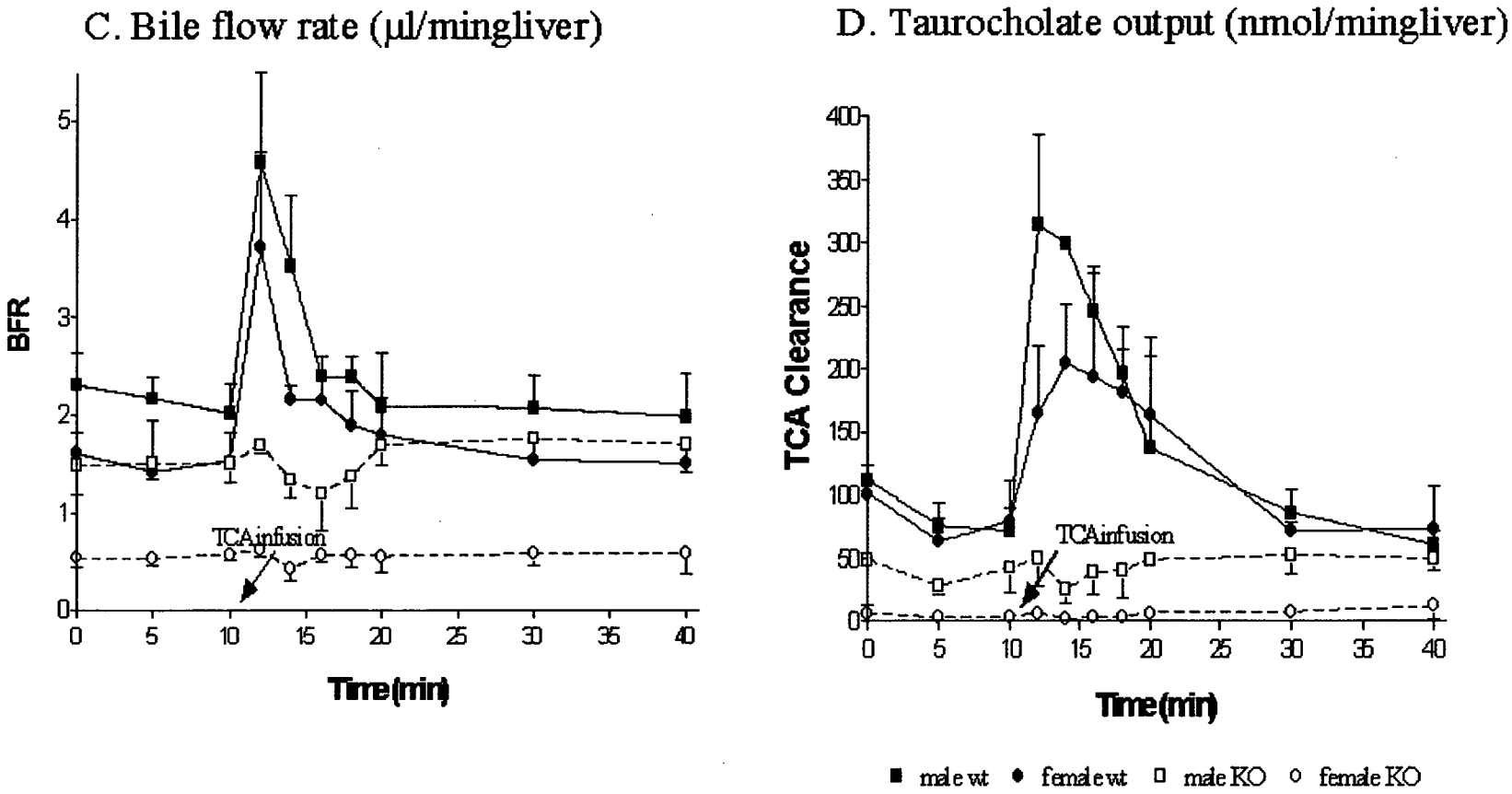
C. Bile flow rate (µl/mingliver)
BFR
Time(min)
TCAinfusion
D. Taurocholate output (nmol/mingliver)
TCA Clearance
Time(min)
TCAinfusion
male wt
female wt
male KO
female KO

3.2.7. ABC transporter expression in *spgp*$^{-/-}$ mice

Cholestasis has been associated with retention of potentially toxic bile acids and alterations in hepatocellular transporters expression. So far, the focus has been on the level of transcription and posttranscriptional regulation. In this study, we investigated the expression of a number of transporters by real-time PCR (Table 14), immunofluorescence staining (Fig. 12) and Western blotting (Fig. 13) to evaluate some of the molecular changes in *spgp*$^{-/-}$ mice. The categories of liver genes chosen consisted mainly of canalicular and basolateral ABC transporters, and the basolateral bile acid transporter, Ntcp. Fig. 14 summarizes the results from these studies. Several interesting expression patterns were noted. All the canalicular ABC transporters examined at the protein level including Mdr1a, Mrp2, Mdr2 and Mrp3 were upregulated in *spgp*$^{-/-}$ mice on normal and CA diet compared to wildtype mice fed the same diet (Fig. 12 and 13). The basolateral bile acid transporting polypeptide Ntcp was downregulated (Fig. 13). These results indicated that protein levels of bile acid transporters such as Ntcp and Mrp3 were regulated consistent with their functions in enterohepatic circulation of bile acids. Ntcp protein level was significantly decreased ($P<0.05$; Fig. 13) in *spgp*$^{-/-}$ mice fed with normal diet, reduced to almost undetectable level under CA diet. CA feeding had no significant effect on *ntcp* and *mrp2* steady state mRNA levels (Table 14). However, Mrp2 protein level was increased 3-fold ($P<0.05$) in *spgp*$^{-/-}$ mice and CA diet did not increase this level further. Mrp2 protein level was also increased in wildtype mice when fed with CA diet. Taken together, these results suggest that cholic acid modulated Mrp2 protein level perhaps by posttranscriptional modifications such as protein targeting.

Fig. 14 illustrates the alterations in hepatocellular transporters expression at the mRNA and protein levels. Under normal diet, the level of bile acids reached in *spgp*$^{-/-}$ mouse liver might not be high enough to trigger induction of transcriptional regulation. Concentrations of bile acid in the range of 50μM have been demonstrated to be sufficient to upregulate *spgp*, *mrp2, mrp3* and to downregulate *ntcp* (Wang et al. 1999b). Although the concentration of liver bile acid of *spgp*$^{-/-}$ mice is in this range, a still higher concentration of bile acid might be required for *in vivo* effect. No significant alterations in a number of the

mRNA expression until mice were fed with CA. Nevertheless, Mdr1a and Mrp3 appeared to have correlated mRNA and protein expressions suggesting that transcriptional regulation was probably the predominant control of their expressions in *spgp*$^{-/-}$ mice. However, posttranscriptional modification of Mdr1 has been sugggested in which Mdr1 protein level may increased (2-4-fold) following administration of bile acid (Kipp, 2001).

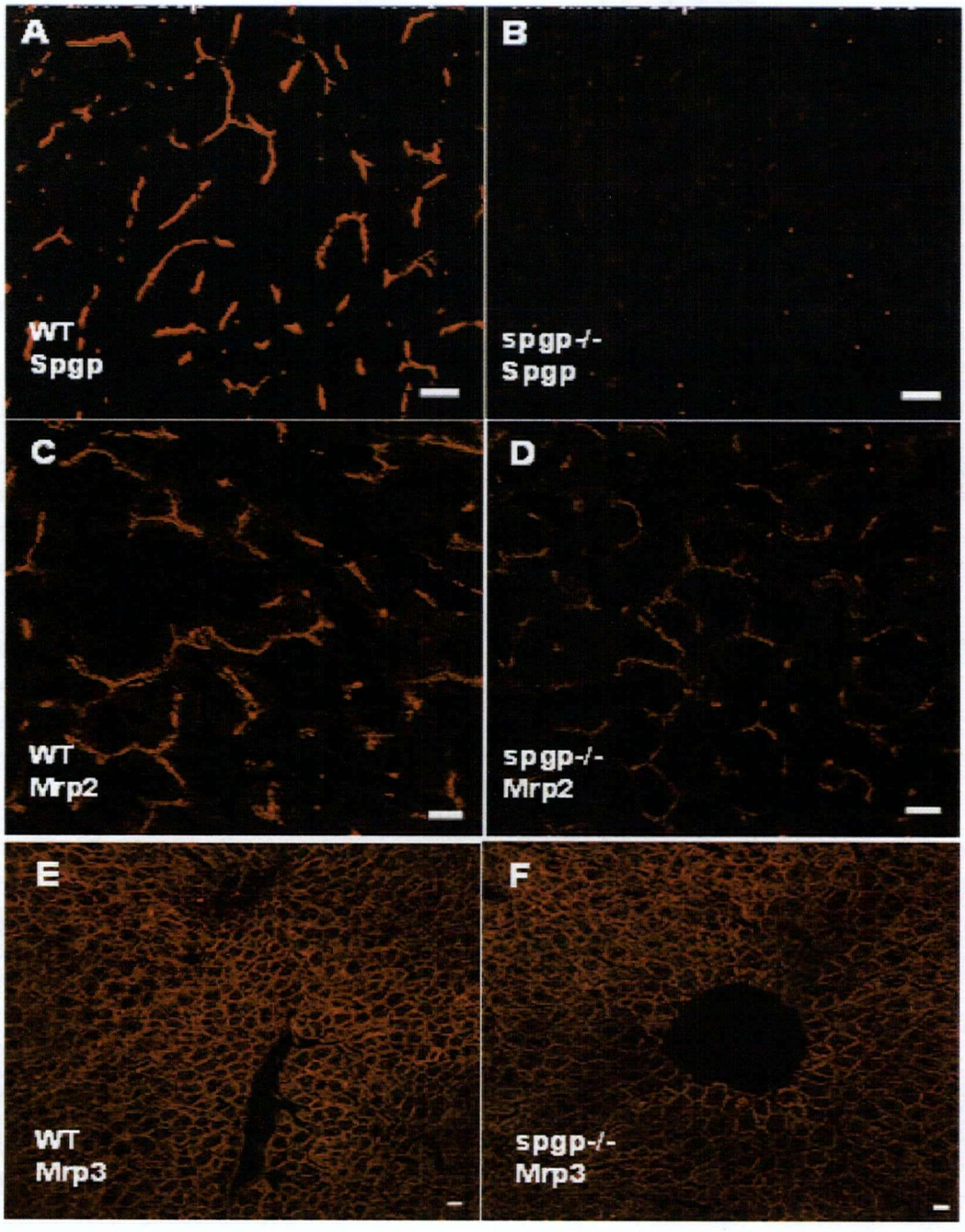

Fig. 12. Immunofluorescent staining of canalicular proteins in wildtype and *spgp*-/- mice.

Liver sections were stained as described in Materials and Methods. IW polyclonal antibody showed canalicular staining of Spgp protein in wildtype mice (left panel) but not in *spgp*$^{-/-}$ mice. EAG15 antibody recognized Mrp2 protein and showed positive canalicular staining in wildtype mice and *spgp*$^{-/-}$ mice. Mrp3 antibody recognized Mrp3 protein and showed positive basolateral staining in wildtype and *spgp*$^{-/-}$ mice. Bar = 10μM

A.

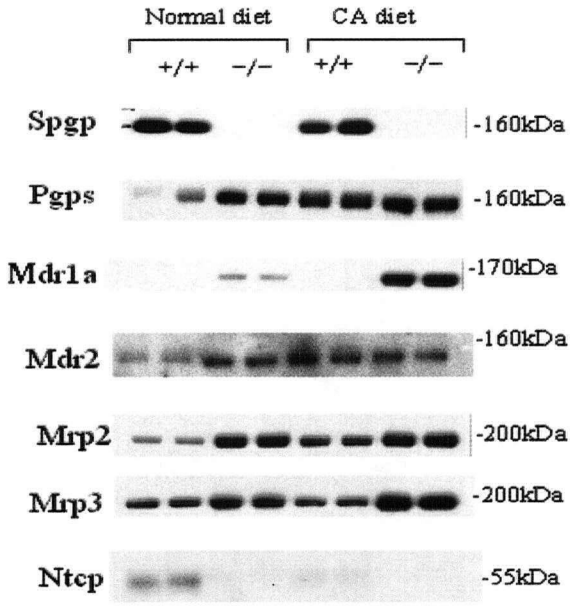

B.

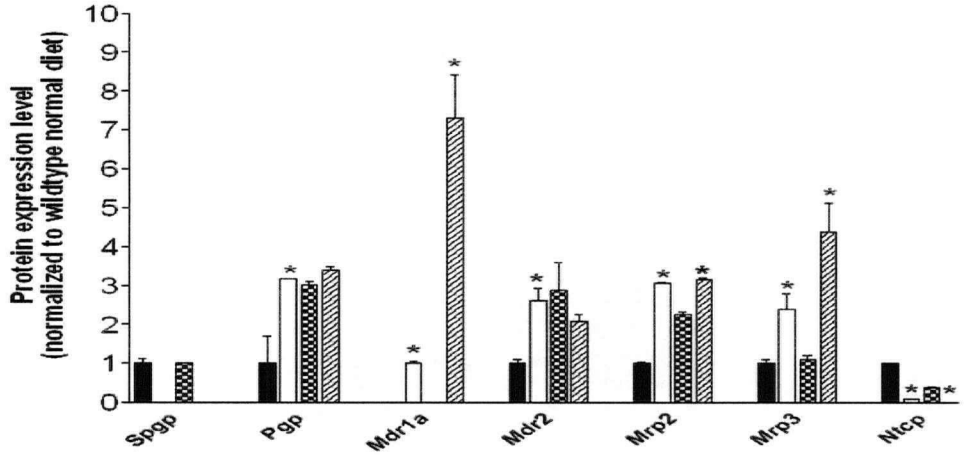

Fig. 13. Effect of disruption of *spgp* on the expression of other canalicular membrane proteins.

Membrane fractions were isolated from livers obtained from wildtype and knockout mice. Representative western blots after probing for Spgp (1:5000 IW); Pgps (1:2000 C219); mdr1a (1:100); Mrp2 (1:5000); Mdr2 (1:100); Ntcp (1:1000) are shown in (A). Compared with wildtype mice, change in expression is determined by band intensities. $P<0.05$ vs. wildtype controls of the same diet (n=4 in each group). WT, normal diet (black bar); *spgp*-/- mice, normal diet (white bar); WT, 0.5% CA diet (checker bar); *spgp*-/- mice, 0.5% CA diet (diagonal bar).

Table 13. Relative mRNA expression of canalicular and basolateral membrane proteins in wildtype and *spgp*$^{-/-}$ mice fed with normal or CA diet.

		Normal diet				CA diet for two days			
Canalicular and Basolateral Membrane Proteins	Gene Symbols	female wt	male wt	female -/-	male -/-	female wt	male wt	female -/-	male -/-
	mdr1a (Abcb1a)	1.00 ± 0.41	0.31 ± 0.08	2.80 ± 0.85 *	1.70 ± 0.78 *	1.53 ± 0.69	0.40 ± 0.09	3.85 ± 0.64 ***	3.39 ± 0.89 **
	mdr1b (Abcb1b)	1.00 ± 0.35	0.83 ± 0.07	1.42 ± 0.28	1.09 ± 0.30	1.31 ± 0.14	0.75 ± 0.17	1.64 ± 0.16 *	1.73 ± 0.54 *
	mdr2 (Abcb4)	1.00 ± 0.38	1.05 ± 0.47	1.99 ± 0.81	1.37 ± 0.83	1.15 ± 0.37	0.83 ± 0.48	1.28 ± 0.26	1.90 ± 0.90
	mrp2 (Abcc2)	1.00 ± 0.21	1.14 ± 0.21	0.96 ± 0.29	0.96 ± 0.42	1.06 ± 0.15	0.98 ± 0.37	1.09 ± 0.35	1.07 ± 0.33
	mrp3 (Abcc3)	1.00 ± 0.27	0.79 ± 0.32	1.47 ± 0.43	1.16 ± 0.58	0.98 ± 0.18	0.55 ± 0.25	1.44 ± 0.12 **	1.74 ± 0.27 ***
	ntcp (Slc10a1)	1.00 ± 0.29	0.82 ± 0.06	0.88 ± 0.33	0.94 ± 0.20	0.62 ± 0.17	0.50 ± 0.12	0.54 ± 0.11	0.49 ± 0.12
	spgp (Abcb11)	1.00 ± 1.05	1.32 ± 1.09	0.00 ± 0.00	0.00 ± 0.00	2.27 ± 2.42	1.17 ± 1.29	0.00 ± 0.00	0.00 ± 0.00

Amount of mRNA was determined by Real Time PCR and normalized against ribosomal protein S15 as described in the Materials and Methods. The level of female wild-type mRNA was set at 1. All numbers are expressed as a ratio of female wild-type mRNA, mean ± standard deviation, n = 2-4. Asterisks indicate statistical significance between the *spgp*$^{-/-}$ mice and the same sex wild-type mice, *, $0.01 < P < 0.05$; **, $0.001 < P < 0.01$; ***, $P < 0.001$.

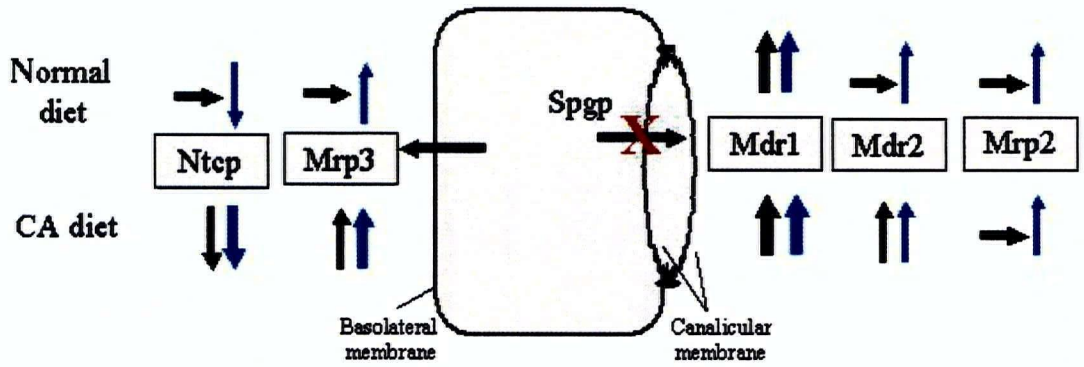

Fig. 14. Schematic representation of alterations in hepatocellular transport expression in *spgp*-/- mice.

Expression of transporters in basolateral and canalicular membranes in *spgp*$^{-/-}$ mice is represented here under normal and 0.5% cholic acid diets (CA). mRNA levels (left arrow) were measured by real time PCR (data not shown) and protein levels (right arrow) were measured by Western immunoblotting.

3.3. Discussion

3.3.1. CA fed *spgp*$^{-/-}$ mice is a good model system for PFIC2

In humans, mutations in the *spgp* gene result in a fatal liver disease, PFIC2. Presentation of PFIC2 is similar to neonatal hepatitis in infancy but it rapidly progresses to liver failure in the first decade. PFIC2 is characterized by growth retardation, jaundice, hepatomegaly, elevated serum bile acids, low levels of γ-GT, elevated aminotransferases, elevated alkaline phosphatase activity, histological features of neonatal hepatitis, marked hepatocellular death, cholangiopathy, cirrhosis and liver failure (Strautnieks et al. 1998; Jansen et al. 1999). In *spgp*$^{-/-}$ mice, changes in the bile acid composition influenced the extent of cholestatic phenotype. We have shown that cholic acid was able to induce pathological, biochemical and molecular changes in *spgp*$^{-/-}$ mice. This is in line with our hypothesis that the severity of the disease is determined by bile acid composition. The observations made in this study suggest CA-fed *spgp*$^{-/-}$ mice recapitulated the phenotypes of PFIC2, and therefore is a good mouse model for the disease. First, symptoms between the two species are similar. These included significant loss in body weight, elevated bile acid accumulation in liver and blood, low γ-GT, high aminotransferases and ALP, liver cell damage and cholangiopathy in females, and marked hepatocellular necrosis/apoptosis and high fatality rate in males. Second, molecular changes in *spgp*$^{-/-}$ mice were consistent with the features of cholestasis. The canalicular multidrug resistance proteins Mdr1a, Mdr1b and Mrp2 were upregulated. The basolateral sodium-dependent bile acid cotransporter, Ntcp, was downregulated. These results are consistent with previous findings in various experimental and clinical cholestatic conditions (Lee et al. 2000) and in CA and UDCA-fed mice (Fickert et al. 2001), which were characterized by elevated bile acid levels.

To determine the extent of the compensation, bile flow rate and bile acid secretion were measured. This addresses two issues, the capacity of the redundant pathway for bile acid secretion and the substrate preference of each transport pathway. The results showed distinct features of bile acid secretion in *spgp*$^{-/-}$ mice from wildtype mice. Infusion of taurocholate increased significantly bile flow and bile acid output only in wildtype and not in *spgp*$^{-/-}$ mice. Bile acid concentration was at the same level for wildtype and *spgp*$^{-/-}$ mice

after CA feeding. These results suggest that a high capacity bile acid transport system was operating under cholestatic condition and was more sensitive to bile acid loading than bile acid flux through the liver. A 'rain barrel' model (Fig. 15) is presented to demonstrate bile acid secretion under two sets of conditions, a physiological condition when Spgp is operational and a cholestatic condition when an alternative transporter is compensatory. Spgp expression and transport activity is highly sensitive to bile acid flux through the liver and low level of bile acids. The alternative transporter seems to be highly responsive only when toxic level of bile acids is accumulated in the liver. So far, our data agree with this model. In *spgp*$^{-/-}$ mice fed with normal diet, tauromuricholic acid secretion was not affected while taurocholic acid secretion was significantly suppressed. However, CA feeding increased the taurocholic acid pool in *spgp*$^{-/-}$ mice that resulted in the concomitant increase in taurocholic acid output.

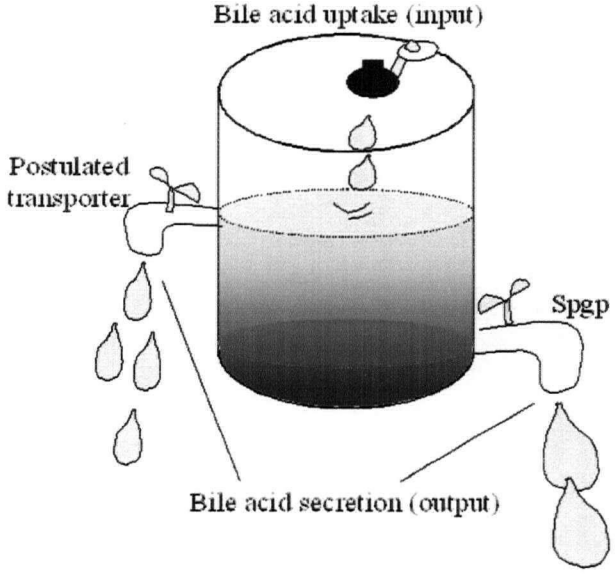

Fig. 15. Water barrel model of the capacity of Spgp and Spgp-independent bile acid transport in the liver of wildtype mice and *spgp*$^{-/-}$ mice.

A dramatic 6-8-fold decrease in plasma high-density cholesterol in *spgp*$^{-/-}$ fed with CA but not in wildtype mice fed with the same diet. These data indicated that *spgp*$^{-/-}$ mice had an altered serum lipoprotein profile that was exacerbated by increased dietary CA. Low serum HDL level and low serum apoA-I have been reported in PFIC patients with low γGT and biochemical characteristics of type 1 and type 2 PFIC (Claudel et al. 2002). Studies from apoA-I transgenic mice, apoA-I promoter construct analysis and electrophoresis mobility shift assays have demonstrated that bile acids activate the nuclear receptor FXR, which negatively regulates apoAI transcription (Srivastava et al. 2000). Therefore, a proposed mechanism of plasma HDL alteration in *spgp*$^{-/-}$ mice was that CA alone activated the nuclear receptor FXR, effectively downregulating apoA-I, which is a major component of the HDL particle. The mRNA level of apoA-I was decreased in *spgp*$^{-/-}$ mice consistent with the hypothesis that HDL formation might be affected.

3.3.2. Sexual dimorphism in alternative bile acid transport in *spgp*$^{-/-}$ mice

The ability to secrete more bile acids when mice are fed with CA does not seem to determine the viability of the mutant mice. S*pgp*$^{-/-}$ male mice died within 5-9 days of feeding on cholic acid diet. *Spgp*$^{-/-}$ female mice, in comparison, secrete significantly less bile acids but continue to thrive on the same diet. The molecular basis of the dietary CA induced phenotype and sex-dependent difference in bile acid secretion in *spgp*$^{-/-}$ mice is not known. It is thought that subtle differences in bile acid retention in the liver may contribute to the cholestatic phenotype. *Spgp*$^{-/-}$ female mice accumulate consistently less bile acid in the liver when fed CA diet. Analysis of fecal bile acids recovered from one mouse so far, showed that *spgp*$^{-/-}$ male and female mice had similar fecal bile acid ouput, although biliary bile acid secretion was at least 2 times higher in *spgp*$^{-/-}$ male mice (data not shown). These results suggest that reabsorption processes from the small intestine might be a limiting step in transporting bile acids back to the liver. Analysis at the molecular changes in the ileum bile acid transporter (I-batp) and other potential bile acid associated protein(s) in both sexes may provide some clues to the gender differences in the biliary physiology of *spgp*$^{-/-}$ mice.

3.3.3. Bile acid selectivity of the alternative bile acid system

In wildtype mice, the amount of individual bile acids in the bile was in the order of taurocholic acid (TCA) > tauromuricholic acids (TMCA) > taurochenodeoxycholic acid (TCDCA) ≥ tauroursodeoxycholic acid (TUDCA) ≥ taurodeoxycholic acid (TDCA). On the other hand, the amounts of TMCA and tetrahydroxylated bile acids were highest in the bile of *spgp*$^{-/-}$ mice (Wang et al. 2001). This study further confirms the idea that Spgp and Spgp-independent system in the canalicular membrane have different specificity for bile acids and that the latter has a preference for hydrophilic bile acids.

Despite the high output of bile acids in *spgp*$^{-/-}$ mice, this capacity was not able to protect *spgp*$^{-/-}$ mice from progressive cholestasis. From this study, it appeared that a number of criteria must be met in order to protect the mice. First, rapid CA and UDCA clearance associated with Spgp is required (Fig. 11). Second, a more efficient system with similar rate of secretion of conjugated CA, taurocholic acid like Spgp is also required (Table 12). Third, an active and continuous hydroxylation system to convert CA to the hydrophilic bile acid as a mechanism of detoxification with accumulated toxic bile acids (Table 12).

Chapter 4: Characterization of Spgp-independent canalicular Transport of taurocholic acid using hepatocyte couplets and canalicular membrane vesicles

4.1. Introduction

The bile canalicular membranes contain a number of primary active transporters that utilize ATP energy to transport bile acids and organic compounds into the bile canaliculus. These proteins are members of the ABC superfamily with transport functions such as multidrug resistance Pgp for organic cations, Mdr2 for phosphatidylcholine, Mrp2 for non-bile acid organic anions and Spgp for bile acids. Recent studies indicate that the functional activity of canalicular ABC transporter may be regulated by the amount of protein trafficking to the canalicular membrane. Intravenous injection to rats of dibutyryl cAMP (dBcAMP) or taurocholate (TCA) rapidly and selectively increased bile acid transport activity and the amount of Mdr1, Mdr2, Spgp and Mrp2 protein level by 3 to 4-fold (Misra et al. 2003). The mobilization of ABC transporters induced by dBcAMP or TCA has been demonstrated in rat hepatocyte couplet system, in WIFB9 hepatoma cell line and in perfused rat liver (Boyer and Soroka 1995; Gatmaitan et al. 1997; Misra et al. 1998; Misra et al. 1999; Misra et al. 2003). The increased in transport and protein amount is inhibitable by prior administration of nocodazole which disrupts microtubule, Wortmannin which inhibits PI3-kinase (Boyer and Soroka 1995; Gatmaitan et al. 1997; Misra et al. 1998; Misra et al. 1999; Misra et al. 2003). These studies indicate that taurocholate-mediated bile acid secretion and recruitment of ABC transporters is phosphatidylinositol 3-kinase (PI3K) dependent and requires an intact microtubular apparatus.

There is considerable evidence that Spgp is the main canalicular bile acid transporter. The report by Gerloff et al., (Gerloff et al. 1998) showing that Spgp expressed in a heterologous insect cell system can mediate ATP-dependent bile acid transport with high affinity and efficiency, convincingly demonstrated that Spgp is a canalicular bile acid transporter *in vitro*. Bile acid secretion is significantly changed in *spgp*$^{-/-}$ mice fed CA diet from results obtained with CA-fed controls although taurocholate secretion is reduced and muricholate and hydroxylated bile acids are increased (Chapter 3). The question is how does a mouse lacking Spgp secrete taurocholate into the bile? The present report concerns

biochemical characterization of the alternative mechanism in *in vitro* systems. The first part of this study is to determine whether *spgp*$^{-/-}$ mice utilized the same secretory pathway as wildtype mice. This study took advantage of our knowledge of fluorescent bile acid analogs to visualize bile acid secretion in hepatocyte couplets using *spgp*$^{-/-}$ mice. In order to shed light on the issues of intracellular bile acid mobilization, fluorescent bile acid secretion is tested in the presence of dBcAMP or nocodozole. The second part of this study is to isolate membrane vesicles from the livers of *spgp*$^{-/-}$ mice and controls to investigate the mechanism of taurocholate transport.

4.2. Results

4.2.1. Assessment of hepatocyte couplets viability and polarity

For hepatocyte couplets, a routine collagenase procedure was used for preparation of hepatocyte couplets from both wildtype and knockout mice with modifications including shorter perfusion times and an added step of percoll centrifugation to remove dead cells. The viability of the cells is 70%-90% for wildtype liver and 50%-66% for *spgp*$^{-/-}$ mice liver as assessed by trypan blue exclusion test. Under light microscopy, we observed a large number of hepatocyte couplets fused together and did not contain a bile canaliculus from *spgp*$^{-/-}$ mice (Fig. 17). In these clumps of cells, the hepatocyte secretory polarity was not established as assessed by immunofluorescent staining of canalicular membrane protein (data not shown). Therefore, secretory experiments used hepatocyte couplets that have expanded canaliculi and secretory polarity were selected for fluorescent bile acid secretion (see section 4.2.2).

To confirm the membrane polarity of the hepatocyte couplet, we first investigated the distribution of the canalicular membrane protein, Spgp, Mrp2 and Pgp. As shown in Fig. 16, these proteins are exclusively localized to the apical domain. As expected, no fluorescence was detectable when cells were incubated with Spgp antibody in *spgp*$^{-/-}$ mice cells or when incubated only with the secondary antibody (Fig. 16). Mrp3 was found highly expressed in mice than in rat liver basolateral membrane.

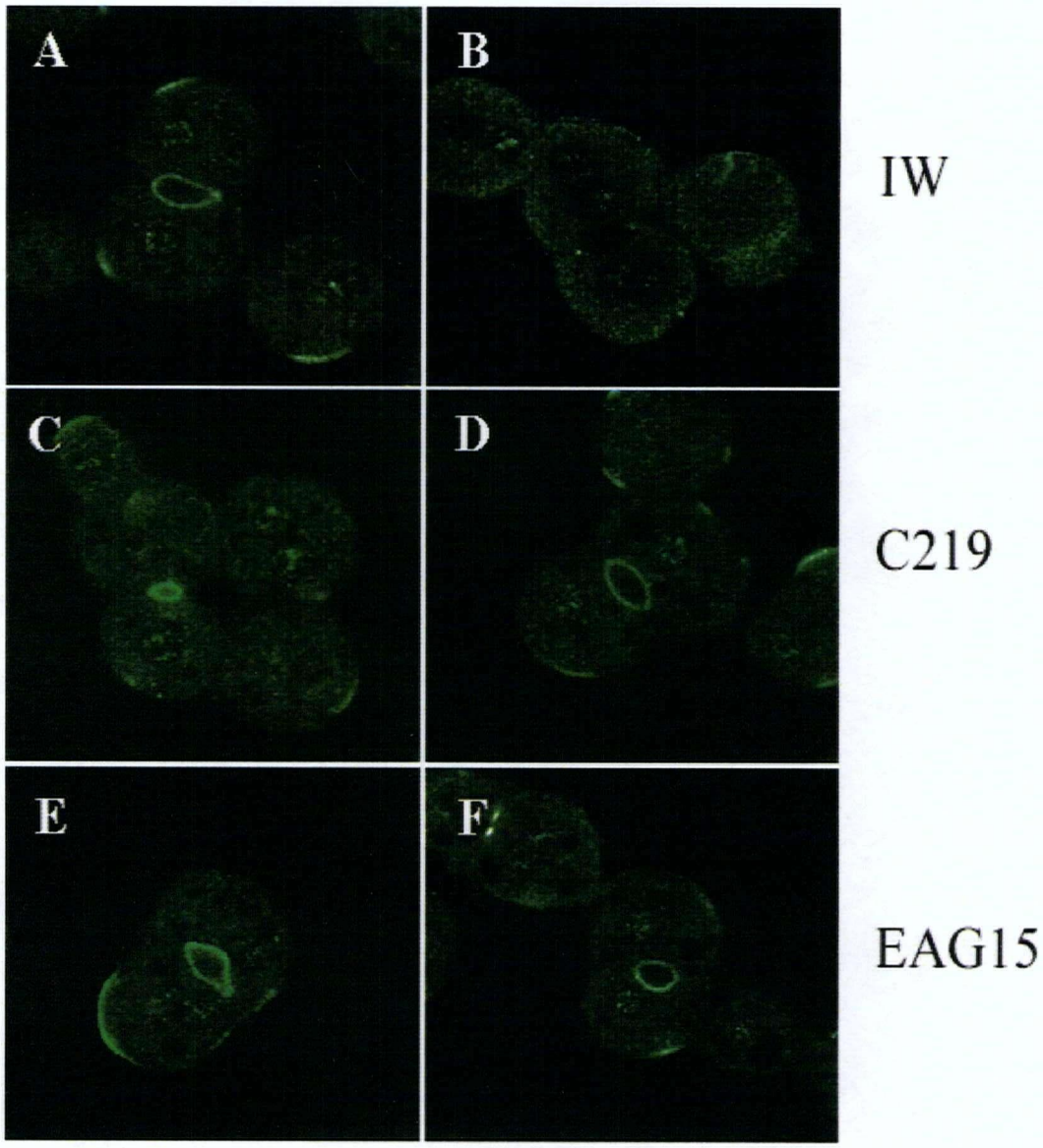

Fig. 16. Expression of different canalicular proteins in hepatocyte couplets from wildtype and *spgp*-/- mice.

A, C, and E are from wildtype mice. B, D, and F are from *spgp*$^{-/-}$ mice. Couplet cells were stained with IW polyclonal antibody recognizes Spgp (A, B), C219 monoclonal antibody recognizes Mdr1, Mdr2 and Spgp (C, D) and EAG15 polyclonal antibody recognizes Mrp2 (E, F).

4.2.2. Assessment of bile secretory functional capacity for bile acids

Fluorescent derivatives of bile acids have been extensively used in *in vivo* and *in vitro* experiments. It has been shown that biliary secretion of the fluorescent bile acid, cholylglycylamidofluorescein (CGamF), was similar to its natural conjugated bile acid, glycocholate (Holzinger et al. 1998). For example, the single pass extraction of CGamF was 85.4%, and that of glycocholate was 94.6% (Holzinger et al. 1998). The cumulative recovery in 60min of CGamF as a percent of uptake was 92.5%, and that of glycocholate was 98.1% (Holzinger et al. 1998). The uptake and recovery of fluorescein alone was incomplete, averaging 68.4% and 59.3% respectively. CGamF was also found to transport across the hepatocyte without undergoing appreciable biotransformation (Holzinger et al. 1998). Based on these criteria, CGamF was used as a surrogate marker for glycocholate secretion.

Confocal microscopy and image analysis were performed according to Boyer and Soroka, (1995) to obtain a more quantitative assessment of the secretory capacity in individual couplets. (Boyer and Soroka 1995). Fig. 17 shows the cumulative percentage of fluorescent bile acids secreted into canalicular lumen. The appearance of the analogue in the lumen was rapid and paralleled the secretion of taurocholate in wildtype and *spgp*$^{-/-}$ mice (section 3.2.5). The presence of fluorescence in the cytoplasm of couplets from *spgp*$^{-/-}$ mice and control mice indicated a transcellular route from medium to bile canaliculi. This confirmed that cells are capable of vectorial transport of bile acids from basolateral membrane to bile canaliculi instead of taking a paracellular pathway directly from blood into bile. These results do not exclude the possibility of additional paracellular permeability through the tight junctions.

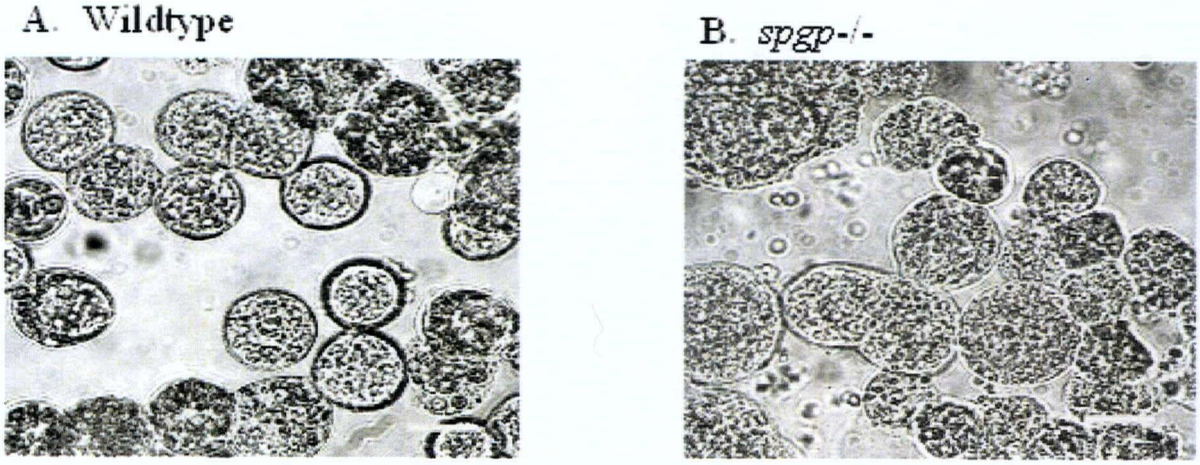

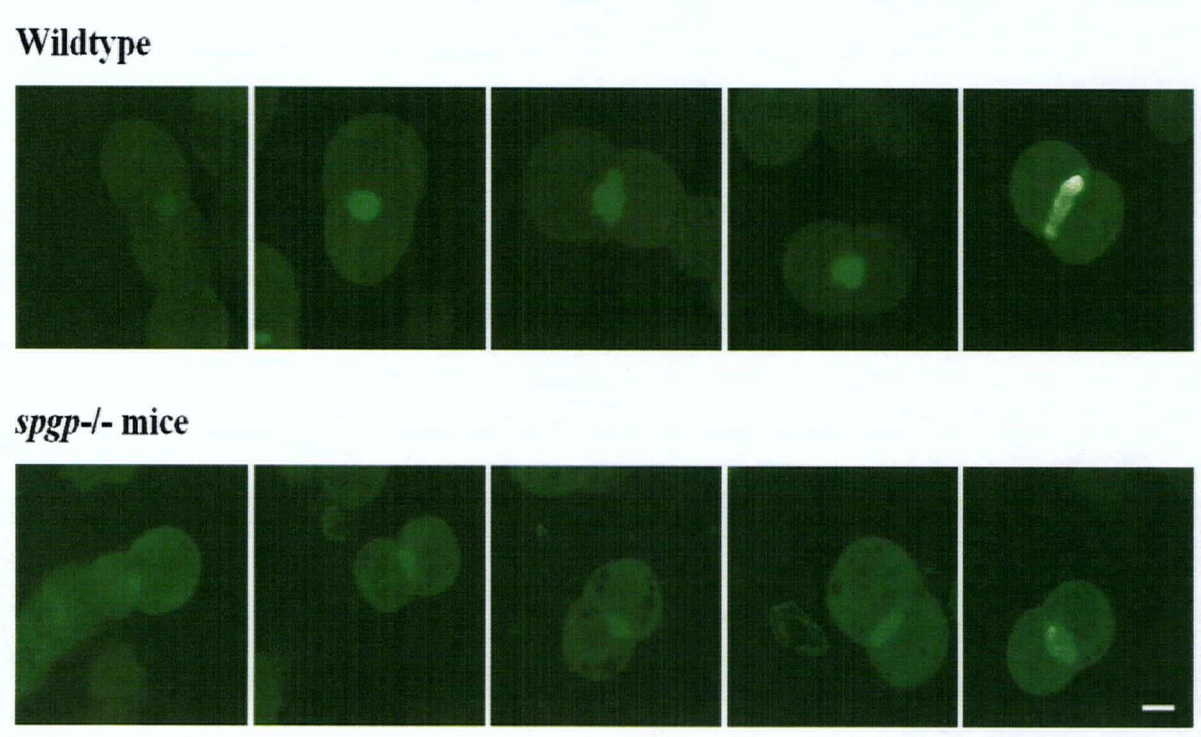

Fig. 17. Representative hepatocyte couplets and fluorescent bile acid secretion in wildtype and *spgp*$^{-/-}$ mice.

Isolated heptocyte couplets from (A) wildtype and (B) *spgp*$^{-/-}$ mice illustrated that the viability of the cells are higher from wildtype mice than *spgp*$^{-/-}$ mice. Fewer hepatocyte couplets with expanded canaliculi were observed from *spgp*$^{-/-}$ mice. (C) Representative hepatocyte couplets from wildtype and *spgp*$^{-/-}$ mice with expanded canaliculi secrete fluorescent bile acid CGamF into the canalicular lumen.
Bar = 10μM.

Cellular and canalicular areas were determined by analysis of images captured during the imaging of canalicular accumulation of CGamF. The canalicular and cellular area are important determinants of the capacity to hold and to secrete CGamF. DBcAMP and nocodozole were shown to increase and decrease the circumference canalicular bile lumen of rat hepatocyte couplets (Boyer and Soroka 1995). In this study, we measured these variables to investigate whether similar changes can be found in *spgp*$^{-/-}$ mice and controls. Quantitative analysis of couplets (n=10) showed that there was high variability in the size, area, and fluorescence accumulation in bile canaliculi and couplets isolated from each animal (Fig. 18). However, comparison of the means ± SD (n=30) of area and fluorescence showed no significant difference between wildtype and *spgp*$^{-/-}$ mice. In addition, dBcAMP and nocodozole did not affect the area or fluorescence accumulation of hepatocyte couplets in *spgp*$^{-/-}$ mice and controls (data not shown), the reasons for this is not yet apparent.

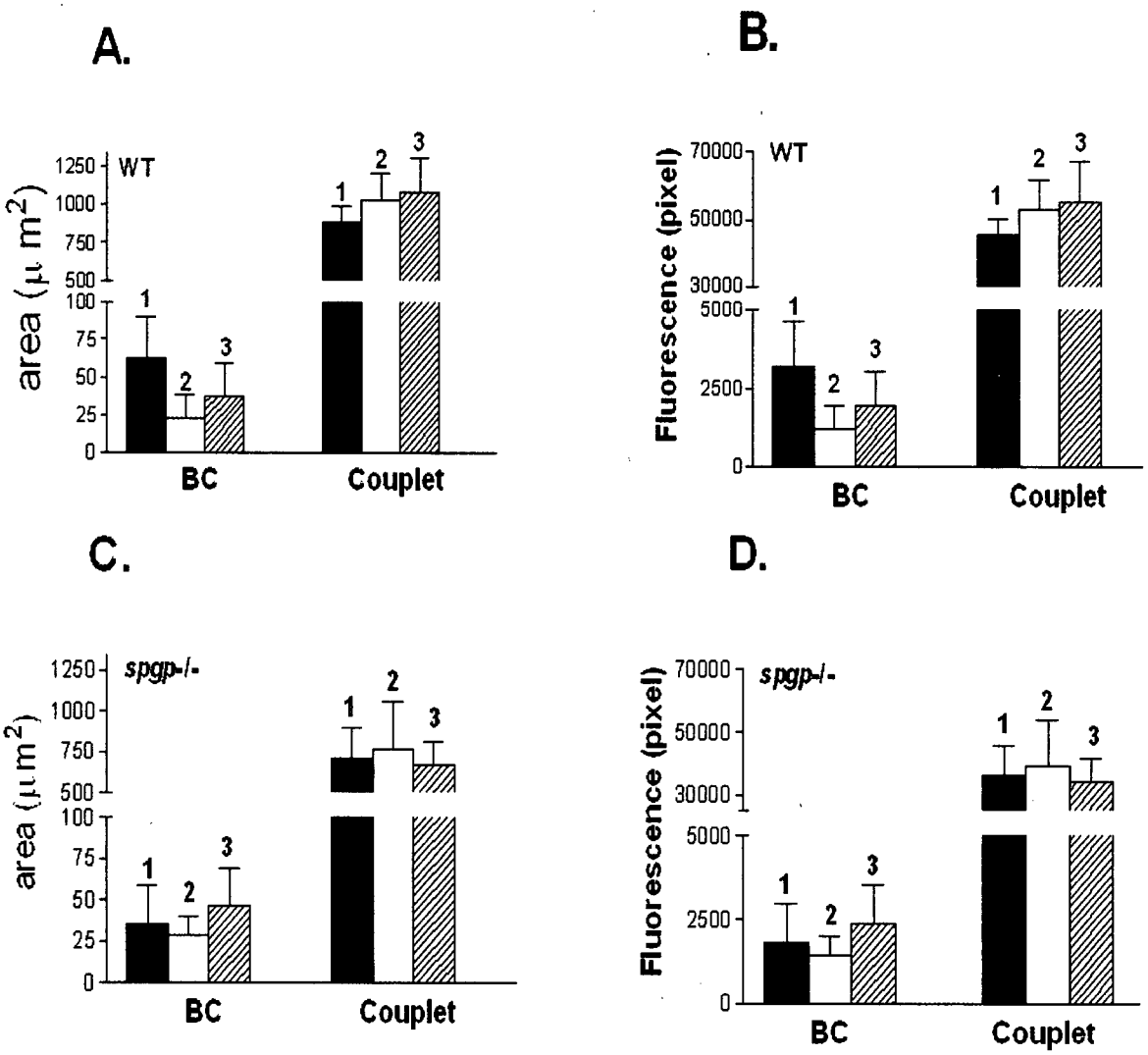

Fig. 18. Bile canalicular area, couplet area and fluorescence accumulation in hepatocyte couplets isolated from wildtype and *spgp*-/- mice.

Total area of a couplet cell (couplet) and total area of a bile canaliculi (BC) was measured in each couplet from (A) wildtype and (C) *spgp*$^{-/-}$ mice. Total fluorescent pixels in each couplet and each bile canaliculi was measured.

Each bar labeled 1, 2, or 3 (black, white and crossed) represents three different animals of each genotype (WT and *spgp*$^{-/-}$). Mean ± S.D. is calculated from 10 couplet cells. The graphs show large variability in cell and couplet areas within each animal and no significant difference between the genotypes.

The % secretion of CGamF for wildtype and *spgp*$^{-/-}$ mouse couplets were 22 ± 15 % and 22 ± 6 % respectively. Another fluorescent bile acid, deoxycholyl-lysyl-fluorescein (DCLF), was also tested. It was secreted at a similar capacity as CGamF and there was no significant difference between wildtype and *spgp*$^{-/-}$ mice (data not shown). To investigate further whether the secretion of other biliary components could be affected in *spgp*$^{-/-}$ mice, we assessed the percentage of fluorescent organic anion derivative, 5-chloromethylfluorescein diacetate (CMFDA), in the canalicular vacuole (Fig. 19). CMFDA was secreted by another canalicular ABC transporter, Mrp2, in rat hepatocyte couplets that are not found in mutant rats of Mrp2 (Roelofsen et al. 1998). Therefore, it is used in this study to investigate the function of Mrp2 in *spgp*$^{-/-}$ mice. As expected, Mrp2 is targeted properly to the canalicular domain in hepatocyte couplets from both wildtype and knockout mice (Fig. 16). CMFDA secretion is at the same level between wildtype and *spgp*$^{-/-}$ mice.

Previously it has been found in rat hepatocyte couplets that DBcAMP stimulates and nocodozole inhibits the accumulation of CGamF within the canalicular lumens. DBcAMP (20μmol/L) increases CGamF secretion by about 2-fold compared to controls (Boyer and Soroka 1995). It was interpreted that DBcAMP mobilizes intracellular bile acids and/or intracellular proteins, like Spgp and Mrp2, destined for the canalicular membrane. Nocodazole on the other hand, has been shown to disrupt microtubule, and the percentage of CGamF secretion is decreased about 2-fold in hepatocyte couplets treated with nocodozole (10μmol/L) compared to control cells. In this study, we were interested to investigate whether CGamF secretion in mice hepatocyte couplets are affected by DBcAMP and nocodozole. From these studies, we measured no significant difference in the percentage of CGamF secretion after treating with DBcAMP or nocodozole using the same experimental condition as for the rat hepatocyte couplet system (Fig. 19). The reason for this discrepancy is not known.

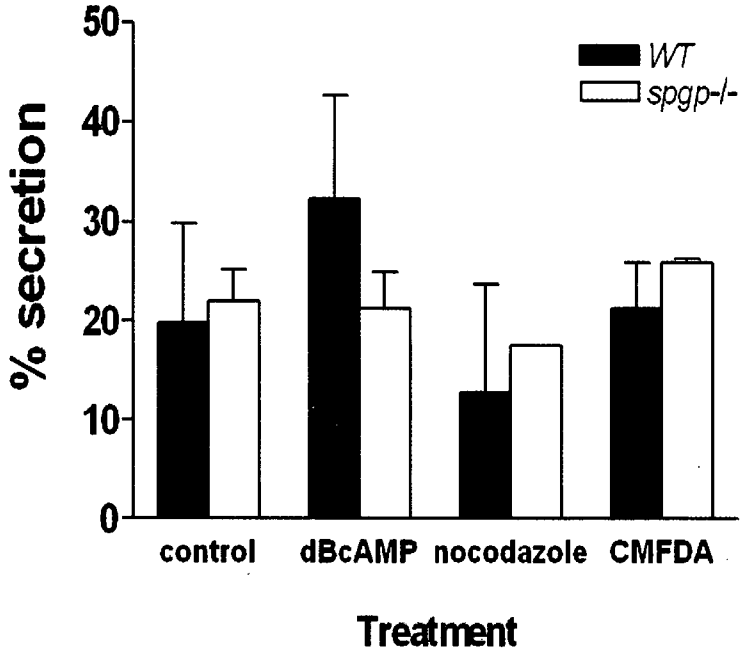

Fig. 19. Secretion of fluorescent bile acid in the presence of different compounds in hepatocyte couplets isolated from wildtype and *spgp*-/- mice.

Enriched functional hepatocyte couplets were isolated from wildtype (black bar) and knockout mice (white bar). The ability to secrete the fluorescent bile acid CGamF in the absence (control) and presence of dBcAMP and nocodazole were measured as the percentage of secretion into the canalicular vacuole in the presence of control cells. The ability to secrete the fluorescent organic anion CMFDA was measured as a control experiment for Mrp2 secretion.

The trend was toward increased secretion in dBcAMP in wildtype couplets (28 ± 11% and 39 ± 14% in control and dBcAMP treated wildtype cells respectively). The trend for nocodozole was toward secretion in wildtype couplets as compared to control (28 ± 11% and 14 ± 11% in control and nocodozole treated wildtype cells respectively). In *spgp*$^{-/-}$ hepatocyte couplets, this trend was not observed.

4.2.3. Biochemical characteristics of isolated membrane vesicles

Canalicular membrane vesicles are routinely isolated from rat liver (Meier and Boyer 1990; Nishida et al. 1991; Bohme et al. 1994). The aim of this study was to isolate canalicular membrane vesicles from wildtype and *spgp*$^{-/-}$ mouse livers. I found that modifications to the original techniques were necessary to isolate enriched canalicular membrane vesicles suitable for transport studies from mouse livers. The poor survival of *spgp*$^{-/-}$ mice and the large number of mice that were required limited the use of nitrogen cavitation and rate zonal rotors procedures that are routinely used for rat canalicular membranes preparations. For practical purposes, a relatively simple methodology was developed that yielded enriched canalicular membrane. These membrane vesicles were used for taurocholate transport studies (section 4.2.6). Earlier studies using the published routine procedures of Meier (Meier et al. 1984b) produced low yield of enriched membrane vesicles (0.05mg/gliver in a total of 10 preparations) and poor enrichment of canalicular membrane marker (~20-fold in a total of 10 preparations). This was partly due to contaminations of organelles such as endoplasmic reticulum, Golgi and mitochondria (fig. 20). Furthermore, I found that livers from older mice were also not suitable for preparation of membrane vesicles. Livers of *spgp*$^{-/-}$ mice also resulted in lower yield and poorer enrichment of canalicular membrane. Therefore, in later studies, only 2-4 months old mice were used. The use of rate zonal centrifugation may improve the purification process if large amount of liver is available.

The procedures in this study were designed to isolate a specific area of the liver cell plasma membrane, the bile canalicular membrane. The method isolated from a low speed "nuclear" fraction containing plasma membrane fragments. The bile canalicular membrane was separated from the attached basolateral membranes and mixed membranes containing tight junction complexes by tissue homogenization and sucrose density gradient centrifugation. To corroborate the claims made for membrane vesicle quality and to monitor the separation, protein yield and distribution of marker enzymes among the liver subfractions were investigated. The balance sheets are described in Table 14, 15, 16, 17 and 18.

4.2.4. Enrichment of canalicular membrane

CMV was isolated from mouse liver with an average yield of 0.08 to 0.10 mg protein/g liver, which was similar to published results (Inoue et al. 1984; Meier and Boyer 1990; Nishida et al. 1991; Bohme et al. 1994). Protein yield was similar between normal and mutant mice (Table 14). The distribution of protein was also similar to other published results. However, the highest percentage of protein was in the MMV fraction compared to the expected BMV or 2ndGP fractions (Table 15). The MMV fraction was a mixed membrane fraction of plasma membrane consisting largely of lateral membranes, basolateral membranes and canalicular membranes. The large amount of protein in this fraction suggested that canalicular and basolateral membranes might not be completely separated and could lead to lower yield of either fraction. However, experiments to improve the separation such as increasing the number of douncing from 50 strokes to 100 strokes did not result in higher yield or purity of each fraction. Such difference might be due to the difference in membrane surface area and membrane components in the plasma membrane of rat and mouse liver.

Table 14. Protein yield in different fractions isolated from wildtype and *spgp*-/- mice liver

	Protein (mg/gliver)				
Sample	Rat liver*	Male wildtype mice (n=26)	Male *spgp*$^{-/-}$ mice (n=13)	Female wildtype mice (n=9)	Female *spgp*$^{-/-}$ mice (n=5)
H	164.7 ± 12.5	157.57 ± 18.24	188.83 ± 42.84	185.44 ± 27.35	168.40 ± 68.42
P		53.66 ± 15.36	75.82 ± 28.61	61.78 ± 29.82	74.67 ± 32.32
S		105.72 ± 18.93	108.92 ± 42.06	124.11 ± 31.98	100.83 ± 31.03
1stG	1.08 ± 0.22	0.93 ± 0.43	1.05 ± 0.86	1.39 ± 0.83	2.10 ± 0.72
1stGP		7.75 ± 3.44	8.06 ± 3.34	6.32 ± 2.13	8.12 ± 6.78
Cyt		1.08 ± 1.20	1.01 ± 1.65	2.44 ± 2.23	1.49 ± 1.58
CMV	0.12 ± 0.03	0.08 ± 0.03	0.08 ± 0.03	0.10 ± 0.04	0.09 ± 0.03
MMV	0.18 ± 0.06	0.16 ± 0.08	0.15 ± 0.10	0.15 ± 0.09	0.17 ± 0.06
BMV	0.20 ± 0.06	0.10 ± 0.10	0.12 ± 0.18	0.16 ± 0.14	0.19 ± 0.08
2ndP	0.52 ± 0.10	0.48 ± 0.64	0.36 ± 0.42	1.62 ± 0.45	1.20 ± 0.71

Homogenate (H), Pellet (P), Supernatant, first sucrose fraction (1stG) and its pellet (1stGP), washing step (Cyt) and three plasma membrane fractions consisting of canalicular (CMV), mixed (MMV) and basolateral (BMV) membranes and the final pellet (2ndGP) were collected for analysis of marker enzyme activities. (See Materials and Methods section 2.4 and 2.5 for details.

*Based on published data (Meier et al. 1984b). See materials and methods section for description of each fraction.

Table 15. Protein recovery from wildtype and *spgp*-/- mouse livers

	% distribution				
Sample	Rat liver*	Male wildtype mice (n=26)	Male *spgp*$^{-/-}$ mice (n=13)	Female wildtype mice (n=9)	Female *spgp*$^{-/-}$ mice (n=5)
H	100	100	100	100	100
P		34.05	40.15	33	44.34
S		67.10	57.68	67	59.88
1stG	0.66	0.59	0.55	0.75	1.25
1stGP		4.92	4.27	3.41	4.82
Cyt		0.68	0.53	1.31	0.88
CMV	0.07	0.05	0.04	0.05	0.05
MMV	0.11	0.10	0.08	0.08	0.10
BMV	0.12	0.06	0.06	0.09	0.11
2ndP	0.32	0.30	0.19	0.87	0.71

* Based on published data (Meier et al. 1984b)

The profile of marker enzyme activities and enrichment compared with starting homogenate indicated that membrane vesicles were derived predominantly from the canalicular domain of the hepatocyte plasma membrane (Table 16). Alkaline phosphatase activity, a marker of the canalicular membrane, was enriched about 60-fold in the final membrane fractions compared with the homogenate (Table 16). Na^+-K^+ ATPase, a marker for basolateral membrane, was enriched about 6-8-fold in membranes from both wildtype and mutant mouse livers compared to about 30-fold in the other plasma membrane fractions (Table 17). The orientation of membrane vesicles was estimated to determine the amount of functional vesicles for transport studies. The vesicles that had the inside-out orientation, i.e. with the ATP-binding domain of Spgp outside, could hydrolyze ATP and thus be functional for tracer uptake studies. Canalicular membrane vesicles isolated were 35-43% inside-out based on the orientation of ectoenzyme nucleotide pyrophosphatase and its activity in the membrane. Table 18 summarizes the results of protein yield, relative enrichment and membrane-sidedness of canalicular membrane vesicles obtained from wildtype and *spgp*$^{-/-}$ mice.

Table 16. Recovery of canalicular marker alkaline phosphatase activity in wildtype and *spgp*-/- mice.

	Relative enrichment of Alkaline Phosphatase				
Sample	Rat liver*	Male wildtype mice (n=26)	Male *spgp*-/- mice (n=13)	Female wildtype mice (n=9)	Female *spgp*$^{-/-}$ mice (n=5)
H	1.0	1.0	1.0	1.0	1.0
P		3.0	2.3	2.6	2.1
S		0.8	0.1	1.1	0.4
1stG		35.0	28.4	20.0	17.2
1stGP		3.6	3.9	4.4	3.1
Cyt		11.8	18.9	8.9	12.4
CMV	71 ± 21	68.7	74.2	61.3	47.4
MMV	22 ± 9	39.9	45.2	38.3	38.9
BMV	12 ± 4	16.5	23.7	39.2	19.3
2ndP		9.6	8.4	3.8	14.7

* Based on published data (Meier et al. 1984b)
Relative enrichment is defined as the ratio of specific activity in the different fractions to specificity in the homogenate.

Table 17. Recovery of basolateral marker Na+K+ ATPase activity in wildtype and *spgp*-/- mice

	Relative enrichment of Na+K+ATPase				
Sample	Rat liver*	Male wildtype mice (n=6)	Male *spgp*$^{-/-}$ mice (n=6)	Female wildtype mice (n=4)	Female *spgp*$^{-/-}$ mice (n=4)
H	1.0	1.0	1.0	1.0	1.0
CMV	ND	6.0	5.9	6.3	7.4
MMV	26 ± 10	31.0	45.2	59.5	33.4
BMV	34 ± 5	27.0	23.7	38.3	23.4

* Based on published data. (Meier et al. 1984b)
N.D. not detectable.
Relative enrichment is defined as the ratio of specific activity in the different fractions to specificity in the homogenate.

Table 18. Protein yield and enzyme enrichment of canalicular membrane vesicles in wildtype and *spgp*-/- mice

	Protein yield (mg/g liver)		Alkaline Phosphatase (RE)		NaK ATPase (RE)		Membrane Sidedness (% inside-out)	
	+/+	-/-	+/+	-/-	+/+	-/-	+/+	-/-
Male	0.08 ± 0.03 (26)	0.08 ± 0.03 (13)	68.7 ± 36.7 (26)	74.2 ± 31.7 (13)	6.0 ± 2.5 (6)	5.9 ± 3.1 (6)	43 ± 12 (10)	41 ± 11 (9)
Female	0.10 ± 0.04 (9)	0.08 ± 0.03 (5)	61.3 ± 13.8 (9)	47.4 ± 11.3 (5)	6.3 ± 0.8 (4)	7.4 ± 1.6 (4)	35 ± 6 (6)	39 ± 5 (4)

The homogenate and the plasma membrane samples were obtained as described in the materials and methods. Enzyme specific activities are reported as μmol/hr/mg protein at 37^{o}C. The total recovery of enzymes was in the range of 86%-110%. Data are given as mean ± S.D. with the numbers of experiments in parentheses. Relative enrichment (RE) is defined as the ratio of specific activity in the subfractions to specific activity in the homogenate.

To evaluate the contamination by intracellular organelles, Western blot analysis using antibodies against specific organelle proteins in each subfraction was carried out. The enrichment of endoplasmic reticulum (ER), Golgi and mitochondria were estimated by density of the band in the canalicular membrane fraction and in the homogenate. Studies of rat livers have shown that mitochondria, endoplasmic reticulum and Golgi represent 2, 24 and 1% of total membrane proteins respectively (Meier et al. 1984b). Assuming that this is the case in mouse, the major contaminations in the canalicular membrane fraction were ER and Golgi. Base on analysis of Na^+K^+ATPase activity, basolateral membrane contamination contributed about 6% of total proteins (Fig. 20A). SDS-Polyacrylamide-gel electrophoresis resolved the proteins of the plasma membrane subfractions into 60 major bands (Fig. 20B). The plasma membrane subfractions contained about 30 proteins with molecular weights between 60kDa and 200kDa.

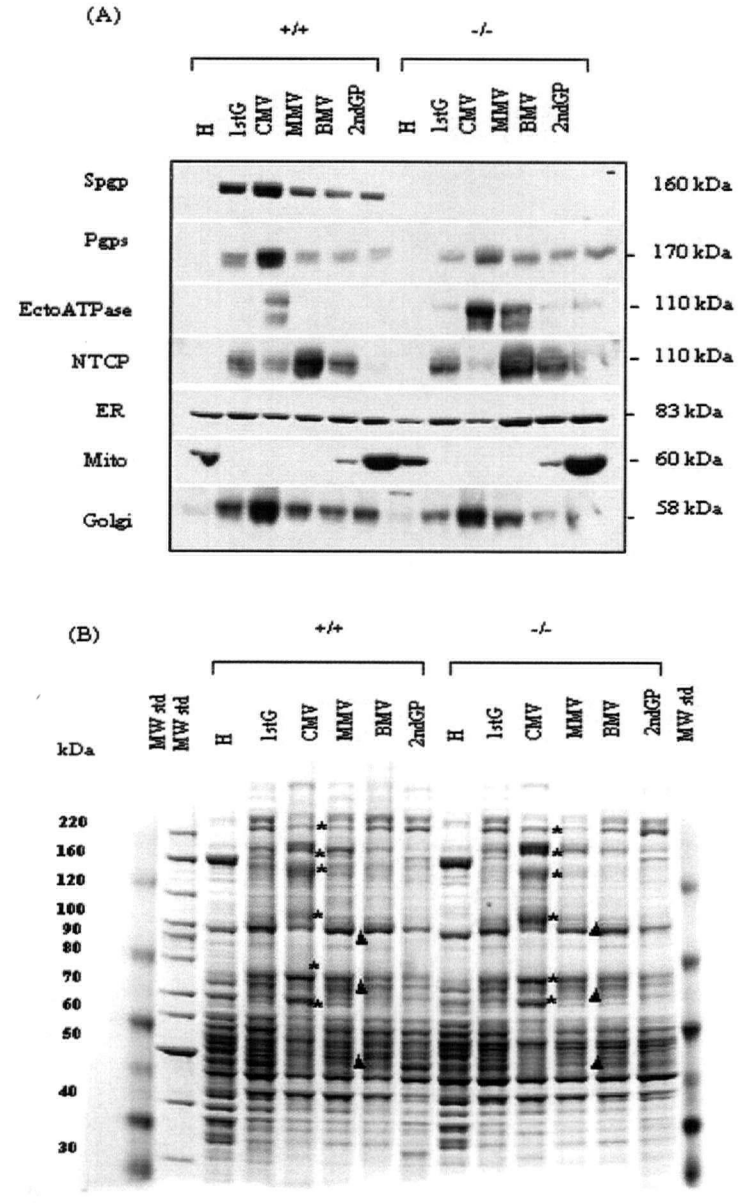

Fig. 20. Protein expression in different liver subfractions isolated from wildtype and *spgp*-/- mice.

Samples were electrophoresed as described in Material and Methods. Samples were either transferred for (A) immunoblotting or (B) Simply Blue protein staining.

(A) The relative enrichment of each subfraction was tested by Western blot analysis. Spgp (sister of P-glycoprotein), Pgp (P-glycoprotein), and EctoATPase are antibodies against canalicular proteins; Ntcp (sodium taurocholate transporting polypeptide), Mito, Golgi and ER are antibodies against basolateral membrane, mitochondria, Golgi and endoplasmic reticulum membranes respectively.

(B) Simply blue protein staining analysis of each subfraction of wildtype and *spgp*$^{-/-}$ mice. Putative canalicular specific proteins (*) and proteins concentrated in basolateral membrane and virtually absent in canalicular membrane (▲).

4.2.5. Transport studies with membrane vesicles- rapid filtration assay

Radiolabeled taurocholate was measured in canalicular membrane vesicles of wildtype and knockout mice as presented in Materials and Methods. As shown in Fig. 21A, membrane vesicles obtained from canalicular- enriched membranes showed ATP-dependent taurocholate uptake at $37^{O}C$. At $4^{O}C$, there was no significance difference between taurocholate uptake in the presence of MgATP and MgAMP (data not shown) confirming that the measured rate at $37^{O}C$ was due to specific taurocholate uptake and not due to non-specific taurocholate adsorption to surface of membrane vesicles as detected at $4^{O}C$.

ATP-dependent uptake of taurocholate was observed only in canalicular membrane vesicles from normal mice and not detectable in the presence of ATP in membrane vesicles from mutant mice (Fig. 21B). To demonstrate that the membrane vesicles isolated from *spgp*$^{-/-}$ mice were functional, ATP-dependent leukotriene C_4 transport was measured in membrane vesicles from *spgp*$^{-/-}$ mice. Leukotriene C_4 has been shown to be transported by Mrp2 in membrane vesicles from transfected cells (Stieger et al. 2000). Table 19 summarizes the initial rates of transport of different bile acids and leukotriene C_4. The initial rate of transport of leukotriene C_4 was 5.0 ± 1.3 pmol/min/mg in *spgp*$^{-/-}$ membrane vesicles whereas in wildtype membrane vesicles, the initial rate of transport was 2.4 ± 0.9 pmol/min/mg protein. The higher rate of transport in *spgp*$^{-/-}$ membrane vesicles suggested that Mrp2 level might be upregulated in the liver. This was supported by my observation that Mrp2 protein level was 3.0-fold higher in *spgp*$^{-/-}$ mice (see Fig. 13). These results confirm that *spgp*$^{-/-}$ membrane vesicles were functionally active and demonstrated that *in vitro* transport activity might reflect closely *in vivo* secretory activity.

In *in vivo* studies, cholic acid diet fed knockout mice had similar bile acid output as wildtype mice (chapter 3). To determine whether bile acid transport could be observed in *in vitro* membrane vesicles in mice, and whether the transport was due an ATP-dependent process, we tested taurocholate uptake in knockout mice that were fed with cholic acid diet along with wildtype controls. The wildtype CMV showed ATP-stimulated taurocholate uptake whereas the knockout CMV showed no ATP-dependent taurocholate activity, further

indicating that the alternative pathway in *spgp*$^{-/-}$ mice likely did not involve a high affinity ATP-dependent process (Fig. 21C, D). ATP-dependent uptake of taurocholate was observed only in canalicular membrane vesicles from normal mice and not from mutant mice lacking Spgp. The apparent Km for taurocholate was 14μM and Vmax was 800pmol/min/mg protein for wildtype CMV (Fig. 22).

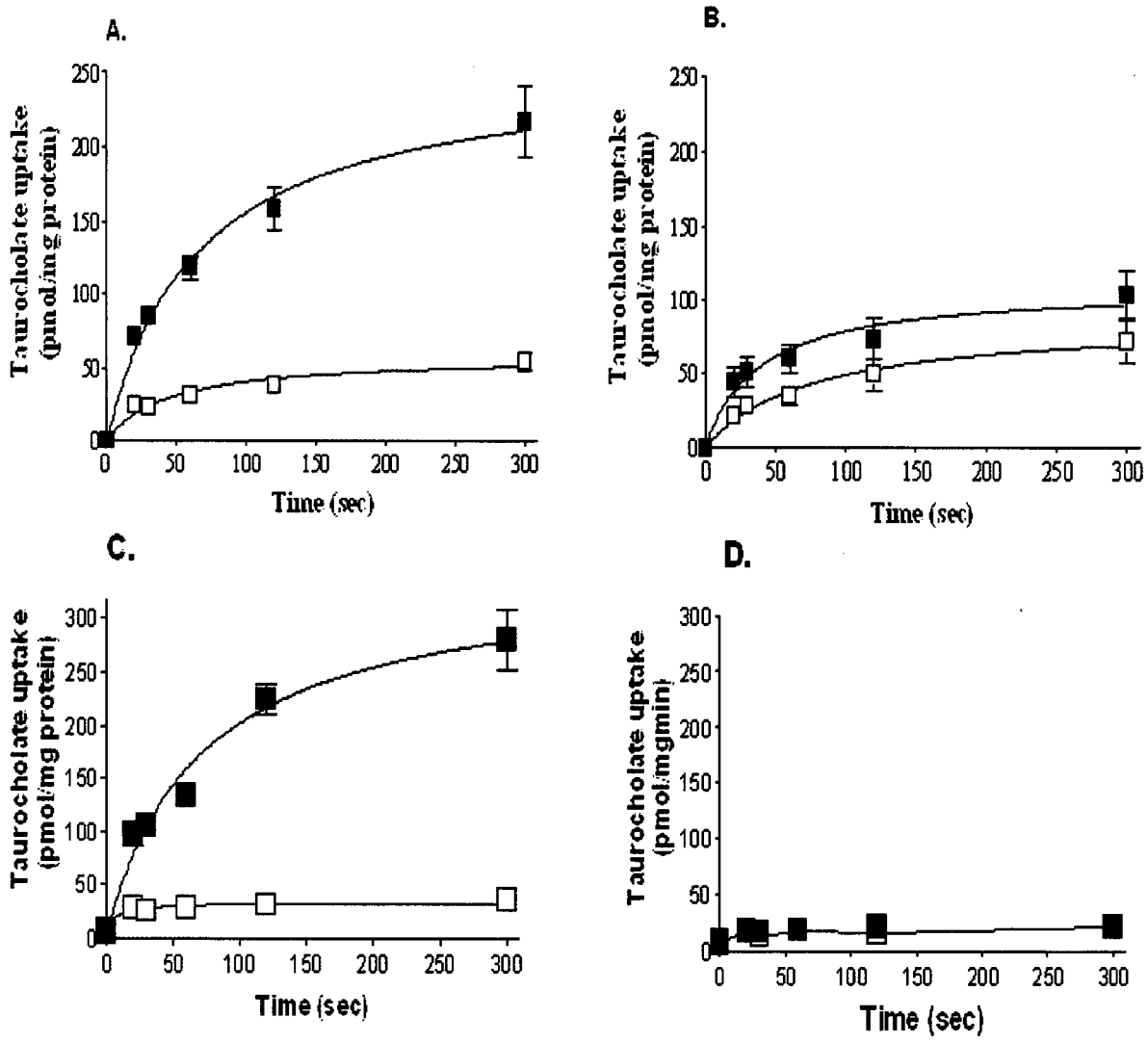

Fig. 21. Time-dependent taurocholate uptake into CMV from wildtype and *spgp*-/- mice.

Uptake of 3μm ^{3}H-taurocholate was measured in the presence of 5mM MgATP (■) or 5mM MgAMP (□) at different time points. The reaction was carried out using canalicular-enriched membrane vesicles isolated from (A) wildtype mice and (B) *spgp*$^{-/-}$ mice fed with normal diet and from (C) wildtype mice and (D) *spgp*$^{-/-}$ mice fed with CA diet. Each symbol and vertical bar represents the mean ± SEM of determinations.

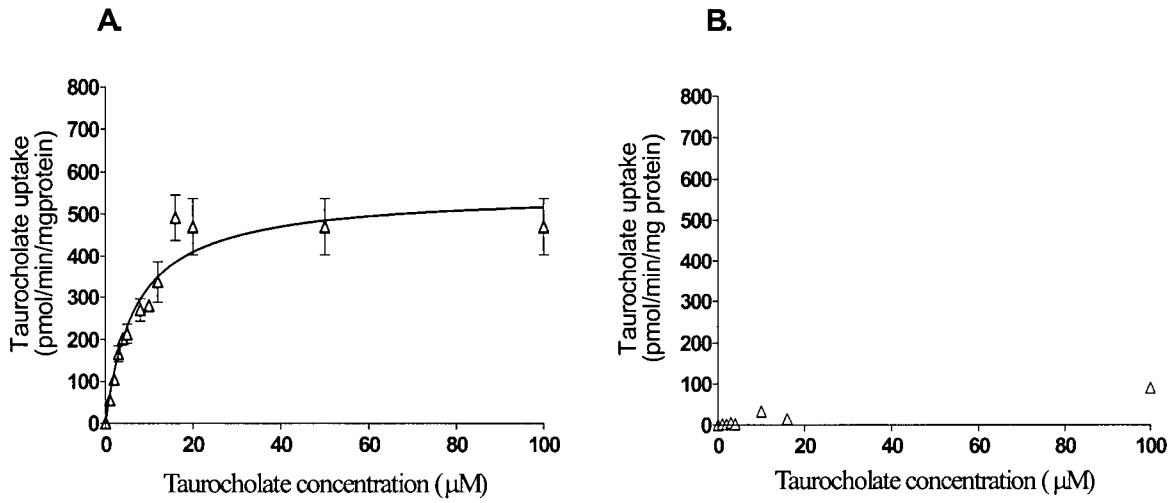

Fig. 22. Concentration dependence of ^{3}H-taurocholate uptake in CMV from wildtype and *spgp*-/- mice.

Membrane vesicles from wildtype (A) and *spgp*$^{-/-}$ mice (B) were incubated with different concentrations of taurocholate (3μM ^{3}H-taurocholate tracer) in reaction mixture (0.25M sucrose, 10mM $MgCl_2$, 10mM Hepes-Tris pH 7.4, 10mM creatine phosphate, 100μg/ml creatine kinase) in the presence of 5mM Na_2ATP or 5mM NaAMP. (A) ATP-dependent taurocholate uptake saturable curve was generated for canalicular membrane vesicles from wildtype mice. Values are rates measured in the presence of MgATP minus rates measured in presence of MgAMP for triplicate determinations; bars represent standard error. Kinetic parameters for taurocholate uptake into CMV is Km~14μM and Vmax~800pmol/mgmin. (B) No significant ATP-dependent taurocholate uptake was measured in canalicular membrane vesicles from *spgp*$^{-/-}$ mice.

4.2.6. Effects of various agents on taurocholic acid transport

The effects of other bile acids and drugs on taurocholate uptake in CMV were tested. These compounds were chosen to demonstrate the specificity of Spgp-mediated transport or to explain their potential *in vivo* effects as inducer of cholestasis by inhibiting Spgp-mediated bile acid transport. Spgp polyclonal antibody (IW) has been produced in this laboratory [Childs, 1995 #] with the peptide encoding the sequence 1170-MDNIKYG-----RGE-1224. Inhibition of taurocholate transport by IW antibody suggests that the transport of taurocholate was mediated by Spgp (Fig. 23A).

Cyclosporin (CsA) has been shown to interfere with normal bile formation and induce cholestasis in mammalian liver (Myara et al. 1996). CsA has been shown previously to *cis*-inhibit ATP-dependent transport in rat CMV with a K_i value of 0.2μmol/L (Bohme et al. 1994) and Spgp-mediated taurocholate transport in Sf9 cell vesicles with a K_i value of 0.3μmol/L (Stieger et al. 2000). CsA also reverses taxol resistance in Spgp transfected cells [Childs, 1995, #]. We found in this study that 1μM of CsA inhibited about 50% of taurocholate transport activity (Fig. 23B).

Ethinylestradiol-17β-glucuronide (E17βG) is a physiological estrogen metabolite that is predominantly excreted into bile by Mrp2 (Vore et al. 1997). E17βG is believed to be transported across the membrane by Mrp2 and intracellular accumulation of E17βG in the vesicles may *trans*-inhibit Spgp-mediated taurocholate transport. Stieger *et al.*, (2000) (Stieger et al. 2000) reported that 100μmol/L of E17βG inhibit ATP-dependent taurocholate uptake by 60% in rat CMV. In this study, I did not observe a significant inhibition of taurocholate uptake in wildtype mouse CMV at concentrations up to 100μmol/L (Fig. 23C). The reason for this discrepancy between the two systems is unknown. One possibility is that a higher concentration of E17βG is required to inhibit taurocholate uptake in mice CMV.

Spgp transfected human SKOV ovarian cell line was moderately resistant (~2-4-fold) to taxol compared to control cell line, suggesting that taxol might also be transported by Spgp (Childs et al. 1998). In this study, 100μM taxol did not significantly inhibit taurocholate uptake into CMV, suggesting that taxol was not a potent inhibitor of Spgp activity (Fig.

23D). This result is consistent with the lack of uptake of taxol in Spgp transfected membrane vesicles (Lecureur et al. 2000). These results also suggest that taxol might not interact with Spgp with high specificity. The Mdr1 protein in the canalicular membrane was likely to be a better transporter of taxol.

Four different bile acid species were tested for their extent of inhibition of taurocholate transport. Previous studies in rat CMV have indicated that the number of hydroxyl groups and the conjugation status of a bile acid affect specificity and efficiency of its transport (Nishida et al. 1995). All four bile acids inhibited taurocholate uptake into CMV but to different extent. Muricholic acids (Fig. 23E) inhibited more than 75% of activity at 100μM, the highest concentration tested. Whether a bile acid was conjugated to taurine or glycine in its free form did not seem to affect taurocholate transport. There is difference observed with different bile acids suggesting that the number and orientation of the hydroxyl groups might be more important in its recognition to Spgp. Ursodeoxycholic acid conjugated to taurine or glycine inhibited taurocholate uptake to the same extent (Fig. 23F). Ursodeoxycholic acid decreased taurocholate uptake to the same level at a much lower concentration than muricholic acid, suggesting that Spgp recognized ursodeoxycholic acid with a higher specificity.

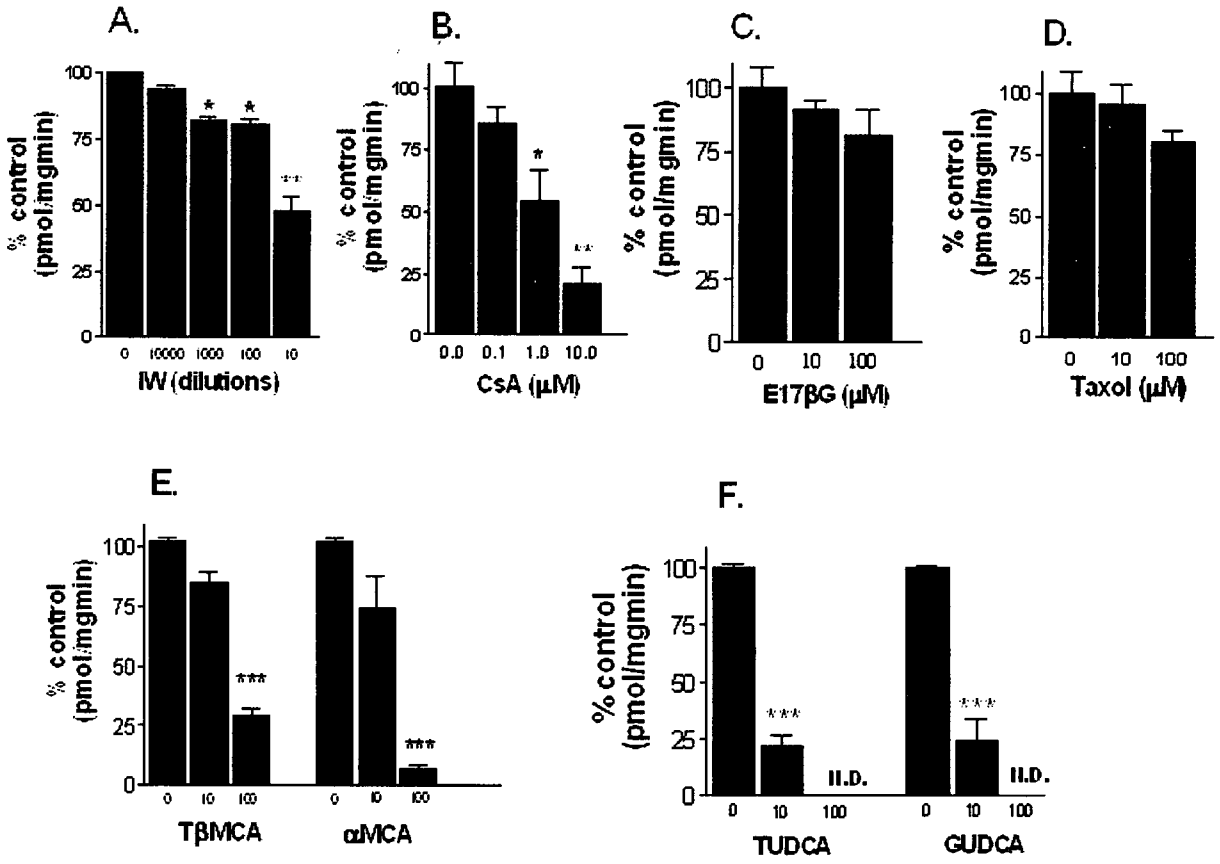

Fig. 23. Effects of bile acids and xenobiotics on the modulation of Spgp-mediated taurocholate uptake transport in CMV.

Uptake of 3μm ^{3}H-taurocholate was measured after 1 min of reaction in the presence of different concentration of inhibitors. (A) Spgp polyclonal antibody, IW; (B) Cyclosporin A; (C) Ethinylestradiol-17β-glucuronide (E17βG); (D) Taxol; (E) Taurobetamuricholic acid (TβMCA) and alphamuricholic acid (αMCA); (F) Tauroursodeoxycholic acid (TUDCA) and glycoursodeoxycholic acid (GUDCA). The data are means ± SD of n=3 experiments. N.D. not detectable. *P<0.05; **0.01<P<0.05; ***P<0.01 indicates significant difference than the corresponding control.

Table 19. Summary of ATP-stimulation of bile acid and leukotriene C4 uptake in CMV from wildtype and *spgp*-/- mice

	ATP-dependent bile acid uptake	
	Wildtype	*spgp*$^{-/-}$
Substrates	pmol/mg/min	
Taurocholate (3μM)	87.1 ± 9.9	N.D.
Glycocholate (3μM)	7.6 ± 0.1	N.D.
Tauroursodeoxycholate (3μM)	92.5 ± 18.4	N.D.
Leukotriene C_4 (50nM)	2.4 ± 0.9	5.0 ± 1.3*

ATP-stimulated uptake was estimated from the difference in radioactivity incorporated in vesicles in the presence of 5mM MgATP and 5mM MgAMP as described in the Materials and Methods. The data are means ± SD of n=3 experiments. * represents value significantly different from wildtype control ($p<0.05$). N.D. not detectable.

4.3. Discussion

4.3.1. Fluorescent bile acid transport in hepatocyte couplets

Hepatocyte couplets were chosen as a first study of bile acid secretion in *spgp*$^{-/-}$ mice. Using standard protocol for rat hepatocyte couplets isolation at the Yale liver center (New Haven, CT), the secretory properties of bile acid secretion into canaliculus of mouse hepatocyte couplets were investigated. In particular, we asked these questions: 1) Are *spgp*$^{-/-}$ mouse liver cells able to form functional couplets that retain secretory polarity in culture over time? 2) If yes, what is the capacity for secretion of fluorescent bile acid analogs into the canalicular vacuole? 3) Can DBcAMP and nocodozole affect CGamF secretion? Couplets of *spgp*$^{-/-}$ mice with expanded canaliculi secreted about 22% fluorescent CGamF into the canalicular vacuole, similar to those of wildtype mice and higher than the expected secretion from rat hepatocyte couplets (Boyer and Soroka 1995). These results are consistent with *in vivo* data demonstrating that wildtype and *spgp*$^{-/-}$ mice have a large capacity to secrete bile acids. The secretory pathway in the couplet cells from wildtype and *spgp*$^{-/-}$ mice also appears to take the common transcellular route. Hence, alterations in the functioning of intracellular components are not expected in *spgp*$^{-/-}$ mice. In summary, establishment of a functional hepatocyte couplet system suitable for studying biliary processes was achieved with wildtype and *spgp*$^{-/-}$ mice. This model system retained membrane and secretory polarity like those of an intact liver.

Bile acid secretion was not modulated in wildtype and *spgp*$^{-/-}$ mice couplets by compounds including nocodozole and DBcAMP. These substances have been postulated to affect bile acid secretion by enhancing or disrupting the molecular machinery of intracellular bile acid transport (Boyer and Soroka 1995; Roelofsen et al. 1998)Misra, 2003 #1573]. One possibility is that the microtubule and microfilament associated pathways that are inhibited by the tested compounds are not involved in bile acid secretion. The possibility that other secretory pathway such as vesicle-mediated exocytosis, is unlikely to contribute to bile acid secretion in *spgp*$^{-/-}$ mice. The lack of obvious punctate fluorescent spots in the cytoplasm of the hepatocyte couplets of *spgp*$^{-/-}$ mice also suggested that the fluorescent bile acids were not retained in postulated vesicles as expected. This is contrary to what has been observed with

rat liver hepatocyte couplets studies, demonstrating that most of these compounds affected secretion of fluorescent bile acid into the vacuole, under similar experimental conditions (Boyer and Soroka 1995; Roelofsen et al. 1998). This incongruity between the two studies may be attributable to species-specific differences in intracellular pathways of bile acid secretion. It is also possible that mice hepatocyte couplets are more resilient to the administered dose of stimulator or inhibitor perhaps by increased efflux back into the medium and limiting the concentration within the cells.

4.3.2. A proposed "leaky" bile acid transporter

Present experiments demonstrating Spgp-mediated transport in wildtype canalicular membrane vesicles to be saturable, temperature- and ATP-dependent, highly efficient, large capacity process that was inhibitable by other bile salts represent little surprise. However, comparison of kinetic parameters of taurocholate transport in wildtype with that in *spgp*$^{-/-}$ mice is necessary to support the conclusion that Spgp is an efficient bile acid transporter in the canalicular membrane. This study not only reaffirms what is found in Spgp transfected heterologous insect cell system but also provided some important kinetics information about the alternative system in the knockout mice. The apparent affinity for taurocholate (Km of 14μM) is compatible with that reported for murine Spgp (Km of 13μM-30μM) and rat liver canalicular membranes (Km of 2-47μM). Similar kinetics has been measured in transfected insect cell membrane vesicles that overexpressed rat, mouse and human Spgp (Gerloff et al. 1998; Green et al. 2000; Byrne et al. 2002; Noe et al. 2002). The affinity for taurocholate in knockout CMV was tested at concentrations up to 200μM, a condition resembling a CA fed diet. The results suggest a molecular model for bile acid secretion. At least two systems exist in mice, Spgp-mediated transport that may be highly specialized for bile acids and another component that is "leaky" to bile acids. The identity of the second component is unknown. Assuming that the substrate concentration gradient generated in CMV was 4-fold based on taurocholate uptake activity in CMV from wildtype mice (with Km~14μM), the affinity in CMV from *spgp*$^{-/-}$ mice would have to be around 50μM or less in order to be detected by such assay with a similar maximum transport rate of 800nmol/min/gliver. Thus,

the low affinity that was speculated for the alternative transporter may be another reason why bile acid transport was not detectable in the CMV system.

Results from the hepatocyte couplets system supports a large capacity transporter with fluorescent bile acid secreted into canalicular vacuole. However, taurocholate transport is not observed in canalicular membrane vesicles isolated from *spgp*$^{-/-}$ mice. Hepatocyte couplets contain hemicanaliculus which were separated from adjacent hepatocytes during preparation (Fig. 16). These hemicanalicular domains traffic their contents (including the canalicular membrane proteins) to the residual apical domain thus the remaining membrane has increased 2-4-fold in protein level (Boyer, 1990). It is possible that the alternative bile acid transporter may be overexpressed in the hepatocyte couplet system due to this artificial process of membrane trafficking. Thus, a low affinity transport process such as the one speculated with the alternative bile acid transporter may be detected. In the isolated canalicular membrane vesicle system, taurocholate uptake is measured against membrane-dependent taurocholate binding. The binding of taurocholate to membranes results from a variety of mainly nonspecific factors and sites that has no physiologic significance.

Chapter 5: P-glycoprotein mediated ATP-dependent taurocholate transport: *in vitro* evidence for an alternative canalicular bile acid transporter

5.1. Introduction

In the previous study of *spgp*$^{-/-}$ mice, the expression levels of a number of ABC canalicular proteins including Mdr1a, Mdr2 and Mrp3 were dramatically increased. This is consistent with the observed upregulation of Pgp and Mrp3 in cholestatic models and in liver of mice fed with cholic acid (Fickert et al. 2001; Zollner et al. 2003b). In *spgp*$^{-/-}$ mice, the increase in *mdr1a* mRNA and protein levels was correlated with the increase in biliary secretion of bile acids in *spgp*$^{-/-}$ mice. Furthermore, biliary bile acid secretion in *spgp*$^{-/-}$ mice was postulated to have the characteristics of a large capacity and low affinity transport by a putative transporter. Whether Pgp acts as a low affinity bile acid transporter responsible for the alternative bile acid secretion in *spgp*$^{-/-}$ mice has not yet been determined.

To date, biochemical data and studies of gene knockout mouse have not indicated that Pgp has bile acid transport activities (Schinkel et al. 1997). Bile acids have been shown to inhibit transport of Pgp substrates, rhodamine 123 and daunomycin in Pgp overexpression cell lines (Mazzanti et al. 1994). However, there has not been any evidence to support Pgp mediated bile acid transport. Furthermore, mice deficient in both *mdr1a* and *mdr1b* genes do not exhibit signs of liver pathology or affect biliary secretion of bile acids (Schinkel et al. 1994). The substrate specificity of Pgp includes a wide range of substances including anticancer drugs, xenobiotics, natural products, steroids, peptides and proteins (reviewed in (Borst and Elferink 2002)). These substrates are usually cationic or neutral hydrophobic molecules. Bile acids, on the other hand, are negatively charged molecules at physiological pH. Based on these results, it is not known if Pgp has a role in biliary bile acid secretion. However, the striking increase in Pgp protein level and in biliary bile acid level in *spgp*$^{-/-}$ mice and in many cholestatic models suggests a potential role of Pgp in biliary bile acid secretion (see section 3.2.6). Therefore, it is postulated that Pgp mediates bile acid transport when the protein is upregulated and operating at bile acid saturated conditions such as those found in intrahepatic cholestasis.

This chapter investigated taurocholate transport properties *in vitro* using Pgp containing plasma membrane vesicles and examined the effects of bile acids on Pgp-mediated drug transport. If bile acids are transport substrates of Pgp, do they affect the transport of other Pgp substrates? Previously, Shapiro *et al.*, (1997) proposed, based on biochemical studies, that Pgp possesses at least two transport-active drug-binding sites (Shapiro and Ling 1997b). The two sites have distinct overlapping substrate specificities and exhibit positive cooperativity. Results in these studies suggest that Pgp mediated the transport of taurocholate and taurocholate inhibited the transport of other Pgp substrates that interacted directly with these two sites.

5.2. Results

5.2.1. ATP-dependent taurocholate uptake into Pgp plasma membrane vesicles

A highly resistant Chinese hamster cell line, CH^RB30, which has been shown to be 640-fold more resistant to colchicine compared to its parental cell line, AuxB1, was used in this study. CH^RB30 cells were grown continuously in colchicine containing culture medium. Pgp represents about 15% of total membrane proteins analyzed by SDS-PAGE and may contain up to 1 x 10^6 Pgp copies/cell.[3] This cell line has been used extensively for studies in Pgp mediated transport.

The purpose of this study was to determine if Pgp containing membrane vesicles transport the bile acid taurocholate. Fig. 24A shows time-dependent ATP-stimulated taurocholate uptake in Pgp-containing plasma membrane vesicles from CH^RB30 cells. No ATP-dependent taurocholate uptake was observed in plasma membrane vesicles from AuxB1 cells or when the reaction occurred at 4^OC (data not shown). These results indicate that transport activity was specific for Pgp-mediated transport. The substrate concentration gradient established in such system was 3-4-fold as expected. When cyclosporin A (CsA), a potent Pgp inhibitor was added, ATP-dependent taurocholate uptake was inhibited. CsA

---

[3] Pgp is a 170kDa protein that is expressed at a level of 15% of total membrane proteins (which in turn represents 2% of total proteins). The total protein in CH^RB30 PMV is measured to be $2x10^{-9}$mg/cell. The calculation for copies of Pgp expressed in a cell would be (6×10^{23} /170000 x 2 $x10^{13}$ x 0.15) ~ 1 x 10^6 Pgps/cell

inhibited 50% taurocholate uptake at a concentration of 3μM (Fig. 24B). With the addition of lower concentrations of CsA (0.1-0.5μM), stimulation of taurocholate transport was reproducibly observed. This is similar to the observed effect of CsA on drug transport reported by Lu P *et al.*, (2001) and is assumed to be caused by complex allosteric interactions affecting substrate binding and transport (Lu et al. 2001).

ATP-dependent taurocholate uptake was also saturable (Fig. 24C). Initial rate of transport had estimated Km and Vmax value of 69μM and 585pmol/min/mg protein respectively (Fig. 24D). It is interesting to compare the rate of secretion based on taurocholate secretion *in vivo* (chapter 3) to taurocholate transport in Pgp containing membrane vesicles *in vitro* (this study). *In vivo*, the basal rate of taurocholate secretion in wildtype mice and in *spgp*$^{-/-}$ mice was not significantly different (12.2 ± 5.2 nmol/min/g liver and 9.6 ± 1.8 nmol/min/g liver respectively). The estimated rate of taurocholate transport into Pgp containing membrane vesicles was 0.5nmol/min/gliver based on Vmax of 585pmol/min/mg protein. This was 20-fold lower than the basal rate of taurocholate transport *in vivo*. These results indicate that Pgp overexpressing membrane vesicles have a low affinity for taurocholate and a moderate capacity for taurocholate transport.

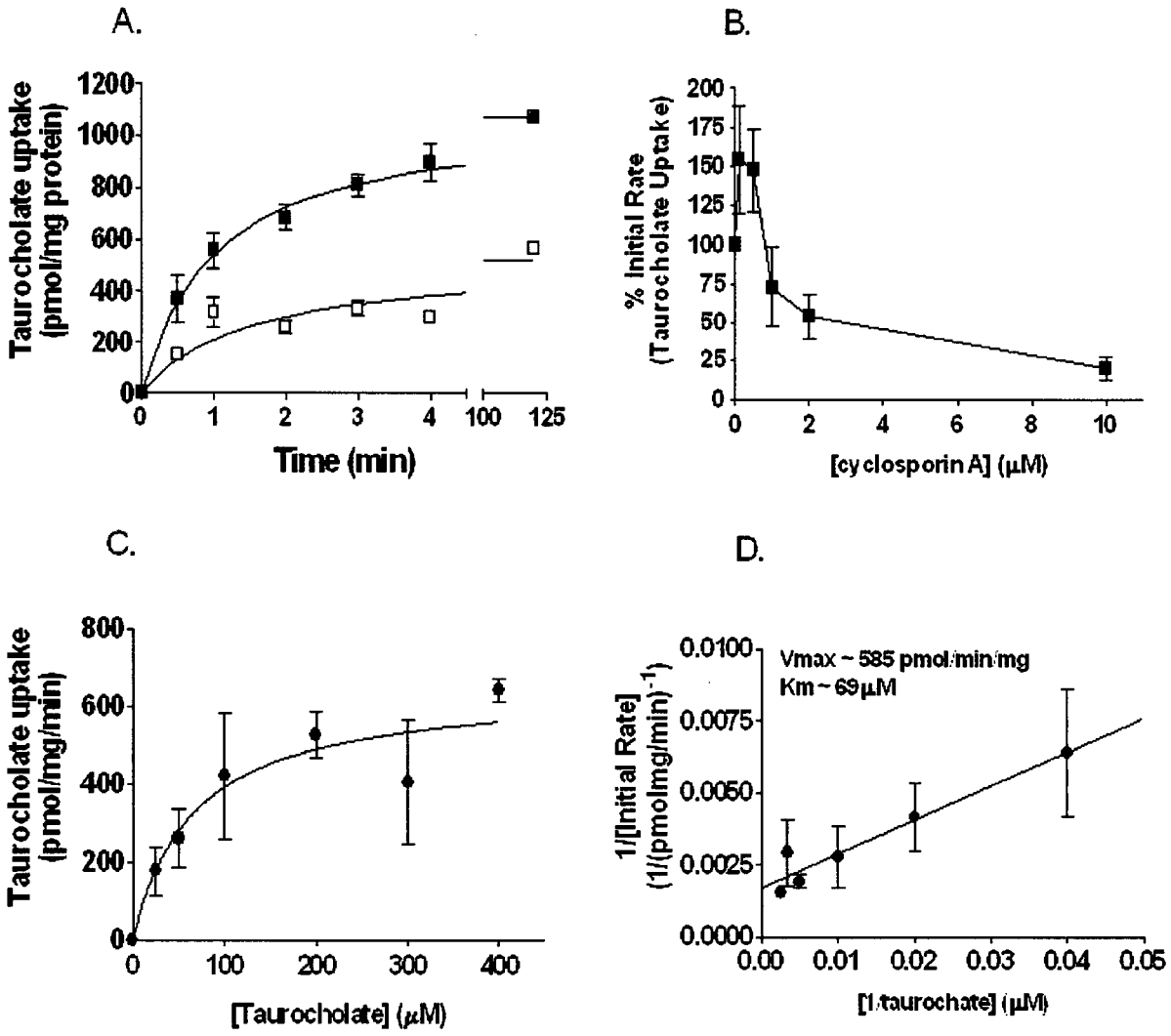

Fig. 24. ATP-dependent taurocholate uptake into Pgp-containing plasma membrane vesicles

(A) Time-dependent taurocholate uptake in the presence of ATP (■) or AMP (□) from Pgp containing CH^RB30 cells. (B) The inhibition of cyclosporin A on ATP-dependent taurocholate uptake in Pgp containing plasma membrane vesicles is shown. (C) ATP-dependent taurocholate uptake (●) is the difference between taurocholate uptake in the presence of ATP and AMP. (D) Transport kinetics parameters are estimated by non-linear regression approach. Apparent Km is 69μM and Vmax is 585pmol/min/mgprotein for ATP-dependent taurocholate transport in Pgp containing plasma membrane vesicles. Results are presented as means ± SEM in triplicate from two experiments.

5.2.2. Rhodamine 123 and Hoechst 33342 transport in Pgp containing membrane vesicles

Pgp has been demonstrated to transport a large number of substrates. Shapiro *et al.*, (1997) have used two fluorescent Pgp substrates to measure initial rate kinetics (Shapiro and Ling 1997b). This approach has the advantage of measuring transport in real time and avoiding the complexity of radiolabel binding to intracellular targets and concentrating within organelles. Fig. 25 illustrates the unique fluorescent properties of Hoechst 33342 and rhodamine 123 transports. Hoechst 33342 is fluorescent when bound to lipid membrane, but not when in aqueous solution. Removal of Hoechst 33342 from the membrane by Pgp in the presence of MgATP was monitored as a loss of fluorescence. Unlike Hoechst 33342, the decrease in fluorescence of rhodamine 123 is due to the entry of the dyes into the aqueous vesicle interior. The initial rate was measured as the decrease in fluorescence due to uptake of the dyes as a function of time. Using this approach, Shapiro *et al.*, (1997) have demonstrated that rhodamine 123 stimulate Hoechst 33342 transport and *vice versa*. This finding has led to the functional model of Pgp containing two positive cooperative sites (R site and H site) for drug binding and transport (Shapiro and Ling 1997b).

Fig. 26 illustrates the time-dependent fluorescence trace of Hoechst 33342 and rhodamine 123 as each one is transported into inside-out Pgp containing membrane vesicles. Addition of MgATP at 0 sec to initiate transport in Pgp containing inside-out membrane vesicles led to a rapid drop in fluorescence, until a new lower steady-state level was reached. Initial rates of fluorescence decrease were measured during the linear part of the trace, typically 4s and 10s for rhodamine 123 and Hoechst 33342 transport measurements, respectively (inset). No ATP-dependent fluorescence decrease occurred when plasma membrane vesicles from AuxB1 cells, the parental cell line of $CH^{R}B30$ cells expressing negligible level of Pgp (data not shown) was added. However, addition of 1μM CsA blocked Pgp transport of rhodamine 123 and Hoechst 33342, rapidly restoring fluorescence to its higher level, indicating that the inhibitor partially collapsed the concentration gradient as the dye passively diffused out of the vesicles (data not shown).

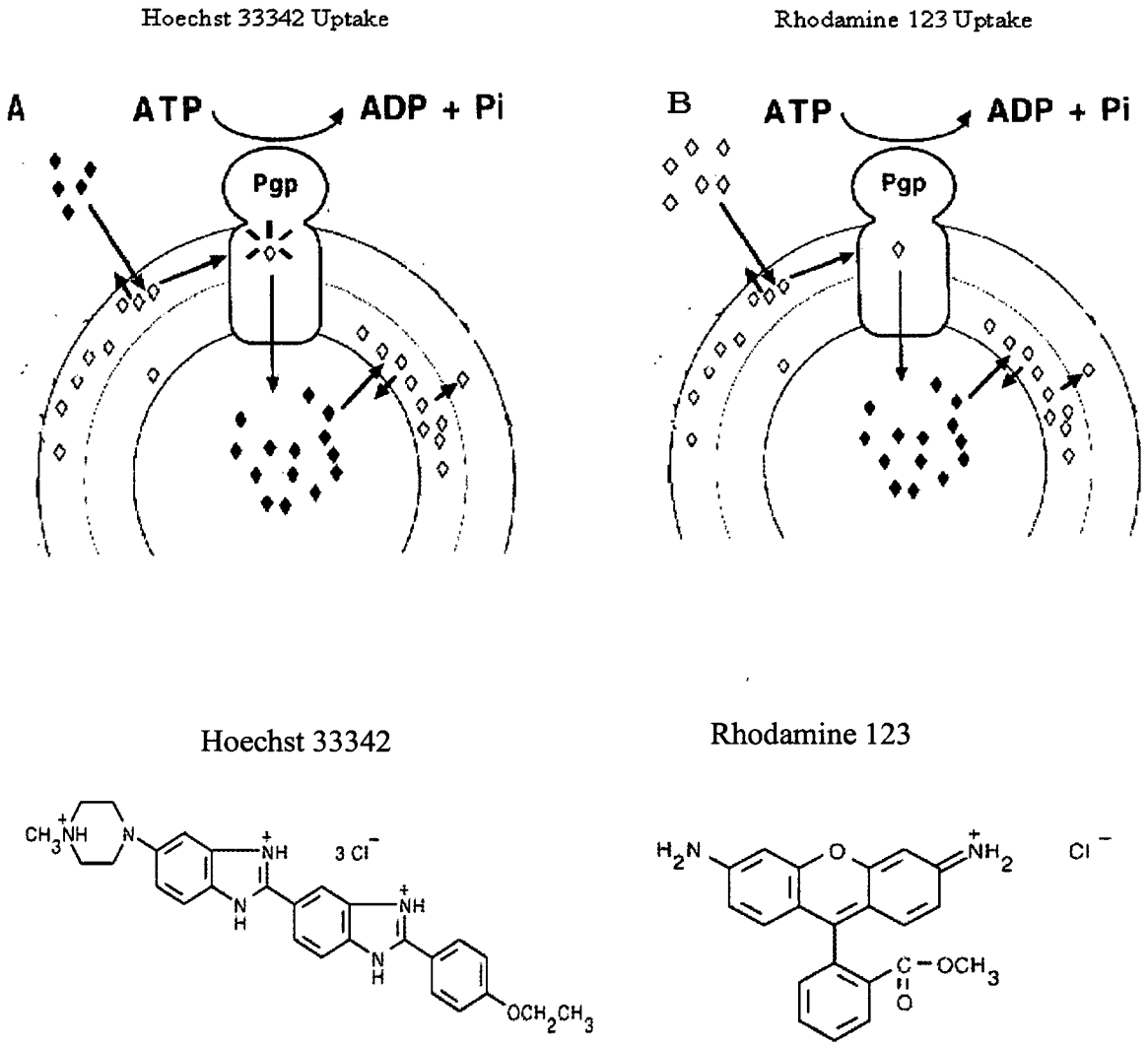

Fig. 25. Cartoon representation of (A) Hoechst 33342 (B) rhodamine 123 uptake by Pgp in isolated $CH^{R}B30$ plasma membrane vesicles.

Hoechst 33342 fluorescence is lipid-dependent (light diamond) in the membrane bilayer and negligible fluorescence in aqueous solution (dark diamond). Rhodamine 123 loses fluorescence when transported into the interior of the vesicles at high concentration. The exact mechanism of this concentration-dependent fluorescence quenching is unknown. Adapted from Shapiro (Shapiro and Ling 1997a).

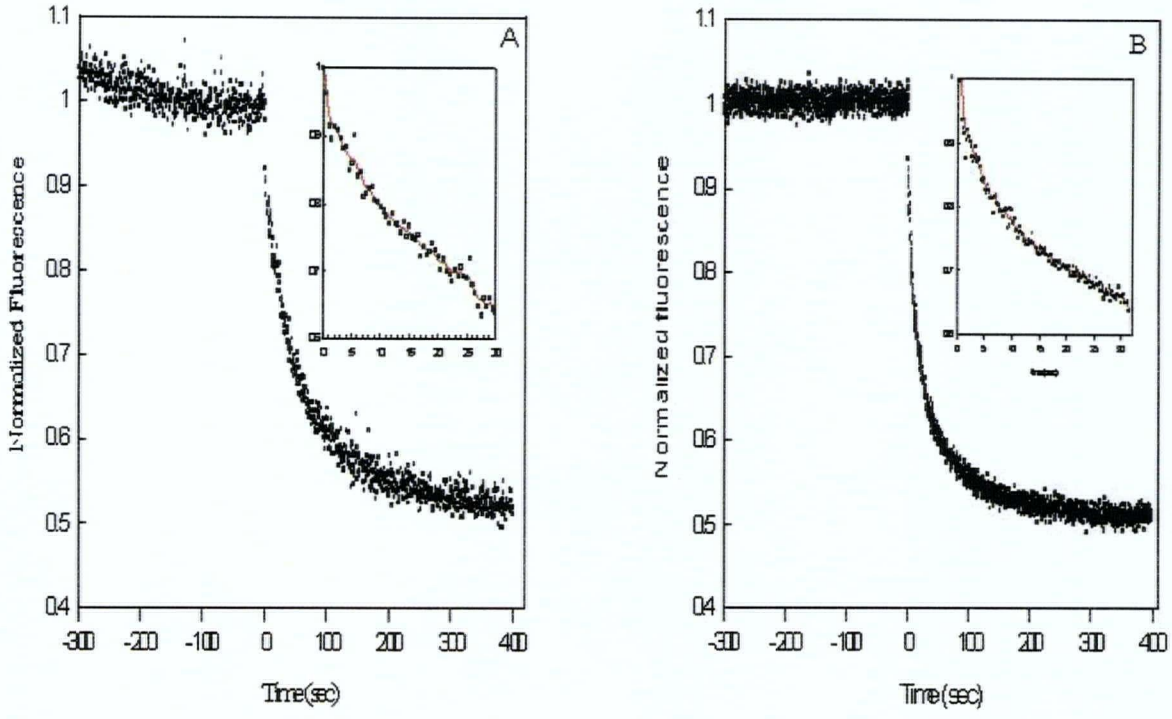

Fig. 26. Transport of (A) Hoechst 33342 (1μM) and (B) rhodamine 123 (1μM) by Pgp in isolated $CH^{R}B30$ plasma membrane vesicles.

The initial rates were measured by linear regression of the traces during the initial linear phase of the fluorescence decrease (inset). Reaction was started at 0 sec by adding 50μl 20xMgATP solution (see Materials and Methods). The fluorescence trace was normalized to a value of 1 at the time of ATP addition. Further details are given in Materials and Methods section.

5.2.3. Effect of drugs on rhodamine 123 and Hoechst 33342 transport in Pgp containing membrane vesicles

Several compounds known to interact with Pgp have been shown to stimulate transport of either Hoechst 33342 or rhodamine 123 and inhibit transport of the other (Shapiro and Ling 1997b). This is interpreted as direct interaction with Pgp at either site. In this study, I wanted to extend the list of substrate specificity of Pgp by studying the interaction of a number of different drugs with Pgp. These drugs were chosen because they may interact with Pgp at either drug-binding site or at a potential third allosteric site. A third site was postulated because progesterone or prazosin has been found to stimulate rhodamine 123 and Hoechst 33342 transport (Shapiro et al. 1999). Using the fluorescent transport assay, any substrates that inhibits rhodamine 123 transport is postulated to bind to the designated R-site and any substrate that inhibits Hoechst 33342 transport is postulated to bind to the designated H-site. In addition, any compound that stimulates both rhodamine 123 and Hoechst 33342 would be thought of as binding to a third allosteric site that regulates the transport of rhodamine 123 and Hoechst 33342.

Dey *et al.*, (1997) reported that (Z)-4-(3-(2-(trifluoromethyl)-9H-thioxanthen-9-ylidene)-propyl)-1-piperazine (*cis*(Z)-flupentixol) increases the affinity of ^{125}I-idoarylazidoprazosin for the C-terminal half of P-glycoprotein without altering the interaction with the N-terminal half (Dey et al. 1997). This result suggests the presence of a third allosteric site to which *cis*(Z)-flupentixol binds. Prenylamine, propanolol and haloperidol caused large enhancements of ^{125}I-iodoarylazidoprazosin photolabeling of Pgp. Therefore, they might also interact with Pgp at the postulated allosteric site. We examined this by testing the effects of these compounds on transports of rhodamine 123 and Hoechst 33342 by Pgp in CH^{R}B30. Haloperidol weakly inhibited the initial rate of Hoechst 33342 transport, and more strongly inhibited the initial rate of rhodamine 123 transport, consistent with a higher affinity for the R site (Fig. 27A). *Cis*(Z)-flupentixol inhibited rhodamine 123 transports at concentrations above 0.2μM. In contrast, Hoechst 33342 transport was slightly stimulated at *cis*(Z)-flupentixol concentrations between 0.1μM and 1μM, but inhibited at higher concentrations (Fig. 27B). These results are consistent with recognition of *cis*(Z)-

flupentixol by both H and R sites, with the R site having greater affinity for *cis*(Z)-flupentixol. *R*(+)propanolol inhibited the initial rates of both rhodamine 123 and Hoechst 33342 transport but with a greater effect on Hoechst 33342 transport, suggesting that that *R*(+) propanolol had slightly higher affinity for the H site than for the R site (Fig. 27C). Sub-micromolar concentrations of prenylamine inhibited the initial rates of both rhodamine 123 and Hoechst 33342 transport (Fig. 27D). These results suggest that prenylamine bound to both H and R sites with the R site having higher affinity. In summary, cis(Z)-flupentixol and haloperidol were more selective for the R-site while *R*(+)propanolol was selective for the H-site and prenylamine bound to both sites with similar affinity.

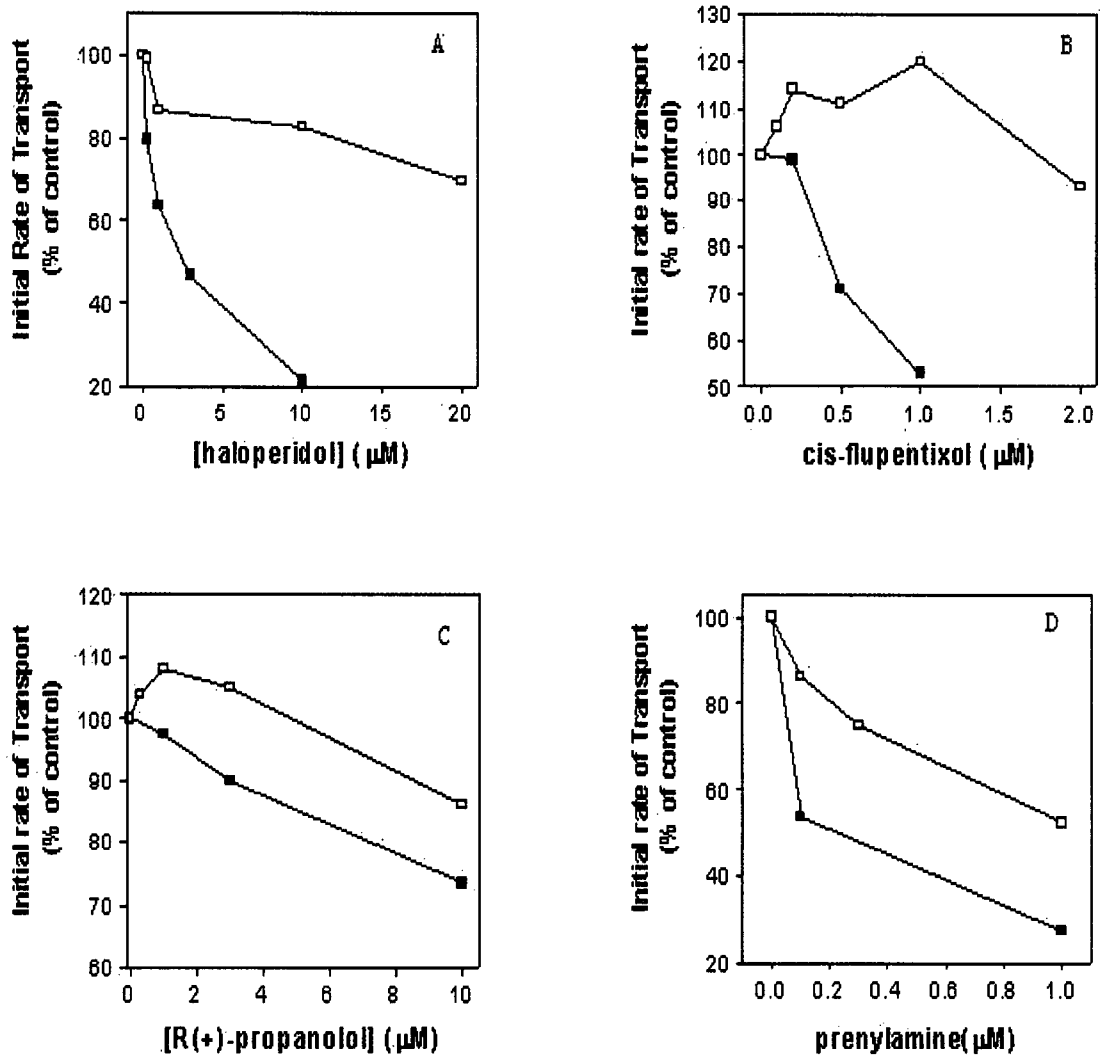

Fig. 27. Effects of different compounds on rhodamine 123 and Hoechst 33342 transports by Pgp in isolated CHRB30 plasma membrane vesicles.

Effects of (A) Haloperidol , (B) cis (*Z*)-flupentixol, (C) *R*(+) propanolol , (D) prenylamine on the initial rate of transport of 1μM rhodamine 123 (■) or 1μM Hoechst 33342 ( ) by P-glycoprotein in isolated $CH^{R}B30$ plasma membrane vesicles. These results are published in (Shapiro et al. 1999).

5.2.4. Effect of bile acids on rhodamine 123 and Hoechst 33342 transport in Pgp containing membrane vesicles

Given that TCA is transported by Pgp, the expectation is that TCA and other bile acids will compete with other Pgp substrates for transport. Most Pgp modulators studied in section 5.2.3 inhibited rhodamine 123 and Hoechst 33342 transport. However, other Pgp modulators such as progesterone and prazosin have been shown to stimulate both rhodamine 123 and Hoechst 33342 transport (Shapiro et al. 1999). This study was to investigate the effects of bile acids on rhodamine 123 and Hoechst 33342 transport. TCA strongly inhibited the initial rate of rhodamine 123 and Hoechst 33342 transport and to the same extent (Fig. 28A). TCDCA also inhibited the transport of rhodamine 123 and Hoechst 33342 to the same extent but at a lower concentration than TCA (Fig. 28B). TUDCA inhibited both rhodamine 123 and Hoechst 33342 transport but to a lesser extent than both TCA and TCDCA (Fig. 28C). In contrast, TBMCA did not inhibit either rhodamine 123 or Hoechst 33342 transport (Fig. 28D). The characteristics of inhibition by bile acids suggest that the three bile acids, TCA, TCDCA and TUDCA, bound to both rhodamine 123 and Hoechst 33342 with equal affinity whereas TBMCA did not bind to either site.

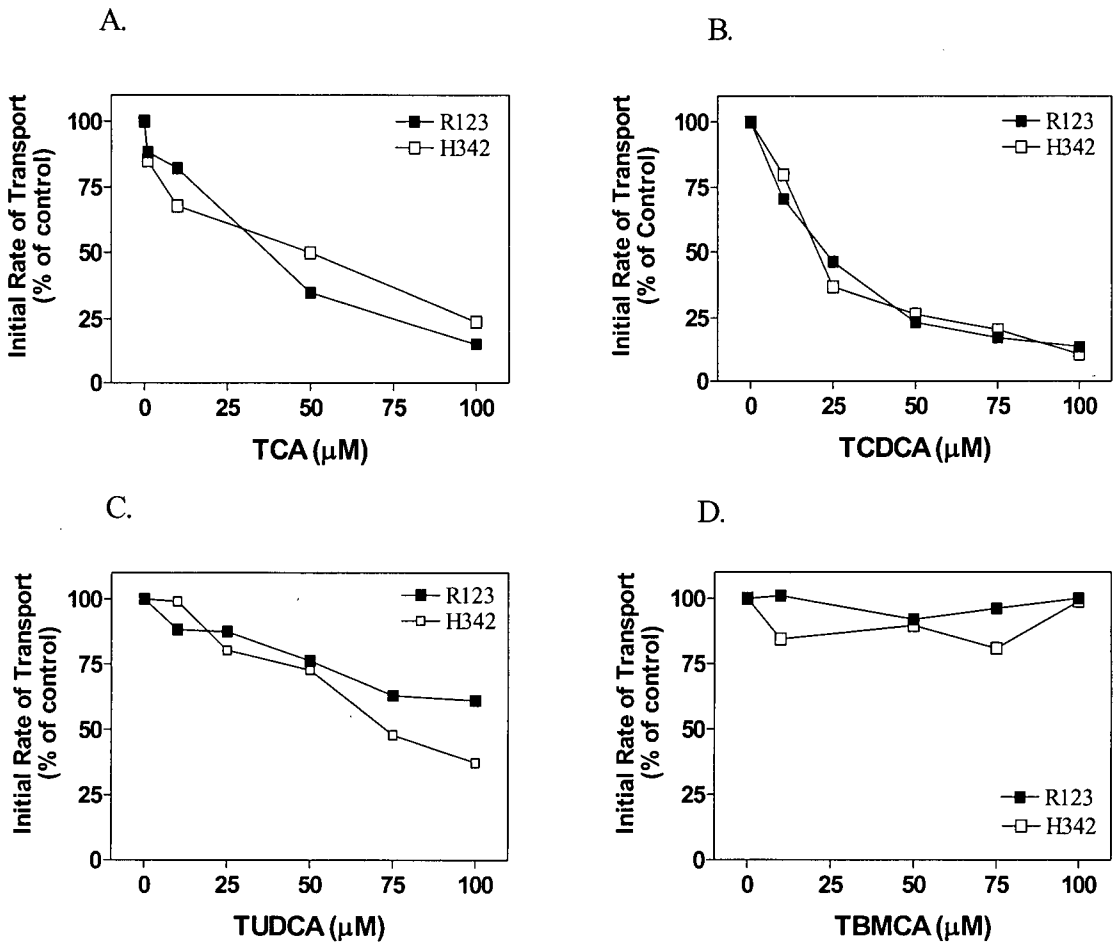

Fig. 28. Effects of bile acids on rhodamine-123 and Hoechst 33342 transport by Pgp in isolated CH^RB30 plasma membrane vesicles.

Effect of (A) taurocholate (TCA), (B) taurochenodeoxycholate (TCDCA), (C) tauroursodeoxycholate (TUDCA) and (D) tauro-betamuricholate (TBMCA) on the initial rate of transport of 1μM rhodamine 123 (■) or 1μM Hoechst 33342 (□) by P-glycoprotein in isolated CH^RB30 PMV.

5.2.5. Effect of bile acids on ATP hydrolysis in Pgp containing membrane vesicles

Since Pgp transport is dependent on ATP hydrolysis, bile acids could inhibit rhodamine 123 and Hoechst 33342 transport by affecting ATP hydrolysis. Fig. 29 shows the effect of bile acids on ATP hydrolysis. Taurocholate (TCA), taurochenodeoxycholate (TCDCA) and tauroursodeoxycholate (TUDCA) inhibited ATPase activity of membrane vesicles isolated from CH^RB30 cells but not from control membrane vesicles from AuxB1 cells. TCDCA, the most hydrophobic bile acid, inhibited ATPase activity at a greater extent. For example, 100μM TCDCA inhibited 40% of ATPase activity, whereas 100μM TCA and 100μM TUDCA inhibited ATPase activity by 20% and 10% respectively. The extent of inhibition was dependent on bile acid concentration. The amount of inhibition of ATP hydrolysis might translate into large effects on the rate of rhodamine 123 or Hoechst 33342 transport (see section 5.2.4). The order of potency of inhibition of ATPase activity was TCDCA > TCA > TUDCA, consistent with the order of potency of inhibition of rhodamine 123 and Hoechst 33342 transports. On the other hand, a more hydrophilic bile acid, taurobetamuricholic acid (TMCA) did not inhibit ATPase activity of membrane vesicles isolated from CH^RB30 cells at 50μM or 100μM. This lack of inhibition of ATP hydrolysis was also consistent with lack of inhibition of rhodamine 123 and Hoechst 33342 transports.

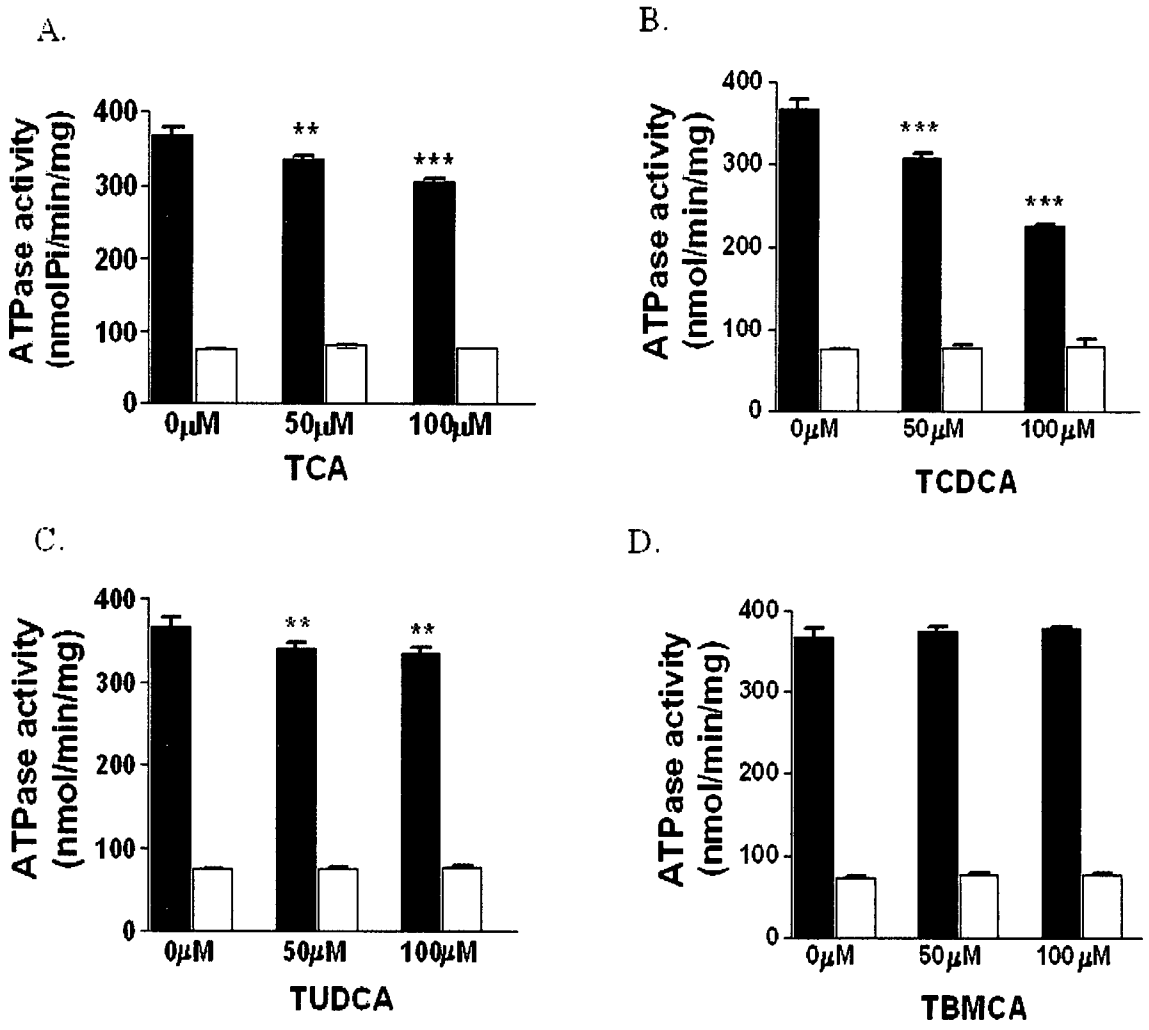

Fig. 29. Effects of bile acids on the ATPase activity of P-glycoprotein in isolated CH^RB30 plasma membrane vesicles (■) and in isolated control AuxB1 plasma membrane vesicles (□).

Each bar represents the mean ± S.D. of three different experiments. Asterisks indicate statistical significance between tested compound and control, *, $0.01 < P < 0.05$; **, $0.001 < P < 0.01$; ***, $P < 0.001$.

5.2.6. Effect of bile acids on equilibrium of rhodamine 123 transports

In the previous sections, I have provided evidence that Pgp may interact directly with bile acids and be transported (section 5.2.1). The presence of bile acids can also inhibit the transport of other Pgp substrates (i.e. rhodamine 123 and Hoechst 33342) (section 5.2.2), or decreased Pgp catalytic ATP hydrolysis (section 5.2.5). In this study, a different strategy was used to show that bile acids interact with Pgp. This study takes advantage of the sophiscated fluorescence assay that allow us to measure transport continuously at a millisecond scale. As demonstrated in section 5.2.2, rhodamine 123 transport is observed in Pgp plasma membrane vesicles. The initial rate of transport is inhibited by most of the bile acids tested with the exception of TBMCA. In this experiment, rhodamine 123 transport is continuously monitored until a steady state is reached (i.e. the rate of rhodamine 123 transport into the vesicles was balanced by the rate of diffusion out of the vesicles), and then bile acids are added to observe the effect on this steady state. As expected, addition of 100μM TCDCA or TCA or TDCA immediately inhibited the rate of rhodamine 123 transport and partially collapsed the concentration gradient to a different level. The extent of the collapse is correlated with the inhibition of initial rate of transport. Addition of 100μM CHAPS was used a control to demonstrate a complete collapse of the gradient. Taken together with the result that TCA is transported by Pgp, it is likely that certain bile acids interact directly with Pgp to inhibit drug transport.

Unexpected is the finding that 100μM TBMCA or 100μM TUDCA stimulated more rhodamine 123 to be transported at steady state (Fig. 30). Like other Pgp substrates, it is likely that these bile acids could affect Pgp activity by altering the fluidity of the lipid bilayer. Bile acid species have been shown to affect membrane fluidity (Asamoto et al. 2001). This observation suggests that TUDCA or TBMCA increased membrane fluidity and thus affected the rate of membrane entry and transbilayer movement of rhodamine 123. This allowed more rhodamine 123 to interact with Pgp, thus increased the concentration gradient that would otherwise equilibrate in the absence of the bile acid.

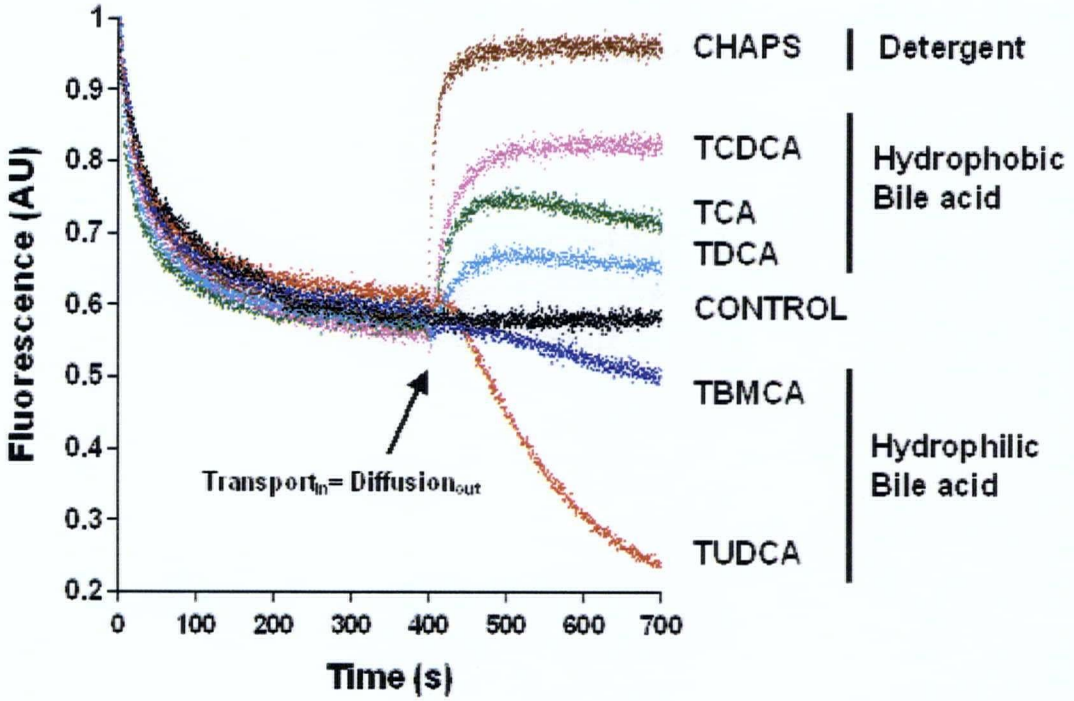

Fig. 30. Effects of bile acids on the rhodamine-123 substrate concentration gradient by Pgp in isolated CH^{R}B30 plasma membrane vesicles.

Fluorescence trace of rhodamine 123 was monitored for 400 sec and then 10µl (100µM final concentration) of bile acid was injected and fluorescence was monitored for another 300 sec as described in Materials and Method. The following bile acids and controls were tested: Tauro-chenodeoxycholate, (TCDCA), taurocholate, (TCA), taurodeoxycholate (TDCA), taurobetamuricholate (TBMCA), tauroursodeoxycholate (TUDCA), CHAPS or methanol (CONTROL).

5.3. Discussion

5.3.1. Finding taurocholate transport by Pgp in CH^RB30 membrane vesicles

There are several aspects that prompted me to study taurocholate transport by Pgp. In *spgp*$^{-/-}$ mice, taurocholate was secreted into the bile at the same rate as wildtype mice when fed with CA diet. Therefore, this alternative system is of large capacity and adaptive to bile acid loading. The reason for the inability to measure taurocholate uptake in canalicular membrane vesicles from *spgp*$^{-/-}$ mice is not known, but may be related to the combined effects of low catalytic efficiency of the alternative transporter (i.e. a high Michaelis Menten Km value) and a comparatively high nonspecific binding of bile acids to the membrane. Bile acid transported into membrane vesicles from *spgp*$^{-/-}$ mice may be difficult to detect above the background. The possibility that membrane vesicles are leaky which leads to the inability to generate a solute gradient is not likely because of its ability to maintain LTC_4 gradient, mediated by Mrp2, in the same canalicular membrane vesicles. To resolve this problem, membrane vesicles of Pgp over-expressing cell line (in which Pgp constitutes 15% of the total membrane proteins) was used, in order to increase the protein to lipid ratio in anticipation of a low affinity bile acid transport.

This work shows that Pgp in plasma membrane vesicles transported taurocholate in a time-dependent, saturable and CsA-inhibitable manner. The transport kinetics was consistent with Pgp being a low affinity and relatively large capacity transporter. Another ABC transporter, Mrp2 has recently been demonstrated to have bile acid transport activity in insect cell membrane vesicles (Bodo et al. 2003). Analogous to Pgp, Mrp2 mediated glycocholate transport with the characteristics of lower affinity (Km ~ 150-200μM) and relatively smaller capacity (Vmax~100pmol/min/mg protein). Two characteristics of Mrp2 suggested that it might not play a significant role in canalicular bile acid transport. First, I found that in *spgp*$^{-/-}$ mice, Mrp2 protein level was increased 2-fold compared to wildtype mice. However, this level of increase was at least 3-fold less than that of Pgp. Second, the physiologic function of bile acid transport by Mrp2 has not been demonstrated. Mrp2 deficient mice have similar level of bile acids in the bile as wildtype controls. Spgp, however, would still be functional in this case and would not require another compensatory bile acid transporter. Mrp2 in the

liver canalicular membrane had been found to transport a number of non-bile acid organic anions including glucuronidated bilirubin, leukotriene C_4 and many glutathione and sulphated conjugates, with different affinity and capacity (Keppler et al. 1997). These compounds were found at relatively high concentrations in the liver. *In vitro*, they have been demonstrated to have high affinity for Mrp2 and therefore would be better physiological substrates than bile acids (Keppler and Konig 2000).

At first, it was not obvious why Pgp would retain bile acid transport activity in the presence of Spgp, a very good bile acid transporter. One possibility was that optimal transport of unidentified physiological substrates might require Pgp to transport bile acids as an unavoidable consequence. Pgp appeared to have broader substrate specificity and were better equipped to secrete high affinity drugs, steroids and peptides (Ueda et al. 1992; Sharom et al. 1999; Lu et al. 2001; Rybczynska et al. 2001). However, the physiological concentrations of these substrates in the liver are well below bile acid concentration. Under high bile acids loading conditions, that is when concentrations become threatening to the function of the liver, the membrane bilayer may be saturated with bile acids. The interaction with Pgp has been postulated to be within the membrane bilayer as found with a number of Pgp substrates *in vitro* (Shapiro and Ling 1997a). The low affinity and high rate of taurocholate transport suggested that Pgp operated at such condition to remove potentially toxic bile acids from the membrane bilayer. Whether Pgp and Spgp shared the same selectivity of all bile acid species needs to be investigated further.

5.3.2. Effect of bile acids on Pgp mediated transport

Transport by Pgp has been shown to be different from other ATP-driven transporters in that it could recognize many different substrates. Most of these substrates are hydrophobic and could passively diffuse into the membrane bilayer (DiDiodato and Sharom 1997). After partitioning in the membrane, Pgp could expel the substrate directly from the membrane bilayer (Shapiro and Ling 1997a). To support this model, there are evidence that showed drug binding affinities were affected by the nature of the lipid environment (Sharom 1997), and lipid-water partition coefficient (Plip) and membrane fluidizing property of Pgp substrates affect activity of Pgp (Romsicki and Sharom 1999). Direct interactions of bile

acids with Pgp have not been reported. My results showed that Pgp interacts and transports taurocholate. This binding is of low affinity and the transport is of low catalytic efficiency. There are also indications that certain bile acids (i.e. tauroursodeoxycholic acid) could also affect Pgp activity by modulating the nature of the lipid environment.

Chapter 6: Conclusions and perspectives for future research

The most surprising finding of this study is that a low affinity bile acid transporter exists in mice. The evidence with canalicular membrane vesicles indeed suggests that an alternative low affinity transporter mediates bile acid transport. Before this discovery, the biliary community has widely accepted that Spgp is the dedicated and exclusive transporter in bile acid secretion from hepatocyte to bile. This study provides direct evidence that at least one of the Pgps in mouse could transport taurocholate *in vitro*. Whether raised levels of Pgps could contribute to bile acid secretion *in vivo* has not yet been studied. This raises the obvious question why is mutation in *spgp* in human result in a more severe liver cholestatic phenotype than in mouse? Complete congenital absence of the Spgp protein result in serious liver cholestasis that manifest shortly after birth. The potential importance of Pgps in cholestasis is therefore, high. The data in this project show that *spgp*$^{-/-}$ mice have at least two compensatory mechanisms: first, the secretion of hydrophilic bile acids such as taurobetamuricholic acids, the highly abundant bile acids in mouse, are not affected and its secretion helps in maintaining bile flow. Human bile acids are more hydrophobic (and therefore aggressive towards membranes) than those of mouse therefore bile acid-induced toxicity in the liver will progress rapidly in human. It is also possible that Pgp(s) are better at recognizing and transporting mouse bile acids. This is supported by data presented in chapter 3 showing that the muricholic acid output is higher than cholic acid in *spgp*$^{-/-}$ mice. Whereas humans have only one Pgp, mice have two, mdr1a and mdr1b. It may be that both Pgps quantitatively contribute to bile acid secretion. It is therefore, of high interest to test whether there is an increased expression of Pgp(s) in livers of PFIC2 patients.

In addition to the diminished bile acid secretion, there are a number of abnormalities in the liver, plasma and bile of the *spgp*$^{-/-}$ mice. Unexpected is the marked decrease in plasma cholesterol, in particular, the HDL component of cholesterol. The apolipoprotein A-I component of HDL has been found to be slightly downregulated in *spgp*$^{-/-}$ mice. CA feeding further suppressed apoA-I mRNA level and plasma HDL cholesterol level in *spgp*$^{-/-}$ mice. This initial analysis may represent an oversimplification of abnormal plasma lipoprotein profile in *spgp*$^{-/-}$ mice. It is possible that we may still find other atypical lipoproteins or

abnormal level of common lipoproteins in *spgp*$^{-/-}$ mice. This study raises the possibility that PFIC2 patients may also have lower plasma apoA-I and HDL cholesterol level. This possibility is supported by evidence from an ealier study that serum apoA-I level is 3-fold lower than normal in patients with PFIC (Claudel et al. 2002). However, the subtype of PFIC has not been characterized at that time.

Unexpected sex dimorphism in bile acid secretion and bile flow was also found in *spgp*$^{-/-}$ mice. The mechanisms underlying sex-specific reduction in bile flow and bile acid secretion in *spgp*$^{-/-}$ female mice are not understood. Sex-dependent differences in bile acid composition, bile acid uptake rate and bile acid metabolism in normal rat have been reported but the molecular basis is incompletely understood (Kuroki et al. 1983; van Nieuwkerk et al. 1997). Plausible explanations for the differences in response of *spgp*$^{-/-}$ mice include: (i) sex related differences in bile acid transporters number or affinity or (ii) sex specific bile acid transporters dynamics that may be regulated by 'female' or 'male' hormonal milieu of the cell. In this study, analysis of mRNA expression level of the liver transporters *mdr1a*, *spgp*, *mdr1b*, *mdr2*, *mrp2*, *mrp3*, and *ntcp* revealed no significant difference between male and female *spgp*$^{-/-}$ mice (Chapter 3). Another possibility, equally speculative is that female sex steroids such as progesterone, which are Pgp substrates, can compete with bile acids for transport thereby lowering the rate and efficiency of bile acid output. Female sex steroids have long been linked to cholestasis (Kreek 1987; Vore 1987). The action of sex hormones on ABC transporters expression and activity and how this is linked to cholestasis are clearly complex. Future research directed at elucidating the specific mechanisms whereby sex hormones regulate bile acid metabolism and ABC transporters are needed.

The discovery that Pgp can transport taurocholate is surprising (Chapter 5) because Pgp has always been associated with drug transporting activity and its physiological role in various tissues is unknown. Mice lacking Mdr1a and Mdr1b are normal but become hypersensitive to drugs suggesting that Pgp play no significant role in physiology, and that its main function, if not exclusive role is in the protection of the organism against naturally occurring toxins (Schinkel et al. 1994). It seems unlikely that Pgps will contribute significantly to bile acid secretion under physiological condition because Spgp appears able

to fully compensate for the absence of mdr1a and mdr1b in knockout mice. In *mdr1a/1b*$^{-/-}$ mice, the other ABC transporters such as *mrp1*, *spgp*, and *cftr* are not upregulated suggesting further compensatory transport activity by these proteins is not required in the absence of Pgp activity (Schinkel et al. 1997). *Spgp*$^{-/-}$/*mdr1a*$^{-/-}$ and *spgp*$^{-/-}$/*mdr1b*$^{-/-}$ mice will be particularly useful for studying the role of Pgp in the liver. If both mdr in mice contribute to biliary bile acid secretion, it will also be useful to study *spgp*$^{-/-}$/*mdr1a*$^{-/-}$/*mdr1b*$^{-/-}$ triple knockout mice to dissect these increasing complex secretory pathways. Rapid analysis of the expression levels of these genes in *spgp*$^{-/-}$ mice will provide a reconstruction of the molecular profile of cholestasis. Whatever these changes may be, the expected diminished capacity to secrete bile acids in a double and a triple knockout mouse will provide a better model for human PFIC2. Moreover, what has to be done is to sort out which Pgps are important in bile acid secretion in humans and how we could make use of this knowledge to treat PFIC2 patients.

The possibility that upregulation of other proteins also contribute to bile acid secretion remains open. Wide-ranging changes in liver genes expression in *spgp*$^{-/-}$ mice have been observed by real time PCR (Chapter 3) and by serial analysis of gene expression (SAGE) (Lin Liu, unpublished). For example, basolateral *mrp3* and *mrp4* are dramatically upregulated in *spgp*$^{-/-}$ mice liver. This is consistent with massive increase in the expression of *mrp3* and *mrp4* observed in the liver of humans and of cholestatic rat (Hirohashi et al. 1998; Ortiz et al. 1999). The role of Mrp3 in bile acid reabsorption from the gut and efflux from the liver into the blood has been postulated (Kool et al. 1999; Hirohashi et al. 2000). The actual importance of Mrp3 in bile acid efflux could be evaluated in *spgp*$^{-/-}$/*mrp3*$^{-/-}$ mice. It would be interesting to see that if both basolateral and canalicular bile acid transporters are knockout, will the mice live? Like *spgp*$^{-/-}$ mice, I expect that *spgp*$^{-/-}$/*mrp3*$^{-/-}$ mice to have further upregulation of *mdr1a* and *mdr1b*, downregulation of *ntcp,* downregulation of bile acid biosynthesis with alterations in bile acid composition to more hydrophilic bile acids. However, *spgp*$^{-/-}$/*mrp3*$^{-/-}$ mice may still exhibit severe cholestasis or is lethal if compensatory mechanisms such as Pgp are not able to help clear the bile acids from the liver.

The ubiquitous functioning of Pgp *in vivo* has not been fully appreciated in the absence of phenotype in *mdr* knockout mice. The capability of Pgp to translocate

taurocholate may radically change our views on the physiological function of the protein. Besides pumping xenobiotics across the apical membranes of cells, Pgp may serve as a compensatory protein in the transport of other physiological substrates, be it bile acids in the liver or cortical hormones in the adrenal gland or other tissue-specific metabolites.

This study conclusively showed that Spgp is the major, high affinity bile acid transporter. Spgp is expressed highly in the liver with very low level detected in the brain gray cortex, small- and large-gut mucosa (Torok et al. 1999). The function of Spgp in other tissues is not known and its low expression presents a challenging task for functional analysis. Apart from the bile acid secretory role of Spgp, there are no indications for additional role of this protein in the liver. However, extensive search for other substrates have not been tested. Lecureur *et al.*, (2000) found no Spgp mediated drug-transporting activity using Pgp substrates such as vincristine, daunomycin, paclitaxel and digoxin, in drug uptake and efflux assays (Lecureur et al. 2000). Transfection of rat Spgp into a human ovarian cancer cell line (SKOV) also did not exhibit dramatic resistance to drugs in cytotoxicity assays (Childs et al. 1998). It seems unlikely that Spgp plays a significant role in drug resistance although studies in clinical tumor samples have not been investigated.

In view of the ability of Pgp to transport bile acids, it would be conceivable that drugs that induced cholestasis may inhibit Pgp transport in the liver. The importance of defining the effect of Pgp inhibitors on bile acid transport is thus, of great clinical value. Cyclosporin A (CsA), commonly used in transplantation surgery caused cholestasis in patients characterized by increase in serum bile acids, and bilirubin levels. CsA can also induced cholestasis in rat model resulting in reduction in bile salt secretion and bile flow (Stone et al. 1987). One possible mode of action of CsA is the inhibition of bile acid transport across the hepatocyte. CsA is a potent inhibitor of Spgp mediated bile acid transport and therefore may represent the molecular mechanism of CsA induced cholestasis (Stieger et al. 2000). This study showed that CsA also inhibit taurocholate transport in Pgp membrane vesicles. It is speculated that like Spgp, inhibition of Pgp transport activity may also account for some forms of drug-induced cholestasis.

Transport of bile acids by Pgp is technically difficult to demonstrate in mice canalicular membrane vesicles (Chapter 4). This experimental difficulty in demonstrating low affinity transport in membrane vesicles has been documented for GSH transport (Ballatori and Rebbeor 1998). Using stably cells expressing human MRP1 and MRP2, investigators have observed a correlation of MRP expression and GSH efflux from the cells but they have not been able to detect GSH transport in isolated membrane vesicles (Paulusma et al. 1999). In my study, it is speculated that the inability to detect taurocholate transport in canalicular membrane vesicles is due to the low catalytic efficiency of transport (Chapter 4). Indeed, this low affinity for taurocholate has been demonstrated in Pgp overexpressing membrane vesicles (Chapter 5). It is expected that canalicular membrane vesicles will still be important in demonstrating high affinity transport in a natural lipid environment. However, in view of the technical problems, alternative approaches of using transfection systems or model cell lines are recommended to study low affinity transport. More experiments with membrane vesicles from transfected cell line containing Pgp and Spgp expressed at a high level are clearly required to settle the issue of overlapping substrate specificity of these transporters. Moreover, by comparing the transport specificity between Pgp and Spgp, one can assess how they contribute individually and together in bile acid transport.

Attempts have been made to define what makes Pgp a drug transporter. The most widely accepted model is Pgp intercepts and directly transports its substrates from the membrane bilayer. This model is consistent with many observations. Pgp has demonstrated flippase activity (Romsicki and Sharom 2001), is able to extract fluorescent dye from the cytoplasmic leaflet of the membrane bilayer (Shapiro and Ling 1997a) and photoaffinity analogs of substrates bind to the transmembrane helices (Ecker et al. 2002). It is compelling to ask what common structural features in Spgp and Pgp are important for bile acid recognition. The availability of different Pgps and Spgp with different substrate specificities should allow for more systematic studies by exchanging different domains and direct mutagenesis to dissect out distinct functional domains of the proteins. It will also be a formidable task for protein biochemists and x-ray crystallographers to elucidate the structure

of such large transmembrane proteins. Homology in sequence and function of Spgp and Pgps should also prove useful in the understanding of how these transporters work.

REFERENCES

Alonso, E.M., D.C. Snover, A. Montag, D.K. Freese, and P.F. Whitington. 1994. Histologic pathology of the liver in progressive familial intrahepatic cholestasis. *J Pediatr Gastroenterol Nutr* **18**: 128-33.

Ambudkar, S.V., S. Dey, C.A. Hrycyna, M. Ramachandra, I. Pastan, and M.M. Gottesman. 1999. Biochemical, cellular, and pharmacological aspects of the multidrug transporter. *Annu Rev Pharmacol Toxicol* **39**: 361-98.

Arias, I.M. 1990. Multidrug resistance genes, p-glycoprotein and the liver. *Hepatology* **12**: 159-65.

Asamoto, Y., S. Tazuma, H. Ochi, K. Chayama, and H. Suzuki. 2001. Bile-salt hydrophobicity is a key factor regulating rat liver plasma-membrane communication: relation to bilayer structure, fluidity and transporter expression and function. *Biochem J* **359**: 605-10.

Ballatori, N. and J.F. Rebbeor. 1998. Roles of MRP2 and oatp1 in hepatocellular export of reduced glutathione. *Semin Liver Dis* **18**: 377-87.

Ballatori, N., J.F. Rebbeor, G.C. Connolly, D.J. Seward, B.E. Lenth, J.H. Henson, P. Sundaram, and J.L. Boyer. 2000. Bile salt excretion in skate liver is mediated by a functional analog of Bsep/Spgp, the bile salt export pump. *Am J Physiol Gastrointest Liver Physiol* **278**: G57-G63.

Ballatori, N. and A.T. Truong. 1992. Glutathione as a primary osmotic driving force in hepatic bile formation. *Am J Physiol* **263**: G617-24.

Barnwell, S.G., P.J. Lowe, and R. Coleman. 1983. Effect of taurochenodeoxycholate or tauroursodeoxycholate upon biliary output of phospholipids and plasma-membrane enzymes, and the extent of cell damage, in isolated perfused rat livers. *Biochem J* **216**: 107-11.

Belinsky, M.G., Z.S. Chen, I. Shchaveleva, H. Zeng, and G.D. Kruh. 2002. Characterization of the drug resistance and transport properties of multidrug resistance protein 6 (MRP6, ABCC6). *Cancer Res* **62**: 6172-7.

Benedetti, A., D. Alvaro, C. Bassotti, A. Gigliozzi, G. Ferretti, T. La Rosa, A. Di Sario, L. Baiocchi, and A.M. Jezequel. 1997. Cytotoxicity of bile salts against biliary epithelium: a study in isolated bile ductule fragments and isolated perfused rat liver. *Hepatology* **26**: 9-21.

Berge, K.E., H. Tian, G.A. Graf, L. Yu, N.V. Grishin, J. Schultz, P. Kwiterovich, B. Shan, R. Barnes, and H.H. Hobbs. 2000. Accumulation of dietary cholesterol in sitosterolemia caused by mutations in adjacent ABC transporters. *Science* **290**: 1771-5.

Berry, M.N. and D.S. Friend. 1969. High-yield preparation of isolated rat liver parenchymal cells. *Journal of Cell Biology* **43**: 506-520.

Bjorkhem, I. 1985. *Mechanism of bile acid biosynthesis in mammalian liver*. Elsevier, Amsterdam.

Bjorkhem, I., U. Andersson, E. Ellis, G. Alvelius, L. Ellegard, U. Diczfalusy, J. Sjovall, and C. Einarsson. 2001. From brain to bile. Evidence that conjugation and omega-hydroxylation are important for elimination of 24S-hydroxycholesterol (cerebrosterol) in humans. *J Biol Chem* **276**: 37004-10.

Bjorkhem, I., U. Andersson, E. Sudjama-Sugiaman, G. Eggertsen, and P. Hylemon. 1993. Studies on the link between HMG-CoA reductase and cholesterol 7 alpha-hydroxylase in lymph-fistula rats: evidence for both transcriptional and post-transcriptional mechanisms for down-regulation of the two enzymes by bile acids. *J Lipid Res* **34**: 1497-503.

Bodo, A., E. Bakos, F. Szeri, A. Varadi, and B. Sarkadi. 2003. Differential modulation of the human liver conjugate transporters MRP2 and MRP3 by bile acids and organic anions. *J Biol Chem* **278**: 23529-37.

Bohme, M., M. Muller, I. Leier, G. Jedlitschky, and D. Keppler. 1994. Cholestasis caused by inhibition of the adenosine triphosphate- dependent bile salt transport in rat liver. *Gastroenterology* **107**: 255-65.

Borst, P. and R.O. Elferink. 2002. Mammalian ABC transporters in health and disease. *Annu Rev Biochem* **71**: 537-92.

Borst, P., R. Evers, M. Kool, and J. Wijnholds. 2000. A family of drug transporters: the multidrug resistance-associated proteins. *J Natl Cancer Inst* **92**: 1295-302.

Boyer, J.L. 1986. *Mechanisms of Bile Secretion and Hepatic Transport.* Plenum, New York.

Boyer, J.L. 1997. Isolated hepatocyte couplets and bile duct units--novel preparations for the in vitro study of bile secretory function. *Cell Biol Toxicol* **13**: 289-300.

Boyer, J.L. and J.R. Bloomer. 1974. Canalicular bile secretion in man. Studies utilizing the biliary clearance of (14C)mannitol. *J Clin Invest* **54**: 773-81.

Boyer, J.L., E. Elias, and T.J. Layden. 1979. The paracellular pathway and bile formation. *Yale J Biol Med* **52**: 61-7.

Boyer, J.L., O.C. Ng, M. Ananthanarayanan, A.F. Hofmann, C.D. Schteingart, B. Hagenbuch, B. Stieger, and P.J. Meier. 1994. Expression and characterization of a functional rat liver Na+ bile acid cotransport system in COS-7 cells. *Am J Physiol* **266**: G382-7.

Boyer, J.L., J.M. Phillips, and J. Graf. 1990. Preparation and specific applications of isolated hepatocyte couplets. *Methods Enzymol* **192**: 501-16.

Boyer, J.L. and C.J. Soroka. 1995. Vesicle targeting to the apical domain regulates bile excretory function in isolated rat hepatocyte couplets. *Gastroenterology* **109**: 1600-11.

Bremmelgaard, A. and B. Alme. 1980. Analysis of plasma bile acid profiles in patients with liver diseases associated with cholestasis. *Scand J Gastroenterol* **15**: 593-600.

Bull, L.N., V.E. Carlton, N.L. Stricker, S. Baharloo, J.A. DeYoung, N.B. Freimer, M.S. Magid, E. Kahn, J. Markowitz, F.J. DiCarlo, L. McLoughlin, J.T. Boyle, B.B. Dahms, P.R. Faught, J.F. Fitzgerald, D.A. Piccoli, C.L. Witzleben, N.C. O'Connell, K.D.

Setchell, R.M. Agostini, Jr., S.A. Kocoshis, J. Reyes, and A.S. Knisely. 1997. Genetic and morphological findings in progressive familial intrahepatic cholestasis (Byler disease [PFIC-1] and Byler syndrome): evidence for heterogeneity. *Hepatology* **26**: 155-64.

Bull, L.N., M.J. van Eijk, L. Pawlikowska, J.A. DeYoung, J.A. Juijn, M. Liao, L.W. Klomp, N. Lomri, R. Berger, B.F. Scharschmidt, A.S. Knisely, R.H. Houwen, and N.B. Freimer. 1998. A gene encoding a P-type ATPase mutated in two forms of hereditary cholestasis. *Nat Genet* **18**: 219-24.

Buschman, E., R.J. Arceci, J.M. Croop, M. Che, I.M. Arias, D.E. Housman, and P. Gros. 1992. mdr2 encodes P-glycoprotein expressed in the bile canalicular membrane as determined by isoform-specific antibodies. *J Biol Chem* **267**: 18093-9.

Buschman, E. and P. Gros. 1994. The inability of the mouse mdr2 gene to confer multidrug resistance is linked to reduced drug binding to the protein. *Cancer Res* **54**: 4892-8.

Byrne, J.A., S.S. Strautnieks, G. Mieli-Vergani, C.F. Higgins, K.J. Linton, and R.J. Thompson. 2002. The human bile salt export pump: characterization of substrate specificity and identification of inhibitors. *Gastroenterology* **123**: 1649-58.

Cabrera-Abreu, J.C. and A. Green. 2002. Gamma-glutamyltransferase: value of its measurement in paediatrics. *Ann Clin Biochem* **39**: 22-5.

Cai, S.Y., L. Wang, N. Ballatori, and J.L. Boyer. 2001. Bile salt export pump is highly conserved during vertebrate evolution and its expression is inhibited by PFIC type II mutations. *Am J Physiol Gastrointest Liver Physiol* **281**: G316-22.

Cali, J.J. and D.W. Russell. 1991. Characterization of human sterol 27-hydroxylase. A mitochondrial cytochrome P-450 that catalyzes multiple oxidation reaction in bile acid biosynthesis. *J Biol Chem* **266**: 7774-8.

Carey, M.C. and D. W.C. 1994. *Enterohepatic circulation.* Raven Press, New York.

Carlton, V.E., A.S. Knisely, and N.B. Freimer. 1995. Mapping of a locus for progressive familial intrahepatic cholestasis (Byler disease) to 18q21-q22, the benign recurrent intrahepatic cholestasis region. *Hum Mol Genet* **4**: 1049-53.

Chen, H.L., P.S. Chang, H.C. Hsu, Y.H. Ni, H.Y. Hsu, J.H. Lee, Y.M. Jeng, W.Y. Shau, and M.H. Chang. 2002. FIC1 and BSEP defects in Taiwanese patients with chronic intrahepatic cholestasis with low gamma-glutamyltranspeptidase levels. *J Pediatr* **140**: 119-24.

Chiang, J.Y., R. Kimmel, C. Weinberger, and D. Stroup. 2000. Farnesoid X receptor responds to bile acids and represses cholesterol 7alpha-hydroxylase gene (CYP7A1) transcription. *J Biol Chem* **275**: 10918-24.

Chifflet, S., A. Torriglia, R. Chiesa, and S. Tolosa. 1988. A method for the determination of inorganic phosphate in the presence of labile organic phosphate and high concentrations of protein: application to lens ATPases. *Anal Biochem* **168**: 1-4.

Childs, S. 1995. New Members of the Mammalian P-glycoprotein Gene Family and Their Evolution. In *Medical Biophysics*. Toronto.

Childs, S. and V. Ling. 1994. The MDR superfamily of genes and its biological implications. *Important Adv Oncol*: 21-36.

Childs, S., R.L. Yeh, E. Georges, and V. Ling. 1995. Identification of a sister gene to P-glycoprotein. *Cancer Res* **55**: 2029-34.

Childs, S., R.L. Yeh, D. Hui, and V. Ling. 1998. Taxol resistance mediated by transfection of the liver-specific sister gene of P-glycoprotein. *Cancer Res* **58**: 4160-7.

Claudel, T., E. Sturm, H. Duez, I.P. Torra, A. Sirvent, V. Kosykh, J.C. Fruchart, J. Dallongeville, D.W. Hum, F. Kuipers, and B. Staels. 2002. Bile acid-activated nuclear receptor FXR suppresses apolipoprotein A-I transcription via a negative FXR response element. *J Clin Invest* **109**: 961-71.

Cohen, D.E., M. Angelico, and M.C. Carey. 1990. Structural alterations in lecithin-cholesterol vesicles following interactions with monomeric and micellar bile salts: physical-chemical basis for subselection of biliary lecithin species and aggregative states of biliary lipids during bile formation. *J Lipid Res* **31**: 55-70.

Cohen, D.E., E.W. Kaler, and M.C. Carey. 1993. Cholesterol carriers in human bile: are "lamellae" involved? *Hepatology* **18**: 1522-31.

Coleman, R. 1987. Biochemistry of bile secretion. *Biochem J* **244**: 249-61.

Corasanti, J.G., N.D. Smith, E.R. Gordon, and J.L. Boyer. 1989. Protein kinase C agonists inhibit bile secretion independently of effects on the microcirculation in the isolated perfused rat liver. *Hepatology* **10**: 8-13.

Crawford, J.M., C.A. Berken, and J.L. Gollan. 1988. Role of the hepatocyte microtubular system in the excretion of bile salts and biliary lipid: implications for intracellular vesicular transport. *J Lipid Res* **29**: 144-56.

de Vree, J.M., E. Jacquemin, E. Sturm, D. Cresteil, P.J. Bosma, J. Aten, J.F. Deleuze, M. Desrochers, M. Burdelski, O. Bernard, R.P. Oude Elferink, and M. Hadchouel. 1998. Mutations in the MDR3 gene cause progressive familial intrahepatic cholestasis. *Proc Natl Acad Sci U S A* **95**: 282-7.

Deroubaix, X., T. Coche, E. Depiereux, and E. Feytmans. 1991. Saturation of hepatic transport of taurocholate in rats in vivo. *Am J Physiol* **260**: G189-96.

Dey, S., M. Ramachandra, I. Pastan, M.M. Gottesman, and S.V. Ambudkar. 1997. Evidence for two nonidentical drug-interaction sites in the human P-glycoprotein. *Proc Natl Acad Sci U S A* **94**: 10594-9.

DiDiodato, G. and F.J. Sharom. 1997. Interaction of combinations of drugs, chemosensitizers, and peptides with the P-glycoprotein multidrug transporter. *Biochem Pharmacol* **53**: 1789-97.

Dietmaier, A., R. Gasser, J. Graf, and M. Peterlik. 1976. Investigations on the sodium dependence of bile acid fluxes in the isolated perfused rat liver. *Biochim Biophys Acta* **443**: 81-91.

Doyle, L.A., W. Yang, L.V. Abruzzo, T. Krogmann, Y. Gao, A.K. Rishi, and D.D. Ross. 1998. A multidrug resistance transporter from human MCF-7 breast cancer cells. *Proc Natl Acad Sci U S A* **95**: 15665-70.

Ecker, G.F., E. Csaszar, S. Kopp, B. Plagens, W. Holzer, W. Ernst, and P. Chiba. 2002. Identification of ligand-binding regions of P-glycoprotein by activated-pharmacophore photoaffinity labeling and matrix-assisted laser desorption/ionization-time-of-flight mass spectrometry. *Mol Pharmacol* **61**: 637-48.

Elferink, R.O. and A.K. Groen. 2002. Genetic defects in hepatobiliary transport. *Biochim Biophys Acta* **1586**: 129-45.

Elferink, R.P., R. Ottenhoff, W. Liefting, J. de Haan, and P.L. Jansen. 1989. Hepatobiliary transport of glutathione and glutathione conjugate in rats with hereditary hyperbilirubinemia. *J Clin Invest* **84**: 476-83.

Elliot, W. 1985. *Metabolism of bile salts in liver and extrahepatic tissues.* Elsevier, New York.

Ellis, E., M. Axelson, A. Abrahamsson, G. Eggertsen, A. Thorne, G. Nowak, B.G. Ericzon, I. Bjorkhem, and C. Einarsson. 2003. Feedback regulation of bile acid synthesis in primary human hepatocytes: evidence that CDCA is the strongest inhibitor. *Hepatology* **38**: 930-8.

Eppens, E.F., S.W. van Mil, J.M. de Vree, K.S. Mok, J.A. Juijn, R.P. Oude Elferink, R. Berger, R.H. Houwen, and L.W. Klomp. 2001. FIC1, the protein affected in two forms of hereditary cholestasis, is localized in the cholangiocyte and the canalicular membrane of the hepatocyte. *J Hepatol* **35**: 436-43.

Erlinger, S. 1996. Review article: new insights into the mechanisms of hepatic transport and bile secretion. *J Gastroenterol Hepatol* **11**: 575-9.

Evans, W.H. 1980. A biochemical dissection of the functional polarity of the plasma membrane of the hepatocyte. *Biochim Biophys Acta* **604**: 27-64.

Falany, C.N., M.R. Johnson, S. Barnes, R.B. Diasio, T. Ide, S. Kano, M. Murata, T. Yanagita, M. Sugano, and J.B. Kwakye. 1994. Glycine and taurine conjugation of bile acids by a single enzyme. Molecular cloning and expression of human liver bile acid CoA:amino acid N-acyltransferase. *J Biol Chem* **269**: 19375-9.

Fickert, P., G. Zollner, A. Fuchsbichler, C. Stumptner, C. Pojer, R. Zenz, F. Lammert, B. Stieger, P.J. Meier, K. Zatloukal, H. Denk, and M. Trauner. 2001. Effects of ursodeoxycholic and cholic acid feeding on hepatocellular transporter expression in mouse liver. *Gastroenterology* **121**: 170-83.

Forker, E.L. 1968. Bile formation in guinea pigs: analysis with inert solutes of graded molecular radius. *Am J Physiol* **215**: 56-62.

Forker, E.L., T. Hicklin, and H. Sornson. 1967. The clearance of mannitol and erythritol in rat bile. *Proc Soc Exp Biol Med* **126**: 115-9.

Frank, N.Y., S.S. Pendse, P.H. Lapchak, A. Margaryan, D. Shlain, C. Doeing, M.H. Sayegh, and M.H. Frank. 2003. Regulation of progenitor cell fusion by ABCB5 P-glycoprotein, a novel human ATP-binding cassette transporter. *J Biol Chem* **7**: 7.

Fuchs, M. 2003. Bile acid regulation of hepatic physiology: III. Regulation of bile acid synthesis: past progress and future challenges. *Am J Physiol Gastrointest Liver Physiol* **284**: G551-7.

Gatmaitan, Z.C., A.T. Nies, and I.M. Arias. 1997. Regulation and translocation of ATP-dependent apical membrane proteins in rat liver. *Am J Physiol* **272**: G1041-9.

Gautam, A., O.C. Ng, and J.L. Boyer. 1987. Isolated rat hepatocyte couplets in short-term culture: structural characteristics and plasma membrane reorganization. *Hepatology* **7**: 216-23.

Georges, E., G. Bradley, J. Gariepy, and V. Ling. 1990. Detection of P-glycoprotein isoforms by gene-specific monoclonal antibodies. *Proc Natl Acad Sci U S A* **87**: 152-6.

Gerloff, T., A. Geier, I. Roots, P.J. Meier, and C. Gartung. 2002. Functional analysis of the rat bile salt export pump gene promoter. *Eur J Biochem* **269**: 3495-503.

Gerloff, T., A. Geier, B. Stieger, B. Hagenbuch, P.J. Meier, S. Matern, and C. Gartung. 1999. Differential expression of basolateral and canalicular organic anion transporters during regeneration of rat liver. *Gastroenterology* **117**: 1408-15.

Gerloff, T., B. Stieger, B. Hagenbuch, J. Madon, L. Landmann, J. Roth, A.F. Hofmann, and P.J. Meier. 1998. The sister of P-glycoprotein represents the canalicular bile salt export pump of mammalian liver. *J Biol Chem* **273**: 10046-50.

Graf, J. 1983. Canalicular bile salt-independent bile formation: concepts and clues from electrolyte transport in rat liver. *Am J Physiol* **244**: G233-46.

Graf, J., R.M. Henderson, B. Krumpholz, and J.L. Boyer. 1987. Cell membrane and transepithelial voltages and resistances in isolated rat hepatocyte couplets. *J Membr Biol* **95**: 241-54.

Green, R.M., F. Hoda, and K.L. Ward. 2000. Molecular cloning and characterization of the murine bile salt export pump. *Gene* **241**: 117-23.

Greim, H., D. Trulzsch, J. Roboz, K. Dressler, P. Czygan, F. Hutterer, F. Schaffner, and H. Popper. 1972. Mechanism of cholestasis. 5. Bile acids in normal rat livers and in those after bile duct ligation. *Gastroenterology* **63**: 837-45.

Guertin, F., A. Loranger, G. Lepage, C.C. Roy, I.M. Yousef, N. Domingo, F. Chanussot, H. Lafont, and B. Tuchweber. 1995. Bile formation and hepatic plasma membrane composition in guinea-pigs and rats. *Comp Biochem Physiol B Biochem Mol Biol* **111**: 523-31.

Hagenbuch, B. and P.J. Meier. 1994. Molecular cloning, chromosomal localization, and functional characterization of a human liver Na+/bile acid cotransporter. *J Clin Invest* **93**: 1326-31.

Hagey, L.R. 1986. Bile Acid Biodiversity in Vertebrates: Chemistry and Evolutionary Implications. In, pp. 205. California, San Diego.

Hagey, L.R., D.L. Crombie, E. Espinosa, M.C. Carey, H. Igimi, and A.F. Hofmann. 1993. Ursodeoxycholic acid in the Ursidae: biliary bile acids of bears, pandas, and related carnivores. *J Lipid Res* **34**: 1911-7.

Hagey, L.R., C.D. Schteingart, S.S. Rossi, H.T. Ton-Nu, and A.F. Hofmann. 1998. An N-acyl glycyltaurine conjugate of deoxycholic acid in the biliary bile acids of the rabbit. *J Lipid Res* **39**: 2119-24.

Hardison, W.G., E. Dalle-Molle, E. Gosink, P.J. Lowe, J.H. Steinbach, and Y. Yamaguchi. 1991. Function of rat hepatocyte tight junctions: studies with bile acid infusions. *Am J Physiol* **260**: G167-74.

Hardison, W.G. and C.A. Wood. 1978. Importance of bicarbonate in bile salt independent fraction of bile flow. *Am J Physiol* **235**: E158-64.

Harris, M.J. and I.M. Arias. 2003. FIC1, a P-type ATPase linked to cholestatic liver disease, has homologues (ATP8B2 and ATP8B3) expressed throughout the body. *Biochim Biophys Acta* **1633**: 127-31.

Hayakawa, T., R. Bruck, O.C. Ng, and J.L. Boyer. 1990. DBcAMP stimulates vesicle transport and HRP excretion in isolated perfused rat liver. *Am J Physiol* **259**: G727-35.

He, D., S. Barnes, C.N. Falany, J. O'Byrne, M.C. Hunt, D.K. Rai, M. Saeki, S.E. Alexson, M.R. Johnson, R.B. Diasio, T. Ide, S. Kano, M. Murata, T. Yanagita, M. Sugano, and J.B. Kwakye. 2003. Rat liver bile acid CoA:amino acid N-acyltransferase: expression, characterization, and peroxisomal localization. *J Lipid Res* **44**: 2242-9. Epub 2003 Sep 1.

Higgins, C.F. 1992. ABC transporters: from microorganisms to man. *Annu Rev Cell Biol* **8**: 67-113.

Hirohashi, T., H. Suzuki, K. Ito, K. Ogawa, K. Kume, T. Shimizu, and Y. Sugiyama. 1998. Hepatic expression of multidrug resistance-associated protein-like proteins maintained in eisai hyperbilirubinemic rats. *Mol Pharmacol* **53**: 1068-75.

Hirohashi, T., H. Suzuki, H. Takikawa, and Y. Sugiyama. 2000. ATP-dependent transport of bile salts by rat multidrug resistance-associated protein 3 (Mrp3). *J Biol Chem* **275**: 2905-10.

Hofmann, A. 1994. *Bile Acids*. Raven Press Ltd., New York.

Hofmann, A.F. 1989. *Enterohepatic circulation of bile acids.* Oxford University Press, New York.

Hofmann, A.F. 1999. The continuing importance of bile acids in liver and intestinal disease. *Arch Intern Med* **159**: 2647-58.

Hofmann, A.F. 2001. Bile secretion in mice and men. *Hepatology* **34**: 848-50.

Holzinger, F., C.D. Schteingart, H.T. Ton-Nu, C. Cerre, J.H. Steinbach, H.Z. Yeh, and A.F. Hofmann. 1998. Transport of fluorescent bile acids by the isolated perfused rat liver: kinetics, sequestration, and mobilization. *Hepatology* **28**: 510-20.

Hosokawa, S., O. Tagaya, T. Mikami, Y. Nozaki, A. Kawaguchi, K. Yamatsu, and M. Shamoto. 1992. A new rat mutant with chronic conjugated hyperbilirubinemia and renal glomerular lesions. *Lab Anim Sci* **42**: 27-34.

Hsing, S., Z. Gatmaitan, and I.M. Arias. 1992. The function of Gp170, the multidrug-resistance gene product, in the brush border of rat intestinal mucosa. *Gastroenterology* **102**: 879-85.

Inoue, M., R. Kinne, T. Tran, and I.M. Arias. 1982. Taurocholate transport by rat liver sinusoidal membrane vesicles: evidence of sodium cotransport. *Hepatology* **2**: 572-9.

Inoue, M., R. Kinne, T. Tran, and I.M. Arias. 1983a. The mechanism of biliary secretion of reduced glutathione. Analysis of transport process in isolated rat-liver canalicular membrane vesicles. *Eur J Biochem* **134**: 467-71.

Inoue, M., R. Kinne, T. Tran, and I.M. Arias. 1984. Taurocholate transport by rat liver canalicular membrane vesicles. Evidence for the presence of an Na+-independent transport system. *J Clin Invest* **73**: 659-63.

Inoue, M., R. Kinne, T. Tran, L. Biempica, and I.M. Arias. 1983b. Rat liver canalicular membrane vesicles. Isolation and topological characterization. *J Biol Chem* **258**: 5183-8.

Ishikawa, T., M. Muller, C. Klunemann, T. Schaub, and D. Keppler. 1990. ATP-dependent primary active transport of cysteinyl leukotrienes across liver canalicular membrane. Role of the ATP-dependent transport system for glutathione S-conjugates. *J Biol Chem* **265**: 19279-86.

Jacquemin, E. 2000. Progressive familial intrahepatic cholestasis. Genetic basis and treatment. *Clin Liver Dis* **4**: 753-63.

Jacquemin, E. 2000. 2001. Role of multidrug resistance 3 deficiency in pediatric and adult liver disease: one gene for three diseases. *Semin Liver Dis* **21**: 551-62.

Jacquemin, E., B. Hagenbuch, B. Stieger, A.W. Wolkoff, and P.J. Meier. 1994. Expression cloning of a rat liver Na(+)-independent organic anion transporter. *Proc Natl Acad Sci U S A* **91**: 133-7.

Jansen, P.L. and M. Muller. 2000. Genetic cholestasis: lessons from the molecular physiology of bile formation. *Can J Gastroenterol* **14**: 233-8.

Jansen, P.L. and M.M. Muller. 1998. Progressive familial intrahepatic cholestasis types 1, 2, and 3. *Gut* **42**: 766-7.

Jansen, P.L., W.H. Peters, and W.H. Lamers. 1985. Hereditary chronic conjugated hyperbilirubinemia in mutant rats caused by defective hepatic anion transport. *Hepatology* **5**: 573-9.

Jansen, P.L., S.S. Strautnieks, E. Jacquemin, M. Hadchouel, E.M. Sokal, G.J. Hooiveld, J.H. Koning, A. De Jager-Krikken, F. Kuipers, F. Stellaard, C.M. Bijleveld, A. Gouw, H. Van Goor, R.J. Thompson, and M. Muller. 1999. Hepatocanalicular bile salt export pump deficiency in patients with progressive familial intrahepatic cholestasis [see comments]. *Gastroenterology* **117**: 1370-9.

Johnson, M.R., S. Barnes, J.B. Kwakye, and R.B. Diasio. 1991. Purification and characterization of bile acid-CoA:amino acid N-acyltransferase from human liver. *J Biol Chem* **266**: 10227-33.

Kamimoto, Y., Z. Gatmaitan, J. Hsu, and I.M. Arias. 1989. The function of Gp170, the multidrug resistance gene product, in rat liver canalicular membrane vesicles. *J Biol Chem* **264**: 11693-8.

Keppler, D. and J. Konig. 2000. Hepatic secretion of conjugated drugs and endogenous substances. *Semin Liver Dis* **20**: 265-72.

Keppler, D., I. Leier, and G. Jedlitschky. 1997. Transport of glutathione conjugates and glucuronides by the multidrug resistance proteins MRP1 and MRP2. *Biol Chem* **378**: 787-91.

Keppler, D., I. Leier, G. Jedlitschky, and J. Konig. 1998. ATP-dependent transport of glutathione S-conjugates by the multidrug resistance protein MRP1 and its apical isoform MRP2. *Chem Biol Interact* **111-112**: 153-61.

Kipp, H. and I.M. Arias. 2000. Newly synthesized canalicular ABC transporters are directly targeted from the Golgi to the hepatocyte apical domain in rat liver. *J Biol Chem* **275**: 15917-25.

Kipp, H., N. Pichetshote, and I.M. Arias. 2001. Transporters on demand: intrahepatic pools of canalicular ATP binding cassette transporters in rat liver. *J Biol Chem* **276**: 7218-24. Epub 2000 Dec 11.

Kitamura, T., Z. Gatmaitan, and I.M. Arias. 1990a. Serial quantitative image analysis and confocal microscopy of hepatic uptake, intracellular distribution and biliary secretion of a fluorescent bile acid analog in rat hepatocyte doublets. *Hepatology* **12**: 1358-64.

Kitamura, T., P. Jansen, C. Hardenbrook, Y. Kamimoto, Z. Gatmaitan, and I.M. Arias. 1990b. Defective ATP-dependent bile canalicular transport of organic anions in mutant (TR-) rats with conjugated hyperbilirubinemia. *Proc Natl Acad Sci U S A* **87**: 3557-61.

Knisely, A.S. 2000. Progressive familial intrahepatic cholestasis: a personal perspective. *Pediatr Dev Pathol* **3**: 113-25.

Kobayashi, K., Y. Sogame, H. Hara, and K. Hayashi. 1990. Mechanism of glutathione S-conjugate transport in canalicular and basolateral rat liver plasma membranes. *J Biol Chem* **265**: 7737-41.

Konig, J., A.T. Nies, Y. Cui, I. Leier, and D. Keppler. 1999a. Conjugate export pumps of the multidrug resistance protein (MRP) family: localization, substrate specificity, and MRP2-mediated drug resistance. *Biochim Biophys Acta* **1461**: 377-94.

Konig, J., D. Rost, Y. Cui, and D. Keppler. 1999b. Characterization of the human multidrug resistance protein isoform MRP3 localized to the basolateral hepatocyte membrane. *Hepatology* **29**: 1156-63.

Kool, M., M. van der Linden, M. de Haas, G.L. Scheffer, J.M. de Vree, A.J. Smith, G. Jansen, G.J. Peters, N. Ponne, R.J. Scheper, R.P. Elferink, F. Baas, and P. Borst. 1999. MRP3, an organic anion transporter able to transport anti-cancer drugs. *Proc Natl Acad Sci U S A* **96**: 6914-9.

Kreek, M.J. 1987. Female sex steroids and cholestasis. *Semin Liver Dis* **7**: 8-23.

Kuipers, F., A. Radominska, P. Zimniak, J.M. Little, R. Havinga, R.J. Vonk, and R. Lester. 1989. Defective biliary secretion of bile acid 3-O-glucuronides in rats with hereditary conjugated hyperbilirubinemia. *J Lipid Res* **30**: 1835-45.

Kuroki, S., S. Muramoto, T. Kuramoto, and T. Hoshita. 1983. Sex differences in gallbladder bile acid composition and hepatic steroid 12 alpha-hydroxylase activity in hamsters. *J Lipid Res* **24**: 1543-9.

Laffitte, B.A., H.R. Kast, C.M. Nguyen, A.M. Zavacki, D.D. Moore, and P.A. Edwards. 2000. Identification of the DNA binding specificity and potential target genes for the farnesoid X-activated receptor. *J Biol Chem* **275**: 10638-47.

Lecureur, V., D. Sun, P. Hargrove, E.G. Schuetz, R.B. Kim, L.B. Lan, and J.D. Schuetz. 2000. Cloning and expression of murine sister of P-glycoprotein reveals a more discriminating transporter than MDR1/P-glycoprotein. *Mol Pharmacol* **57**: 24-35.

Lee, J.M., M. Trauner, C.J. Soroka, B. Stieger, P.J. Meier, and J.L. Boyer. 2000. Expression of the bile salt export pump is maintained after chronic cholestasis in the rat. *Gastroenterology* **118**: 163-72.

Lee, M.H., K. Lu, S. Hazard, H. Yu, S. Shulenin, H. Hidaka, H. Kojima, R. Allikmets, N. Sakuma, R. Pegoraro, A.K. Srivastava, G. Salen, M. Dean, and S.B. Patel. 2001. Identification of a gene, ABCG5, important in the regulation of dietary cholesterol absorption. *Nat Genet* **27**: 79-83.

Leier, I., G. Jedlitschky, U. Buchholz, S.P. Cole, R.G. Deeley, and D. Keppler. 1994. The MRP gene encodes an ATP-dependent export pump for leukotriene C4 and structurally related conjugates. *J Biol Chem* **269**: 27807-10.

Leveille-Webster, C.R. and I.M. Arias. 1994. Mdr 2 knockout mice link biliary phospholipid deficiency with small bile duct destruction. *Hepatology* **19**: 1528-31.

Lowe, P.J., K. Miyai, J.H. Steinbach, and W.G. Hardison. 1988. Hormonal regulation of hepatocyte tight junctional permeability. *Am J Physiol* **255**: G454-61.

Lu, P., R. Liu, and F.J. Sharom. 2001. Drug transport by reconstituted P-glycoprotein in proteoliposomes. Effect of substrates and modulators, and dependence on bilayer phase state. *Eur J Biochem* **268**: 1687-97.

Luketic, V.A. and M.L. Shiffman. 1999. Benign recurrent intrahepatic cholestasis. *Clin Liver Dis* **3**: 509-28, viii.

Lykavieris, P., S. van Mil, D. Cresteil, M. Fabre, M. Hadchouel, L. Klomp, O. Bernard, and E. Jacquemin. 2003. Progressive familial intrahepatic cholestasis type 1 and extrahepatic features: no catch-up of stature growth, exacerbation of diarrhea, and appearance of liver steatosis after liver transplantation. *J Hepatol* **39**: 447-52.

Madon, J., U. Eckhardt, T. Gerloff, B. Stieger, and P.J. Meier. 1997. Functional expression of the rat liver canalicular isoform of the multidrug resistance-associated protein. *FEBS Lett* **406**: 75-8.

Mathisen, O. and M. Raeder. 1983. Mechanism of hepatic bicarbonate secretion and bile acid independent bile secretion. *Eur J Clin Invest* **13**: 193-200.

Mauad, T.H., C.M. van Nieuwkerk, K.P. Dingemans, J.J. Smit, A.H. Schinkel, R.G. Notenboom, M.A. van den Bergh Weerman, R.P. Verkruisen, A.K. Groen, R.P. Oude Elferink, and et al. 1994. Mice with homozygous disruption of the mdr2 P-glycoprotein gene. A novel animal model for studies of nonsuppurative inflammatory cholangitis and hepatocarcinogenesis. *Am J Pathol* **145**: 1237-45.

Mazer, N.A., P. Schurtenberg, M.C. Carey, R. Preisig, K. Weigand, and W. Kanzig. 1984. Quasi-elastic light scattering studies of native hepatic bile from the dog: comparison with aggregative behavior of model biliary lipid systems. *Biochemistry* **23**: 1994-2005.

Mazzanti, R., O. Fantappie, Y. Kamimoto, Z. Gatmaitan, P. Gentilini, and I.M. Arias. 1994. Bile acid inhibition of P-glycoprotein-mediated transport in multidrug-resistant cells and rat liver canalicular membrane vesicles. *Hepatology* **20**: 170-6.

Meier, P.J. and J.L. Boyer. 1990. Preparation of basolateral (sinusoidal) and canalicular plasma membrane vesicles for the study of hepatic transport processes. *Methods Enzymol* **192**: 534-45.

Meier, P.J., U. Eckhardt, A. Schroeder, B. Hagenbuch, and B. Stieger. 1997. Substrate specificity of sinusoidal bile acid and organic anion uptake systems in rat and human liver. *Hepatology* **26**: 1667-77.

Meier, P.J., A.S. Meier-Abt, and J.L. Boyer. 1987. Properties of the canalicular bile acid transport system in rat liver. *Biochem J* **242**: 465-9.

Meier, P.J., A. St Meier-Abt, C. Barrett, and J.L. Boyer. 1984a. Mechanisms of taurocholate transport in canalicular and basolateral rat liver plasma membrane vesicles. Evidence for an electrogenic canalicular organic anion carrier. *J Biol Chem* **259**: 10614-22.

Meier, P.J., E.S. Sztul, A. Reuben, and J.L. Boyer. 1984b. Structural and functional polarity of canalicular and basolateral plasma membrane vesicles isolated in high yield from rat liver. *J Cell Biol* **98**: 991-1000.

Misra, S., P. Ujhazy, Z. Gatmaitan, L. Varticovski, and I.M. Arias. 1998. The role of phosphoinositide 3-kinase in taurocholate-induced trafficking of ATP-dependent canalicular transporters in rat liver. *J Biol Chem* **273**: 26638-44.

Misra, S., P. Ujhazy, L. Varticovski, and I.M. Arias. 1999. Phosphoinositide 3-kinase lipid products regulate ATP-dependent transport by sister of P-glycoprotein and multidrug resistance associated protein 2 in bile canalicular membrane vesicles. *Proc Natl Acad Sci U S A* **96**: 5814-9.

Misra, S., L. Varticovski, and I.M. Arias. 2003. Mechanisms by which cAMP increases bile acid secretion in rat liver and canalicular membrane vesicles. *Am J Physiol Gastrointest Liver Physiol* **285**: G316-24.

Myara, A., J.F. Cadranel, R. Dorent, F. Lunel, E. Bouvier, M. Gerhardt, B. Bernard, J.J. Ghoussoub, A. Cabrol, I. Gandjbakhch, P. Opolon, and F. Trivin. 1996. Cyclosporin A-mediated cholestasis in patients with chronic hepatitis after heart transplantation. *Eur J Gastroenterol Hepatol* **8**: 267-71.

Nathanson, M.H. and J.L. Boyer. 1991. Mechanisms and regulation of bile secretion. *Hepatology* **14**: 551-66.

Nathanson, M.H., A. Gautam, R. Bruck, C.M. Isales, and J.L. Boyer. 1992. Effects of Ca2+ agonists on cytosolic Ca2+ in isolated hepatocytes and on bile secretion in the isolated perfused rat liver. *Hepatology* **15**: 107-16.

Nemeth, A. and B. Strandvik. 1984. Urinary excretion of tetrahydroxylated bile acids in children with alpha 1-antitrypsin deficiency and neonatal cholestasis. *Scand J Clin Lab Invest* **44**: 387-92.

Nies, A.T., Z. Gatmaitan, and I.M. Arias. 1996. ATP-dependent phosphatidylcholine translocation in rat liver canalicular plasma membrane vesicles. *J Lipid Res* **37**: 1125-36.

Nishida, T., M. Che, Z. Gatmaitan, and I.M. Arias. 1995. Structure-specific inhibition by bile acids of adenosine triphosphate-dependent taurocholate transport in rat canalicular membrane vesicles. *Hepatology* **21**: 1058-62.

Nishida, T., Z. Gatmaitan, M. Che, and I.M. Arias. 1991. Rat liver canalicular membrane vesicles contain an ATP-dependent bile acid transport system. *Proc Natl Acad Sci U S A* **88**: 6590-4.

Nishida, T., Z. Gatmaitan, J. Roy-Chowdhry, and I.M. Arias. 1992a. Two distinct mechanisms for bilirubin glucuronide transport by rat bile canalicular membrane vesicles. Demonstration of defective ATP-dependent transport in rats (TR-) with inherited conjugated hyperbilirubinemia. *J Clin Invest* **90**: 2130-5.

Nishida, T., C. Hardenbrook, Z. Gatmaitan, and I.M. Arias. 1992b. ATP-dependent organic anion transport system in normal and TR- rat liver canalicular membranes. *Am J Physiol* **262**: G629-35.

Noe, B., B. Hagenbuch, B. Stieger, and P.J. Meier. 1997. Isolation of a multispecific organic anion and cardiac glycoside transporter from rat brain. *Proc Natl Acad Sci U S A* **94**: 10346-50.

Noe, J., B. Hagenbuch, P.J. Meier, and M.V. St-Pierre. 2001. Characterization of the mouse bile salt export pump overexpressed in the baculovirus system. *Hepatology* **33**: 1223-31.

Noe, J., B. Stieger, and P.J. Meier. 2002. Functional expression of the canalicular bile salt export pump of human liver. *Gastroenterology* **123**: 1659-66.

Northfield, T.C., N.F. LaRusso, A.F. Hofmann, and J.L. Thistle. 1975. Biliary lipid output during three meals and an overnight fast. II. Effect of chenodeoxycholic acid treatment in gallstone subjects. *Gut* **16**: 12-7.

O'Byrne, J., M.C. Hunt, D.K. Rai, M. Saeki, and S.E. Alexson. 2003. The human bile acid-CoA:amino acid N-acyltransferase functions in the conjugation of fatty acids to glycine. *J Biol Chem* **278**: 34237-44. Epub 2003 Jun 16.

Ortiz, D.F., S. Li, R. Iyer, X. Zhang, P. Novikoff, and I.M. Arias. 1999. MRP3, a new ATP-binding cassette protein localized to the canalicular domain of the hepatocyte. *Am J Physiol* **276**: G1493-500.

Paigen, B., A. Morrow, C. Brandon, D. Mitchell, and P. Holmes. 1985. Variation in susceptibility to atherosclerosis among inbred strains of mice. *Atherosclerosis* **57**: 65-73.

Paulusma, C.C., P.J. Bosma, G.J. Zaman, C.T. Bakker, M. Otter, G.L. Scheffer, R.J. Scheper, P. Borst, and R.P. Oude Elferink. 1996. Congenital jaundice in rats with a mutation in a multidrug resistance- associated protein gene. *Science* **271**: 1126-8.

Paulusma, C.C., M.A. Geer, R. Evers, M. Heijn, R. Ottenhoff, P. Borst, and R.P. Oude Elferink. 1999. Canalicular multispecific organic anion transporter/multidrug resistance protein 2 mediates low-affinity transport of reduced glutathione. *Biochem J* **338**: 393-401.

Perwaiz, S., D. Forrest, D. Mignault, B. Tuchweber, M.J. Phillip, R. Wang, V. Ling, and I.M. Yousef. 2003. Appearance of atypical 3 alpha,6 beta,7 beta,12 alpha-tetrahydroxy-5 beta-cholan-24-oic acid in spgp knockout mice. *J Lipid Res* **44**: 494-502.

Plass, J.R., O. Mol, J. Heegsma, M. Geuken, K.N. Faber, P.L. Jansen, and M. Muller. 2002. Farnesoid X receptor and bile salts are involved in transcriptional regulation of the gene encoding the human bile salt export pump. *Hepatology* **35**: 589-96.

Poupon, R., Y. Chretien, M. Parquet, F. Ballet, C. Rey, and R. Infante. 1988. Hepatic transport of bile acids in the isolated perfused rat liver. Structure-kinetic relationship. *Biochem Pharmacol* **37**: 209-12.

Preisig, R., H.L. Cooper, and H.O. Wheeler. 1962. The relationship between taurocholate secretion rate and bile production in the unanesthetized dog during cholinergic blockade and during secretin administration. *J Clin Invest* **41**: 1152-62.

Reichel, C., B. Gao, J. Van Montfoort, V. Cattori, C. Rahner, B. Hagenbuch, B. Stieger, T. Kamisako, and P.J. Meier. 1999. Localization and function of the organic anion-transporting polypeptide Oatp2 in rat liver. *Gastroenterology* **117**: 688-95.

Reid, G., P. Wielinga, N. Zelcer, M. De Haas, L. Van Deemter, J. Wijnholds, J. Balzarini, and P. Borst. 2003. Characterization of the transport of nucleoside analog drugs by the human multidrug resistance proteins MRP4 and MRP5. *Mol Pharmacol* **63**: 1094-103.

Roelofsen, H., C.J. Soroka, D. Keppler, and J.L. Boyer. 1998. Cyclic AMP stimulates sorting of the canalicular organic anion transporter (Mrp2/cMoat) to the apical domain in hepatocyte couplets. *J Cell Sci* **111**: 1137-45.

Romsicki, Y. and F.J. Sharom. 1999. The membrane lipid environment modulates drug interactions with the P-glycoprotein multidrug transporter. *Biochemistry* **38**: 6887-96.

Romsicki, Y. and F.J. Sharom. 2001. Phospholipid flippase activity of the reconstituted P-glycoprotein multidrug transporter. *Biochemistry* **40**: 6937-47.

Rosenberg, M.F., R. Callaghan, R.C. Ford, and C.F. Higgins. 1997. Structure of the multidrug resistance P-glycoprotein to 2.5 nm resolution determined by electron microscopy and image analysis. *J Biol Chem* **272**: 10685-94.

Rossi, S.S., J.L. Converse, and A.F. Hofmann. 1987. High pressure liquid chromatographic analysis of conjugated bile acids in human bile: simultaneous resolution of sulfated

and unsulfated lithocholyl amidates and the common conjugated bile acids. *J Lipid Res* **28**: 589-95.

Ruetz, S. and P. Gros. 1994. Phosphatidylcholine translocase: a physiological role for the mdr2 gene. *Cell* **77**: 1071-81.

Ruetz, S., G. Hugentobler, and P.J. Meier. 1988. Functional reconstitution of the canalicular bile salt transport system of rat liver. *Proc Natl Acad Sci U S A* **85**: 6147-51.

Rybczynska, M., R. Liu, P. Lu, F.J. Sharom, E. Steinfels, A.D. Pietro, M. Spitaler, H. Grunicke, and J. Hofmann. 2001. MDR1 causes resistance to the antitumour drug miltefosine. *Br J Cancer* **84**: 1405-11.

Sathirakul, K., H. Suzuki, K. Yasuda, M. Hanano, O. Tagaya, T. Horie, and Y. Sugiyama. 1993. Kinetic analysis of hepatobiliary transport of organic anions in Eisai hyperbilirubinemic mutant rats. *J Pharmacol Exp Ther* **265**: 1301-12.

Scharschmidt, B.F., E.B. Keeffe, N.M. Blankenship, and R.K. Ockner. 1979. Validation of a recording spectrophotometric method for measurement of membrane-associated Mg- and NaK-ATPase activity. *J Lab Clin Med* **93**: 790-9.

Schinkel, A.H., U. Mayer, E. Wagenaar, C.A. Mol, L. van Deemter, J.J. Smit, M.A. van der Valk, A.C. Voordouw, H. Spits, O. van Tellingen, J.M. Zijlmans, W.E. Fibbe, and P. Borst. 1997. Normal viability and altered pharmacokinetics in mice lacking mdr1-type (drug-transporting) P-glycoproteins. *Proc Natl Acad Sci U S A* **94**: 4028-33.

Schinkel, A.H., J.J. Smit, O. van Tellingen, J.H. Beijnen, E. Wagenaar, L. van Deemter, C.A. Mol, M.A. van der Valk, E.C. Robanus-Maandag, H.P. te Riele, and et al. 1994. Disruption of the mouse mdr1a P-glycoprotein gene leads to a deficiency in the blood-brain barrier and to increased sensitivity to drugs. *Cell* **77**: 491-502.

Schinkel, A.H., E. Wagenaar, L. van Deemter, C.A. Mol, and P. Borst. 1995. Absence of the mdr1a P-Glycoprotein in mice affects tissue distribution and pharmacokinetics of dexamethasone, digoxin, and cyclosporin A. *J Clin Invest* **96**: 1698-705.

Schmitt, M., R. Kubitz, S. Lizun, M. Wettstein, and D. Haussinger. 2001. Regulation of the dynamic localization of the rat Bsep gene-encoded bile salt export pump by anisoosmolarity. *Hepatology* **33**: 509-18.

Schwarz, M., E.G. Lund, K.D. Setchell, H.J. Kayden, J.E. Zerwekh, I. Bjorkhem, J. Herz, and D.W. Russell. 1996. Disruption of cholesterol 7alpha-hydroxylase gene in mice. II. Bile acid deficiency is overcome by induction of oxysterol 7alpha-hydroxylase. *J Biol Chem* **271**: 18024-31.

Setchell, K.D., C.M. Rodrigues, C. Clerici, A. Solinas, A. Morelli, C. Gartung, and J. Boyer. 1997. Bile acid concentrations in human and rat liver tissue and in hepatocyte nuclei. *Gastroenterology* **112**: 226-35.

Shapiro, A.B., K. Fox, P. Lam, and V. Ling. 1999. Stimulation of P-glycoprotein-mediated drug transport by prazosin and progesterone. Evidence for a third drug-binding site. *Eur J Biochem* **259**: 841-50.

Shapiro, A.B. and V. Ling. 1994. ATPase activity of purified and reconstituted P-glycoprotein from Chinese hamster ovary cells. *J Biol Chem* **269**: 3745-54.

Shapiro, A.B. and V. Ling. 1995. Reconstitution of drug transport by purified P-glycoprotein. *J Biol Chem* **270**: 16167-75.

Shapiro, A.B. and V. Ling. 1997a. Extraction of Hoechst 33342 from the cytoplasmic leaflet of the plasma membrane by P-glycoprotein. *Eur J Biochem* **250**: 122-9.

Shapiro, A.B. and V. Ling. 1997b. Positively cooperative sites for drug transport by P-glycoprotein with distinct drug specificities. *Eur J Biochem* **250**: 130-7.

Sharom, F.J. 1995. Characterization and functional reconstitution of the multidrug transporter. *J Bioenerg Biomembr* **27**: 15-22.

Sharom, F.J. 1997. The P-glycoprotein multidrug transporter: interactions with membrane lipids, and their modulation of activity. *Biochem Soc Trans* **25**: 1088-96.

Sharom, F.J., X. Yu, P. Lu, R. Liu, J.W. Chu, K. Szabo, M. Muller, C.D. Hose, A. Monks, A. Varadi, J. Seprodi, and B. Sarkadi. 1999. Interaction of the P-glycoprotein multidrug transporter (MDR1) with high affinity peptide chemosensitizers in isolated membranes, reconstituted systems, and intact cells. *Biochem Pharmacol* **58**: 571-86.

Sinal, C.J., M. Tohkin, M. Miyata, J.M. Ward, G. Lambert, and F.J. Gonzalez. 2000. Targeted disruption of the nuclear receptor FXR/BAR impairs bile acid and lipid homeostasis [In Process Citation]. *Cell* **102**: 731-44.

Sinicrope, F.A., P.K. Dudeja, B.M. Bissonnette, A.R. Safa, and T.A. Brasitus. 1992. Modulation of P-glycoprotein-mediated drug transport by alterations in lipid fluidity of rat liver canalicular membrane vesicles. *J Biol Chem* **267**: 24995-5002.

Sippel, C.J., M.J. McCollum, and D.H. Perlmutter. 1994. Bile acid transport by the rat liver canalicular bile acid transport/ecto-ATPase protein is dependent on ATP but not on its own ecto-ATPase activity. *J Biol Chem* **269**: 2820-6.

Smit, J.J., A.H. Schinkel, R.P. Oude Elferink, A.K. Groen, E. Wagenaar, L. van Deemter, C.A. Mol, R. Ottenhoff, N.M. van der Lugt, M.A. van Roon, and et al. 1993. Homozygous disruption of the murine mdr2 P-glycoprotein gene leads to a complete absence of phospholipid from bile and to liver disease. *Cell* **75**: 451-62.

Smit, J.W., A.H. Schinkel, M. Muller, B. Weert, and D.K. Meijer. 1998a. Contribution of the murine mdr1a P-glycoprotein to hepatobiliary and intestinal elimination of cationic drugs as measured in mice with an mdr1a gene disruption. *Hepatology* **27**: 1056-63.

Smit, J.W., A.H. Schinkel, B. Weert, and D.K. Meijer. 1998b. Hepatobiliary and intestinal clearance of amphiphilic cationic drugs in mice in which both mdr1a and mdr1b genes have been disrupted. *Br J Pharmacol* **124**: 416-24.

Soroka, C.J., J.M. Lee, F. Azzaroli, and J.L. Boyer. 2001. Cellular localization and up-regulation of multidrug resistance-associated protein 3 in hepatocytes and cholangiocytes during obstructive cholestasis in rat liver. *Hepatology* **33**: 783-91.

Srivastava, R.A., N. Srivastava, and M. Averna. 2000. Dietary cholic acid lowers plasma levels of mouse and human apolipoprotein A-I primarily via a transcriptional mechanism. *Eur J Biochem* **267**: 4272-80.

Staudinger, J.L., B. Goodwin, S.A. Jones, D. Hawkins-Brown, K.I. MacKenzie, A. LaTour, Y. Liu, C.D. Klaassen, K.K. Brown, J. Reinhard, T.M. Willson, B.H. Koller, and S.A. Kliewer. 2001. The nuclear receptor PXR is a lithocholic acid sensor that protects against liver toxicity. *Proc Natl Acad Sci U S A* **98**: 3369-74.

Stieger, B., K. Fattinger, J. Madon, G.A. Kullak-Ublick, and P.J. Meier. 2000. Drug- and estrogen-induced cholestasis through inhibition of the hepatocellular bile salt export pump (Bsep) of rat liver. *Gastroenterology* **118**: 422-30.

Stieger, B., B. O'Neill, and P.J. Meier. 1992. ATP-dependent bile-salt transport in canalicular rat liver plasma-membrane vesicles. *Biochem J* **284**: 67-74.

Stolz, A., H. Takikawa, M. Ookhtens, and N. Kaplowitz. 1989. The role of cytoplasmic proteins in hepatic bile acid transport. *Annu Rev Physiol* **51**: 161-76.

Stone, B.G., M. Udani, A. Sanghvi, V. Warty, K. Plocki, C.D. Bedetti, and D.H. Van Thiel. 1987. Cyclosporin A-induced cholestasis. The mechanism in a rat model. *Gastroenterology* **93**: 344-51.

Strandvik, B. and S.A. Wikstrom. 1982. Tetrahydroxylated bile acids in healthy human newborns. *Eur J Clin Invest* **12**: 301-5.

Strautnieks, S.S., L.N. Bull, A.S. Knisely, S.A. Kocoshis, N. Dahl, H. Arnell, E. Sokal, K. Dahan, S. Childs, V. Ling, M.S. Tanner, A.F. Kagalwalla, A. Nemeth, J. Pawlowska, A. Baker, G. Mieli-Vergani, N.B. Freimer, R.M. Gardiner, and R.J. Thompson. 1998. A gene encoding a liver-specific ABC transporter is mutated in progressive familial intrahepatic cholestasis. *Nat Genet* **20**: 233-8.

Strautnieks, S.S., A.F. Kagalwalla, M.S. Tanner, A.S. Knisely, L. Bull, N. Freimer, S.A. Kocoshis, R.M. Gardiner, and R.J. Thompson. 1997. Identification of a locus for progressive familial intrahepatic cholestasis PFIC2 on chromosome 2q24. *Am J Hum Genet* **61**: 630-3.

Suchy, F.J., J.C. Bucuvalas, and D.A. Novak. 1987. Determinants of bile formation during development: ontogeny of hepatic bile acid metabolism and transport. *Semin Liver Dis* **7**: 77-84.

Takikawa, H., K. Nishikawa, N. Sano, M. Yamanaka, and T. Horie. 1995. Mechanisms of biliary excretion of lithocholate-3-sulfate in Eisai hyperbilirubinemic rats (EHBR). *Dig Dis Sci* **40**: 1792-7.

Thompson, R. and P.L. Jansen. 2000. Genetic defects in hepatocanalicular transport. *Semin Liver Dis* **20**: 365-72.

Tomer, G., M. Ananthanarayanan, A. Weymann, N. Balasubramanian, and F.J. Suchy. 2003. Differential developmental regulation of rat liver canalicular membrane transporters Bsep and Mrp2. *Pediatr Res* **53**: 288-94.

Torok, M., H. Gutmann, G. Fricker, and J. Drewe. 1999. Sister of P-glycoprotein expression in different tissues. *Biochem Pharmacol* **57**: 833-5.

Ueda, K., N. Okamura, M. Hirai, Y. Tanigawara, T. Saeki, N. Kioka, T. Komano, and R. Hori. 1992. Human P-glycoprotein transports cortisol, aldosterone, and dexamethasone, but not progesterone. *J Biol Chem* **267**: 24248-52.

Ujhazy, P., D. Ortiz, S. Misra, S. Li, J. Moseley, H. Jones, and I.M. Arias. 2001. Familial intrahepatic cholestasis 1: studies of localization and function. *Hepatology* **34**: 768-75.

Urbatsch, I.L., B. Sankaran, S. Bhagat, and A.E. Senior. 1995. Both P-glycoprotein nucleotide-binding sites are catalytically active. *J Biol Chem* **270**: 26956-61.

van Asperen, J., A.H. Schinkel, J.H. Beijnen, W.J. Nooijen, P. Borst, and O. van Tellingen. 1996. Altered pharmacokinetics of vinblastine in Mdr1a P-glycoprotein-deficient Mice. *J Natl Cancer Inst* **88**: 994-9.

van Mil, S.W., L.W. Klomp, L.N. Bull, and R.H. Houwen. 2001. FIC1 disease: a spectrum of intrahepatic cholestatic disorders. *Semin Liver Dis* **21**: 535-44.

van Nieuwerk, C.M., A.K. Groen, R. Ottenhoff, M. van Wijland, M.A. van den Bergh Weerman, G.N. Tytgat, J.J. Offerhaus, and R.P. Oude Elferink. 1997. The role of bile salt composition in liver pathology of mdr2 (-/-) mice: differences between males and females. *J Hepatol* **26**: 138-45.

Vlahcevic, Z.R., G. Eggertsen, I. Bjorkhem, P.B. Hylemon, K. Redford, and W.M. Pandak. 2000. Regulation of sterol 12alpha-hydroxylase and cholic acid biosynthesis in the rat. *Gastroenterology* **118**: 599-607.

Vore, M. 1987. Estrogen cholestasis. Membranes, metabolites, or receptors? *Gastroenterology* **93**: 643-9.

Vore, M., Y. Liu, and L. Huang. 1997. Cholestatic properties and hepatic transport of steroid glucuronides. *Drug Metab Rev* **29**: 183-203.

Wagner, M., P. Fickert, G. Zollner, A. Fuchsbichler, D. Silbert, O. Tsybrovskyy, K. Zatloukal, G.L. Guo, J.D. Schuetz, F.J. Gonzalez, H.U. Marschall, H. Denk, and M. Trauner. 2003. Role of farnesoid X receptor in determining hepatic ABC transporter expression and liver injury in bile duct-ligated mice. *Gastroenterology* **125**: 825-38.

Wang, D.P. and J.Y. Chiang. 1994. Structure and nucleotide sequences of the human cholesterol 7 alpha-hydroxylase gene (CYP7). *Genomics* **20**: 320-3.

Wang, D.Q., F. Lammert, D.E. Cohen, B. Paigen, and M.C. Carey. 1999a. Cholic acid aids absorption, biliary secretion, and phase transitions of cholesterol in murine cholelithogenesis. *Am J Physiol* **276**: G751-60.

Wang, D.Q., B. Paigen, and M.C. Carey. 1997. Phenotypic characterization of Lith genes that determine susceptibility to cholesterol cholelithiasis in inbred mice: physical-chemistry of gallbladder bile. *J Lipid Res* **38**: 1395-411.

Wang, D.Q., S. Tazuma, D.E. Cohen, and M.C. Carey. 2003a. Feeding natural hydrophilic bile acids inhibits intestinal cholesterol absorption: studies in the gallstone-susceptible mouse. *Am J Physiol Gastrointest Liver Physiol* **285**: G494-502. Epub 2003 May 14.

Wang, H., J. Chen, K. Hollister, L.C. Sowers, and B.M. Forman. 1999b. Endogenous bile acids are ligands for the nuclear receptor FXR/BAR. *Mol Cell* **3**: 543-53.

Wang, L., C.J. Soroka, and J.L. Boyer. 2002. The role of bile salt export pump mutations in progressive familial intrahepatic cholestasis type II. *J Clin Invest* **110**: 965-72.

Wang, R., P. Lam, L. Liu, D. Forrest, I.M. Yousef, D. Mignault, M.J. Phillips, and V. Ling. 2003c. Severe cholestasis induced by cholic acid feeding in knockout mice of sister of P-glycoprotein. *Hepatology* **38**: 1489-99.

Wang, R., M. Salem, I.M. Yousef, B. Tuchweber, P. Lam, S.J. Childs, C.D. Helgason, C. Ackerley, M.J. Phillips, and V. Ling. 2001. Targeted inactivation of sister of P-glycoprotein gene (spgp) in mice results in nonprogressive but persistent intrahepatic cholestasis. *Proc Natl Acad Sci U S A* **98**: 2011-6.

Watanabe, N., N. Tsukada, C.R. Smith, and M.J. Phillips. 1991. Motility of bile canaliculi in the living animal: implications for bile flow. *J Cell Biol* **113**: 1069-80.

Weinman, S.A., J. Graf, and J.L. Boyer. 1989. Voltage-driven, taurocholate-dependent secretion in isolated hepatocyte couplets. *Am J Physiol* **256**: G826-32.

Wheeler, H.O., E.D. Ross, and S.E. Bradley. 1968. Canalicular bile production in dogs. *Am J Physiol* **214**: 866-74.

Whitington, P.F. 1996. Chronic cholestasis of infancy. *Pediatr Clin North Am* **43**: 1-26.

Whitington, P.F., D.K. Freese, E.M. Alonso, S.J. Schwarzenberg, and H.L. Sharp. 1994. Clinical and biochemical findings in progressive familial intrahepatic cholestasis. *J Pediatr Gastroenterol Nutr* **18**: 134-41.

Wolters, H., B.M. Elzinga, J.F. Baller, R. Boverhof, M. Schwarz, B. Stieger, H.J. Verkade, and F. Kuipers. 2002. Effects of bile salt flux variations on the expression of hepatic bile salt transporters in vivo in mice. *J Hepatol* **37**: 556-63.

Xie, W., A. Radominska-Pandya, Y. Shi, C.M. Simon, M.C. Nelson, E.S. Ong, D.J. Waxman, and R.M. Evans. 2001. An essential role for nuclear receptors SXR/PXR in detoxification of cholestatic bile acids. *Proc Natl Acad Sci U S A* **98**: 3375-80.

Xu, G., L.X. Pan, H. Li, B.M. Forman, S.K. Erickson, S. Shefer, J. Bollineni, A.K. Batta, J. Christie, T.H. Wang, J. Michel, S. Yang, R. Tsai, L. Lai, K. Shimada, G.S. Tint, and G. Salen. 2002. Regulation of the farnesoid X receptor (FXR) by bile acid flux in rabbits. *J Biol Chem* **277**: 50491-6.

Yanagisawa, J., M. Itoh, M. Ishibashi, H. Miyazaki, and F. Nakayama. 1980. Microanalysis of bile acid in human liver tissue by selected ion monitoring. *Anal Biochem* **104**: 75-86.

Yoon, Y.B., L.R. Hagey, A.F. Hofmann, D. Gurantz, E.L. Michelotti, and J.H. Steinbach. 1986. Effect of side-chain shortening on the physiologic properties of bile acids: hepatic transport and effect on biliary secretion of 23-nor-ursodeoxycholate in rodents. *Gastroenterology* **90**: 837-52.

Yousef, I.M., G. Bouchard, B. Tuchweber, and G.L. Plaa. 1997. Monohydroxy bile acid induced cholestasis: role of biotransformation. *Drug Metab Rev* **29**: 167-81.

Zelcer, N., G. Reid, P. Wielinga, A. Kuil, I. van der Heijden, J.D. Schuetz, and P. Borst. 2003a. Steroid and bile acid conjugates are substrates of human multidrug-resistance protein (MRP) 4 (ATP-binding cassette C4). *Biochem J* **371**: 361-7.

Zelcer, N., T. Saeki, I. Bot, A. Kuil, and P. Borst. 2003b. Transport of bile acids in multidrug-resistance-protein 3-overexpressing cells co-transfected with the ileal Na+-dependent bile-acid transporter. *Biochem J* **369**: 23-30.

Zollner, G., P. Fickert, A. Fuchsbichler, D. Silbert, M. Wagner, S. Arbeiter, F.J. Gonzalez, H.U. Marschall, K. Zatloukal, H. Denk, and M. Trauner. 2003a. Role of nuclear bile acid receptor, FXR, in adaptive ABC transporter regulation by cholic and ursodeoxycholic acid in mouse liver, kidney and intestine. *J Hepatol* **39**: 480-8.

Zollner, G., P. Fickert, D. Silbert, A. Fuchsbichler, H.U. Marschall, K. Zatloukal, H. Denk, and M. Trauner. 2003b. Adaptive changes in hepatobiliary transporter expression in primary biliary cirrhosis. *J Hepatol* **38**: 717-27.